

# Yukawa Coupling Thresholds: Application to the MSSM and the Minimal Supersymmetric SU(5) GUT

BRIAN D. WRIGHT<sup>†</sup>

*Physics Department, University of Wisconsin  
Madison, WI 53706, USA*

## ABSTRACT

We consider a particular class of threshold corrections to Yukawa couplings and mass relations in the MSSM and supersymmetric grand unified models. We give a complete treatment of Yukawa coupling thresholds at the unification scale  $M_{GUT}$  and the effective supersymmetry scale  $M_{SUSY}$  and apply them to corrections to the tree-level prediction  $y_b(M_{GUT}) = y_\tau(M_{GUT})$  in minimal supersymmetric SU(5). We apply both gauge and Yukawa coupling thresholds to gauge unification and the above Yukawa unification condition to find predictions for the top quark mass,  $M_t$ , the superheavy vector boson mass  $M_V$  and the colored Higgs triplet mass  $M_{H_3}$ . We discuss the dependencies of  $M_{GUT}$  and  $M_{H_3}$  on  $\alpha_s(M_Z)$ ,  $M_t$  and the sparticle spectrum as well as those of  $M_t$  on  $\tan\beta$ ,  $\alpha_s(M_Z)$  and the bottom quark mass,  $M_b$ . The effect of the Yukawa coupling thresholds on  $M_t$  are given for representative sparticle spectra. We describe the quantitative differences between these effects for low and high  $\tan\beta$ . We also give new bounds on superheavy masses, incorporating proton decay as well as unification constraints, the former leading to a lower bound on  $\alpha_s$ .

Submitted to *Physical Review D*

---

<sup>†</sup> E-mail address: wright@phenot.physics.wisc.edu

# 1. Introduction

In light of the current renewal of interest in renormalization group (RG) constraints arising from supersymmetric grand unified theories (SUSY-GUTs), it has become increasingly important to quantify corrections to GUT scale predictions. Recently several two loop renormalization group analyses of SUSY-GUTs with soft supersymmetry-breaking induced via minimal N=1 supergravity have been performed.<sup>[1-7]</sup> In certain scenarios, these analyses have made predictions for the sparticle spectrum and low energy parameters arising from GUT scale constraints. Emphasis should be placed on determining the uncertainties in these predictions and their dependence on the unknown heavy mass spectrum as well as the details of supersymmetry breaking. However, only some of these analyses treat the one loop threshold matching conditions which are necessary for a consistent two loop analysis of the gauge coupling unification and few consider thresholds occurring in Yukawa couplings and mass parameters in general. Usually threshold effects are considered only for the gauge couplings.<sup>1</sup> We find that the Yukawa coupling thresholds are typically at least as important as the gauge coupling threshold effects.

The purpose of this article is to present a complete treatment of Yukawa threshold corrections in the Standard Model (SM), the Minimal Supersymmetric Standard Model (MSSM) and the minimal supersymmetric SU(5) GUT. We also review the gauge coupling threshold corrections in these models and attempt to quantify both types of correction terms. These effects are applied in the context of gauge and third generation Yukawa unification in minimal SU(5), and are used to probe the superheavy spectrum and the top quark mass. For definiteness, we consider the scenario in which these unifications, modulo grand unified scale thresholds, are used to solve for the physical top mass  $M_t$ , the colored Higgs triplet mass  $M_{H_3}$  and an effective GUT scale  $M_{GUT}$ . These solutions are considered for experimental ranges of values of  $\sin\theta_W$ , the strong coupling  $\alpha_s$  and the physical bottom quark

---

<sup>1</sup> For a discussion of this indirect influence of gauge coupling thresholds on the prediction of  $m_b(M_Z)$  from Yukawa unification, see Ref. 8.

mass  $M_b$  and central values of the remaining weak scale parameters. We also give, especially for the  $M_t$  solution, the dependence on  $\tan\beta$ , the ratio of the VEVs of the two Higgs doublets in the MSSM (see Appendix A for conventions). We highlight the importance of threshold effects in these solutions by displaying their quantitative dependence on the sparticle and GUT scale spectrum.

We find significant variation of the solutions for  $M_{H_3}$  and  $M_{GUT}$  with top masses in the range  $130 < M_t < 200$  GeV. The corresponding weak threshold corrections are between 1 and 40% for the  $M_{GUT}$  solution and between 6 and  $-95\%$  for the  $M_{H_3}$  solution. The latter solution is more sensitive to the large  $\alpha_s$  error bars, two loop effects and boundary corrections at  $M_Z$  and  $M_{SUSY}$ , particularly since  $M_{H_3}$  itself only appears in threshold matching functions. The decline of the  $M_{H_3}$  solution with  $M_t$  is to be contrasted with the increase in the lower bound on  $M_{H_3}$  from proton decay in which a large top Yukawa enhances the corresponding effective dimension 5 operator through renormalization group effects. We allude to the possibilities for constraining the minimal SUSY-SU(5) model using proton decay limits without introducing theoretical prejudices about the GUT scale spectrum. We also re-emphasize the sensitivities of  $M_{GUT}$  and  $M_{H_3}$  on the gluino and Higgsino masses respectively.

The effect of the Yukawa thresholds is seen in the  $M_t$  solution or, equivalently,  $m_b(M_Z)$  for fixed  $M_t$ . We discuss the robustness of the former solution compared to the latter in the context of both Yukawa threshold corrections at  $M_{SUSY}$  and  $M_{GUT}$ . We find that these GUT scale corrections to  $M_t$  typically range from  $+10$  to  $-5\%$  for extreme ranges of the ratio of the superheavy vector and adjoint scalar masses. We dissect the various supersymmetric Yukawa coupling threshold corrections, in particular the various sources of enhancements in the large  $\tan\beta$  region coming from certain vertex diagrams involving gluinos and charginos. Quantitative effects for  $M_t$  are given for sample sparticle spectra for low, intermediate and large  $\tan\beta$ . Characteristically, we find positive corrections to  $M_t$  of order 2 - 7% for low  $\tan\beta = 1.5$  and for both signs of the supersymmetric Higgs mass parameter  $\mu_H$ . For higher  $\tan\beta$  and  $\mu_H > 0$ , we find typically negative corrections of up to 10%

for  $\tan\beta = 15$ . For  $\tan\beta \gtrsim 40$ , the corrections are larger and highly spectrum dependent. The inclusion of the Yukawa coupling thresholds can also significantly modify perturbativity constraints on third generation Yukawa couplings.

The importance of Yukawa coupling thresholds has come to the attention of several authors recently.<sup>[9–11]</sup> Loop corrections to low energy mass parameters have been treated in certain cases such as the well-known case of radiative corrections to the Higgs boson masses in the MSSM<sup>[12]</sup> although usually not explicitly in the form of threshold conditions on running mass parameters except in the case of the Standard Model<sup>[13]</sup> and for  $y_b$  and  $y_\tau$  in ordinary GUTs.<sup>[14]</sup> However, in the context of renormalization group analyses of high scale predictions they have not been treated generally.

This work is organized as follows. We first consider in Section 2 the general treatment of Yukawa and mass parameter thresholds. This analysis provides a framework which can be applied to more complicated mass and mixing angle textures. In Section 3 we give a complete calculation of the GUT scale matching functions for the Yukawa couplings in minimal SUSY-SU(5). In the spirit of quantifying uncertainties in SUSY-GUT predictions, we consider in particular the one loop threshold corrections to the tree-level relation  $y_b(M_{GUT}) = y_\tau(M_{GUT})$  and highlight its sensitivity to the top Yukawa coupling  $y_t(M_{GUT})$  and the possible splitting of the colored Higgs triplet superfields from the other superheavy fields. This is one of many threshold corrections to various mass relations discussed recently in Refs. 15 - 19 when a specific GUT or string model is taken to generate certain textures in the fermion mass matrices at the unification scale. We also review the GUT scale matching functions for the gauge couplings.

In Section 4 we give the most important contributions to the Yukawa coupling matching conditions at  $M_{SUSY}$  in the MSSM in the case of one light Higgs doublet in the effective SM below  $M_{SUSY}$ . We show the origin of the large enhancements which occur for large  $\tan\beta$ . We discuss the sensitivity of these corrections to the soft supersymmetry breaking parameters of the model. A complete calculation of

these thresholds for a general sparticle spectrum is given in Appendix A. We also review the gauge coupling thresholds at  $M_{SUSY}$  as well as the top mass dependent gauge and Yukawa thresholds when the top quark together with the light Higgs and  $W$  and  $Z$  bosons are integrated out at  $M_Z$ . Finally we describe our procedure for extracting the heavy quark pole masses.

In Section 5 we apply these threshold corrections to analytic predictions for  $M_{GUT} = (M_V^2 M_\Sigma)^{\frac{1}{3}}$ ,  $M_{H_3}$  and  $m_t(M_Z)$ , where  $M_V$  and  $M_\Sigma$  are the superheavy vector and the superheavy adjoint scalar masses, respectively. The first two predictions are essentially determined by gauge coupling unification. Generally gauge unification can be used to determine the unification scale  $M_{GUT}$ , the value of the couplings at  $M_{GUT}$ ,  $\alpha_G$ , and either  $\alpha_s(M_Z)$ ,  $\sin \theta_W(M_Z)$  or  $M_{H_3}$ . In the latter case the mismatch of the gauge couplings at the GUT scale determines the colored Higgs triplet mass through threshold corrections. We choose this somewhat unconventional case as it is more useful in discussing proton decay constraints. We quantify the importance of threshold corrections at  $M_Z$  and  $M_{SUSY}$  on the  $M_{GUT}$  and  $M_{H_3}$  solutions. In particular, we describe the importance of the top mass dependence of  $\sin^2 \theta_W(M_Z)$  and the gluino and Higgsino masses, respectively, on these two solutions. For the last prediction, we give a semi-analytic solution for  $m_t$  which allows one to identify the relative importance of the various correction terms. We note the robustness of the  $m_t$  solution in all but the extreme large  $\tan \beta$  region and relate this to the attraction of the infrared quasi-fixed point in  $y_t$ . For all the solutions we show their dependence on the experimental uncertainties in low scale parameters.

In Section 6 we briefly review the proton decay bound on  $M_{H_3}$  and indicate how conservative bounds can be improved when applied to the context considered here. We also review how perturbativity arguments are used to put theoretical bounds on the GUT scale spectrum. We apply these, together with the condition that all masses lie below the Planck mass  $M_{Planck}$ , only to delineate the cases in which a perturbative analysis is appropriate.

We give the full two loop numerical solutions for  $M_{GUT}$ ,  $M_{H_3}$  and  $M_t$  in Section 7. We give the extreme ranges of  $M_{GUT}$  and  $M_{H_3}$  consistent with gauge coupling unification and low energy data. We display the effects of the weak and supersymmetry scale threshold corrections as well as the error bars on  $\alpha_s$  of these solutions in graphical form. The effects of the thresholds at  $M_{SUSY}$  and  $M_{GUT}$  on the  $M_t$  solution are separately discussed. In the former case we quantify the effects in the low, intermediate and high  $\tan\beta$  regions for sample sparticle spectra. In the latter case we show how the GUT scale spectrum can modify the prediction for  $M_t$  as a function of  $\tan\beta$ . We also show the dominant effects of the uncertainties in  $M_b$  and  $\alpha_s$  on  $M_t$ .

Finally we make two general remarks. The first concerns our restriction to minimal SUSY-SU(5). This restriction is chosen merely for its relative simplicity. The minimal case may also be indicative of what one may expect in more general GUTs. Thus we do not address the less appealing features of minimal SU(5) such as the doublet-triplet splitting problem and the unsuccessful mass relations for the first and second generation fermions. These difficulties can be resolved by complicating the GUT scale superpotential.<sup>[20]</sup> Instead we regard minimal SUSY-SU(5) as a toy model for investigation. In general, one expects the threshold corrections in more complicated models to be at least as large as those in the minimal case.

Second, we would like to advocate a particular philosophy for the treatment of threshold corrections in minimal subtraction (MS) schemes. From the Appelquist-Carrazzone decoupling theorem<sup>[21]</sup> we expect the physics at energies below a given mass scale to be independent of the particles with masses higher than this threshold. However, MS schemes are not physical in the sense that they are scale dependent and mass independent so that the decoupling theorem is not manifest. As described in Refs. 22 - 24, one implements the decoupling in MS schemes by formulating a low energy effective theory obtained by integrating out the heavy fields to one loop. The effect of this procedure is to give relations between renormalized parameters just above and below the particle mass(es), the so-called matching

functions, and to modify the various  $\beta$  function coefficients so that in the lower scale theory the contribution of the particle(s) to these coefficients is removed. The running parameters are typically discontinuous at the boundary at which the matching function is applied unless one tunes the boundary scale. In either case reliable values for the parameters of the theory are obtained asymptotically away from the boundary.

In the treatment of gauge coupling thresholds, particularly in the MSSM and in GUTs, many authors have identified a threshold with each sparticle (often assuming small mixings or large degeneracies) or superheavy particle mass, and modified the beta function coefficients between each threshold. Here the couplings are usually taken to be continuous at the boundary, which is justified since the gauge matching functions in supersymmetric theories in the dimensional reduction (DR) scheme vanish at the mass of the particle defining the boundary. However this procedure can be complicated when the effect of integrating out the particle breaks the gauge symmetry of the higher scale theory. In the case of split multiplets (such as the Higgs  $\mathbf{5}$  of  $SU(5)$ ), one typically must use different sets of  $\beta$  functions depending on different mass orderings of the spectrum. Also, when Yukawa thresholds are included the Yukawa and mass parameters are in general not continuous at threshold boundaries even in DR schemes.

Instead we use the arguably simpler scheme advocated by Hall<sup>[23]</sup> in which one integrates out together all particles with similar masses at a single scale. If one uses one loop matching functions then this is justified as long as one loop  $\beta$  functions can be used between the different particle masses.<sup>[23]</sup> This is generally the case. This is simpler both from the analytic and numerical standpoint when it is applied to the MSSM and its grand unified extensions. For example, in the analysis below in which one has a light SM Higgs doublet below  $M_{SUSY}$ , the top quark as well as the  $W$ ,  $Z$ , and SM Higgs are integrated out at  $M_Z$ , all sparticles including the heavier Higgs doublet can be integrated out at a fixed scale,  $M_{SUSY}$  (with complicated matching functions incorporating the details of the spectrum) and all superheavy particles at  $M_{GUT}$ . With more generality and without a loss of

accuracy, the proliferation of scales and sets of  $\beta$  functions is reduced to at most three.

## 2. Yukawa Thresholds: The General Case

The treatment of Yukawa coupling and mass parameter thresholds in minimal subtraction (MS) schemes is analogous to the treatment of gauge thresholds given by Weinberg,<sup>[22]</sup> Hall<sup>[23]</sup> and Ovrut and Schnitzer.<sup>[24]</sup> For completeness we outline the procedure for Yukawa coupling and mass thresholds below.

Consider a generic gauge theory in which the kinetic and Yukawa contributions to the bare Lagrangian are

$$\begin{aligned}\mathcal{L}_{kin} &= \mathcal{L}_{gauge} + i\bar{\psi}_{Li} \not{\partial}\psi_{Li} + i\bar{\psi}_{Ri} \not{\partial}\psi_{Ri} + \partial_\mu\phi_a^\dagger\partial^\mu\phi_a + \dots \\ \mathcal{L}_Y &= -\bar{\psi}_{Li}M_{ij}\psi_{Rj} - \bar{\psi}_{Li}Y_{ij}^a\psi_{Rj}\phi_a + \text{h.c.} ,\end{aligned}\tag{2.1}$$

where  $\psi_i$  is a generic fermion of type  $i$ ,  $\phi_a$  is a generic scalar field with vacuum expectation value  $v_a$ , and  $M_{ij} = Y_{ij}^a v_a$ . We assume that it is possible to decompose the fields  $\psi_i$  and  $\phi_a$  into light components  $\hat{\psi}_i$ ,  $\hat{\phi}_a$  and heavy components  $\Psi_I$  and  $\Phi_\alpha$ . When the heavy fields are integrated out to one loop we generate the following low energy effective Lagrangian,

$$\begin{aligned}\mathcal{L}_{kin}^{eff} &= \mathcal{L}_{gauge}^{eff} + i\bar{\hat{\psi}}_{Li} \not{\partial}Z_L^{ij}\hat{\psi}_{Lj} + i\bar{\hat{\psi}}_{Ri} \not{\partial}Z_R^{ij}\hat{\psi}_{Rj} + \partial_\mu\hat{\phi}_a^\dagger Z_\phi^{ab}\partial^\mu\hat{\phi}_b + \dots \\ \mathcal{L}_Y^{eff} &= -\bar{\hat{\psi}}_{Li}\hat{M}_{ij}\hat{\psi}_{Rj} - \bar{\hat{\psi}}_{Li}\hat{Y}_{ij}^a\hat{\psi}_{Rj}\hat{\phi}_a + \text{h.c.} + \text{NR} ,\end{aligned}\tag{2.2}$$

where NR indicates induced nonrenormalizable interactions. The matrix parameters  $Z_{(L,R)}$  can be written as

$$Z_{(L,R)} = 1 + K_{(L,R)} ,\tag{2.3}$$

where  $K_{(L,R)}$  come from light fermion wavefunction renormalization diagrams with

heavy fields in the loop. The parameters  $K_\phi$  in

$$Z_\phi = 1 + K_\phi , \quad (2.4)$$

comes from analogous light scalar wavefunction renormalization. The matrices  $\hat{M}$  and  $\hat{Y}$  can be written as

$$\begin{aligned} \hat{M} &= M + \delta M \equiv M(1 + K_M) , \\ \hat{Y} &= Y + \delta Y \equiv Y(1 + K_Y) , \end{aligned} \quad (2.5)$$

where  $\delta M$  and  $\delta Y$  come from one loop light field self energy and three point Yukawa vertex diagrams, respectively, with heavy fields in the loop.

To properly normalize the kinetic terms one must first diagonalize the hermitian matrices  $Z_{(L,R)}$  and then rescale each bare fermion field by the appropriate eigenvalue. Let  $Z_L = U_L^\dagger Z_L^d U_L$  where  $Z_L^d$  is diagonal and  $U_L$  is unitary, with similar definitions for  $U_R$  and  $U_\phi$ . We redefine the fields via

$$\begin{aligned} \psi'_{Li} &= (Z_{Li}^d)^{\frac{1}{2}} U_L^{ij} \hat{\psi}_{Lj} , \\ \psi'_{Ri} &= (Z_{Ri}^d)^{\frac{1}{2}} U_R^{ij} \hat{\psi}_{Rj} , \\ \phi'_a &= (Z_{\phi a}^d)^{\frac{1}{2}} U_\phi^{ab} \hat{\phi}_b . \end{aligned} \quad (2.6)$$

In terms of the primed fields, the kinetic terms are canonical and the bare effective mass and Yukawa matrices are

$$M^{eff} = (Z_L^d)^{-\frac{1}{2}} U_L (M + \delta M) U_R^\dagger (Z_R^d)^{-\frac{1}{2}} , \quad (2.7)$$

$$Y^{eff a} = (Z_L^d)^{-\frac{1}{2}} U_L (Y + \delta Y)^b U_R^\dagger (Z_R^d)^{-\frac{1}{2}} U_\phi^{\dagger ba} (Z_{\phi a}^d)^{-\frac{1}{2}} , \quad (2.8)$$

To get the one loop matching functions one must turn these bare relations into renormalized ones. The divergent parts in  $M^{eff}$  and  $Y^{eff a}$  are just the difference between the self energy counterterms of the effective theory and those of the full

theory. So by replacing all parameters in (2.7) and (2.8) by their finite parts (indicated by a bar over the quantity) as defined in  $\overline{\text{MS}}$  and neglecting higher order corrections, one obtains the renormalized relations:

$$M_{ij}^{eff}(\mu) = (U_L M(\mu) U_R^\dagger)_{ij} + M_{ij}(\mu) (\overline{K}_{Mij} - \frac{1}{2}(\overline{K}_{Li}^d + \overline{K}_{Rj}^d)) , \quad (2.9)$$

$$Y_{ij}^{eff a}(\mu) = (U_L Y^b(\mu) U_R^\dagger)^{ij} U_\phi^{\dagger ba} + Y_{ij}^a(\mu) (\overline{K}_{Yij}^a - \frac{1}{2}(\overline{K}_{Li}^d + \overline{K}_{Rj}^d + \overline{K}_{\phi a}^d)) , \quad (2.10)$$

In practice  $M^{eff}$  must be diagonalized by a biunitary transformation even if the original theory is written in terms of mass eigenstates. In the case of the MSSM, for example, this leads to threshold corrections in the renormalized Cabibbo-Kobayashi-Maskawa matrix at the effective scale  $M_{SUSY}$  when the superparticles are integrated out. The effect of such thresholds, of potential relevance to RG analyses of GUT scale mass textures, will be discussed in a future work.<sup>[25]</sup>

### 3. Yukawa and Gauge Thresholds in Minimal SUSY-SU(5)

Next we apply the preceding formalism to the one loop GUT threshold corrections to the tree-level relation  $y_b(M_{GUT}) = y_\tau(M_{GUT})$  in minimal supersymmetric SU(5). This is of particular interest since this condition strongly constrains the allowed range of the top quark mass in an experimentally accessible region.<sup>[26–29]</sup> Here we find two contributions, one proportional to the square of the top Yukawa coupling coming from integrating out heavy color triplet Higgs and Higgsino fields, the other proportional to the GUT scale gauge coupling coming from integrating out superheavy vector bosons. Since the soft supersymmetry breaking mass parameters are much smaller than typical GUT scale masses we can work in an approximately supersymmetric formalism in which both light fields along with their superpartners are treated as massless in loops involving superheavy fields. We therefore use supergraph methods to simplify the calculations.

We start with a superpotential of the form

$$\begin{aligned}
P = & \sqrt{2}\Psi_a Y^{(d)} \chi^{ab} H_b^{(1)} - \frac{1}{4}\epsilon_{abcde} \chi^{ab} Y^{(u)} \chi^{cd} H^{(2)e} \\
& + M_2 H^{(2)a} H_a^{(1)} + \lambda_2 H^{(2)a} \Sigma_a^b H_b^{(1)} + \frac{\lambda_1}{3} \text{Tr} \Sigma^3 + \frac{M_1}{2} \text{Tr} \Sigma^2, \tag{3.1}
\end{aligned}$$

where  $\Psi$ ,  $H^{(1)}$ ,  $H^{(2)}$ ,  $\chi$  and  $\Sigma$  are SU(5) superfields transforming as the **5**, **5**,  $\bar{\mathbf{5}}$ , **10** and **24** dimensional representations, respectively. In the usual way we associate these superfields with the SU(3)  $\times$  SU(2)  $\times$  U(1) decomposition by

$$\chi = \frac{1}{\sqrt{2}} \begin{pmatrix} 0 & U_3^c & -U_2^c & -U^1 & -D^1 \\ -U_3^c & 0 & U_1^c & -U^2 & -D^2 \\ U_2^c & -U_1^c & 0 & -U^3 & -D^3 \\ U^1 & U^2 & U^3 & 0 & -E^c \\ D^1 & D^2 & D^3 & E^c & 0 \end{pmatrix}, \tag{3.2}$$

and  $\Psi^T = (D_\alpha^c, E, -\nu)$ , where lowercase Greek/Latin indices denote SU(3) and SU(5) indices, respectively. In component fields the charge conjugate Weyl fermion fields will be related to the right-handed component of Dirac fermions. The five dimensional Higgs supermultiplets are likewise split into color triplet and SU(2) doublet components according to

$$H^{(1)} = (H_{3\alpha}^{(1)}, H^{(1)-}, -H_0^{(1)}) \quad \text{and} \quad H^{(2)} = (H_3^{(2)\alpha}, H^{(2)+}, H_0^{(2)}), \tag{3.3}$$

where the 3 denotes the strongly interacting triplets. These superfields couple to the SU(5) vector supermultiplet in the usual way. In addition to the component field interactions obtained from (3.1), one also can add the most general set of SU(5) invariant soft supersymmetry breaking terms. In the threshold calculations that follow, however supersymmetry as well as electroweak symmetry breaking effects are unimportant as the corresponding mass scales are much smaller than  $M_{GUT}$ . The SU(5) symmetry is broken without breaking supersymmetry when the adjoint Higgs field gets the vacuum expectation value  $\langle \Sigma \rangle = V \text{diag}(1, 1, 1, -3/2, -3/2)$ ,

where  $V = 2M_1/\lambda_1$ . This gives the following mass spectrum in the minimal model: two degenerate Higgs triplet superfields of mass  $M_{H_3}$ , degenerate  $X$  and  $Y$  leptoquark gauge superfields of mass  $M_V$ , color octet and  $SU(2)$  triplet superfields of mass  $M_\Sigma$  along with a singlet of mass  $0.2M_\Sigma$ . The electroweak doublets remain light as long as the fine-tuning constraint  $\lambda_1 M_2 - 3\lambda_2 M_1 \approx M_{EW}$  is satisfied, where  $M_{EW}$  is a typical electroweak scale mass. This can of course be relaxed in the missing doublet model for example,<sup>[20]</sup> but we limit our discussion to the minimal model for simplicity.

The GUT scale threshold corrections are obtained by integrating out the superheavy  $X$  and  $Y$  gauge supermultiplets, the Higgs triplet, and the Higgs adjoint superfields to obtain an effective MSSM. These were obtained for the gauge couplings long ago in Refs. 30 and 31, and have recently been reanalyzed in the present context in Refs. 32 and 33. However, explicit model dependent threshold corrections for the  $SU(5)$  Yukawa couplings have not been computed and studied. To properly generalize the analysis of Weinberg and Hall<sup>[22,23]</sup> to construct an effective MSSM, one must gauge-fix the superfield Lagrangian in a so-called supersymmetric S-covariant gauge so that the low energy gauge symmetry  $S$  is  $SU(3) \times SU(2) \times U(1)$ . One essentially replaces derivatives by S-covariant derivatives in the  $R_\xi$  gauge-fixing functional of the high energy theory. Details in the superfield formalism can be found in Refs. 34 and 35, but the corresponding vertices are not involved in the Yukawa threshold calculation. As mentioned above, at the high scale we can use the supergraph formalism<sup>[36]</sup> to construct the effective action in Feynman gauge ( $\xi = 1$ ) obtained when the aforementioned heavy fields are integrated out. The one loop divergences are naturally regulated by dimensional reduction ( $\overline{DR}$ ),<sup>[37]</sup> which preserves supersymmetry at least up to one loop.

Due to the supersymmetric nonrenormalization theorems,<sup>[36,38]</sup> the only modifications to the parameters of the superpotential in the effective action arise through superfield wavefunction renormalizations. Hence if the original action has the form

$$S = \int d^4x \int d^4\theta (\Phi_a^\dagger e^{2gV} \Phi_a + P[\Phi] \delta^2(\bar{\theta}) + P^\dagger[\Phi] \delta^2(\theta) + \dots) , \quad (3.4)$$

with  $\Phi_a = (\Phi_I, \phi_i)$  being the decomposition into heavy/light superfields respectively, then the effective action (with an unconventional normalization of the kinetic term), suppressing gauge kinetic and interaction terms, is

$$S^{eff} = \int d^4x \int d^4\theta (Z_{ij} \phi_i^\dagger e^{2g\nu} \phi_j + P'[\phi] \delta^2(\bar{\theta}) + P'^\dagger[\phi] \delta^2(\theta) + \text{NR} + \dots) . \quad (3.5)$$

As before, NR denotes effective nonrenormalizable interactions suppressed by inverse powers of superheavy masses which, in the GUT case, will include operators responsible for proton decay. To evaluate Yukawa coupling corrections one need only consider supergraph two point functions with external light MSSM matter (s)fermion and Higgs doublet superfields and at least one superheavy superfield in the loop. Using the methods of Ref. 36 we find that the effective action contributions to the light electron family, down quark family, up quark family and neutral Higgs superfield kinetic terms relevant for the Yukawa thresholds are

$$\begin{aligned} S^{eff} = \int d^4x \int d^4\theta & (E^\dagger Z_E E + E^{c\dagger} Z_{E^c} E^c + D^\dagger Z_D D + D^{c\dagger} Z_{D^c} D^c \\ & + U^\dagger Z_U U + U^{c\dagger} Z_{U^c} U^c + Z_{H_0^{(1)}} H_0^{(1)\dagger} H_0^{(1)} + Z_{H_0^{(2)}} H_0^{(2)\dagger} H_0^{(2)} + \dots (3.6) \\ & + E Y^{(e)} E^c H_0^{(1)} + D^c Y^{(d)} D H_0^{(1)} + U^c Y^{(u)} U H_0^{(2)} \\ & + \text{h.c.} + \text{NR} + \dots) , \end{aligned}$$

where  $Z_{E,D,U}$  are matrices in family and color space. Writing  $Z = 1 + K$  we find

$$\begin{aligned} K_E &= -3\bar{g}^2 A(0, M_V^2, 0) 1 + 3(Y^{(d)} Y^{(d)\dagger})^T A(0, M_{H_3}^2, 0) , \\ K_{E^c} &= -6\bar{g}^2 A(0, M_V^2, 0) 1 + 3Y^{(u)\dagger} Y^{(u)} A(0, M_{H_3}^2, 0) , \\ K_D &= -3\bar{g}^2 A(0, M_V^2, 0) 1 + (2Y^{(u)\dagger} Y^{(u)} + Y^{(d)\dagger} Y^{(d)}) A(0, M_{H_3}^2, 0) , \\ K_{D^c} &= -2\bar{g}^2 A(0, M_V^2, 0) 1 + 2(Y^{(d)} Y^{(d)\dagger})^T A(0, M_{H_3}^2, 0) , \\ K_U &= -3\bar{g}^2 A(0, M_V^2, 0) 1 + (2Y^{(u)\dagger} Y^{(u)} + Y^{(d)\dagger} Y^{(d)}) A(0, M_{H_3}^2, 0) , \\ K_{U^c} &= -2\bar{g}^2 A(0, M_V^2, 0) 1 + (Y^{(u)\dagger} Y^{(u)} + 2Y^{(d)\dagger} Y^{(d)}) A(0, M_{H_3}^2, 0) , \\ K_{H_0^{(1)}} &= K_{H_0^{(2)}} = -3\bar{g}^2 A(0, M_{H_3}^2, M_V^2) + |\lambda_2|^2 \left( 3A(0, M_{H_3}^2, M_V^2) \right. \\ & \quad \left. + \frac{3}{2} A(0, 0, M_\Sigma^2) + \frac{3}{10} A(0, 0, \frac{1}{5} M_\Sigma^2) \right) , \end{aligned} \quad (3.7)$$

where  $\bar{g}$  is the GUT scale gauge coupling. Here the universal function  $A$  arising from the  $d$  dimensional loop integrals is

$$A(p, M_A^2, M_B^2) = -i\mu^{2\epsilon} \int \frac{d^d k}{(2\pi)^d} \frac{1}{(p+k)^2 - M_A^2} \frac{1}{k^2 - M_B^2}, \quad (3.8)$$

where  $\epsilon = 2 - \frac{d}{2}$ . In the case  $p = 0$  we get

$$A(0, M_A^2, M_B^2) = \frac{1}{(4\pi)^2} \left( \frac{1}{\eta} - F_1(M_A^2, M_B^2) \right), \quad (3.9)$$

where  $\frac{1}{\eta} = \frac{1}{\epsilon} + \ln 4\pi - \gamma_E$  and  $F_1$  is defined in Appendix B.

To determine the Yukawa threshold corrections we simply follow the generic component field analysis. First redefine the bare low scale effective light superfields so that they have a conventionally normalized kinetic term. This gives a relation between the bare high and low scale Yukawa matrices. The running relation is obtained by absorbing the divergent parts from the wavefunction renormalizations using the definition of the high and low scale  $\beta$  functions. The resulting threshold matching functions relating the renormalized couplings in the region of the unification scale then depend only on the finite parts of the  $Z$ s. We obtain  $y_\alpha(\mu) = \bar{y}_\alpha(\mu)(1 + \Delta_{y_\alpha}^{GUT})$ , where

$$\begin{aligned} 16\pi^2 \Delta_{y_t}^{GUT} &= -\frac{\bar{g}^2}{2} (5F_1(M_{GUT}^2, 0) + 3F_1(M_{H_3}^2, M_{GUT}^2)) \\ &\quad + \frac{3}{2}(\bar{y}_t^2 + \bar{y}_b^2)F_1(M_{H_3}^2, 0) \\ &\quad + \frac{\lambda^2}{2} (3F_1(M_{H_3}^2, M_{GUT}^2) + \frac{3}{2}F_1(M_\Sigma^2, 0) + \frac{3}{10}F_1(\frac{1}{5}M_\Sigma^2, 0)), \\ 16\pi^2 \Delta_{y_b}^{GUT} &= -\frac{\bar{g}^2}{2} (5F_1(M_{GUT}^2, 0) + 3F_1(M_{H_3}^2, M_{GUT}^2)) \\ &\quad + (\bar{y}_t^2 + \frac{3}{2}\bar{y}_b^2)F_1(M_{H_3}^2, 0) \\ &\quad + \frac{\lambda^2}{2} (3F_1(M_{H_3}^2, M_{GUT}^2) + \frac{3}{2}F_1(M_\Sigma^2, 0) + \frac{3}{10}F_1(\frac{1}{5}M_\Sigma^2, 0)), \\ 16\pi^2 \Delta_{y_\tau}^{GUT} &= -\frac{\bar{g}^2}{2} (9F_1(M_{GUT}^2, 0) + 3F_1(M_{H_3}^2, M_{GUT}^2)) \end{aligned} \quad (3.10)$$

$$\begin{aligned}
& + \frac{3}{2}(\bar{y}_t^2 + \bar{y}_b^2)F_1(M_{H_3}^2, 0) \\
& + \frac{\lambda_2}{2}(3F_1(M_{H_3}^2, M_{GUT}^2) + \frac{3}{2}F_1(M_\Sigma^2, 0) + \frac{3}{10}F_1(\frac{1}{5}M_\Sigma^2, 0)) ,
\end{aligned}$$

and where the (un)barred couplings are (low) GUT scale parameters ( $\bar{y}_b = \bar{y}_\tau$ ). The  $y_b/y_\tau$  threshold matching function is therefore

$$\frac{y_b}{y_\tau}(\mu) = 1 + \frac{1}{16\pi^2}(2\bar{g}^2(\mu)(2\ln\frac{M_V}{\mu} - 1) - \frac{1}{2}\bar{y}_t^2(\mu)(2\ln\frac{M_{H_3}}{\mu} - 1)) , \quad (3.11)$$

and can be applied for  $\mu \simeq M_{GUT}$ .

We also quote the gauge matching conditions for minimal SUSY-SU(5) in the  $\overline{\text{DR}}$  scheme<sup>[30,31]</sup>:

$$\frac{1}{\alpha_i(\mu)} = \frac{1}{\alpha_G(\mu)} - \Delta_i^{GUT}(\mu) , \quad (3.12)$$

where  $\alpha_G = \bar{g}^2/4\pi$  and

$$\begin{aligned}
\Delta_1^{GUT}(\mu) &= -\frac{5}{\pi}\ln\frac{M_V}{\mu} + \frac{1}{5\pi}\ln\frac{M_{H_3}}{\mu} , \\
\Delta_2^{GUT}(\mu) &= -\frac{3}{\pi}\ln\frac{M_V}{\mu} + \frac{1}{\pi}\ln\frac{M_\Sigma}{\mu} , \\
\Delta_3^{GUT}(\mu) &= -\frac{2}{\pi}\ln\frac{M_V}{\mu} + \frac{3}{2\pi}\ln\frac{M_\Sigma}{\mu} + \frac{1}{2\pi}\ln\frac{M_{H_3}}{\mu} .
\end{aligned} \quad (3.13)$$

In the interest of simplicity and minimality we do not include the effects of gravity-induced nonrenormalizable operators<sup>[39]</sup> here. As noted in Ref. 33, differences of the  $\Delta_i$  depend on  $M_V$  and  $M_\Sigma$  in the combination  $M_{GUT} = (M_V^2 M_\Sigma)^{\frac{1}{3}}$  which we will take as GUT scale at which the matching functions are applied in the analysis to follow.

## 4. Electroweak and Supersymmetric Thresholds

In addition to the GUT scale thresholds there are also thresholds at the electroweak scale and the effective supersymmetry scale  $M_{SUSY}$ . At the electroweak scale,  $M_Z$ , we integrate out the top quark, the weak gauge bosons and the SM Higgs. The definition of the inverse electromagnetic coupling  $\alpha(M_Z) = 127.9 \pm 0.1$  and the Weinberg angle  $s_0^2(M_Z) = 0.2324 \pm 0.0003$  includes one loop corrections from electroweak gauge bosons and the top quark<sup>[40]</sup> for a pole mass  $M_{t0} = 143$  GeV. This must be corrected for different top masses above  $M_Z$ . The result is<sup>[41]</sup>

$$\begin{aligned} \frac{1}{\alpha_1(M_Z)} &= \frac{3}{5}(1 - s^2(M_Z)) \left( \frac{1}{\alpha(M_Z)} + \frac{8}{9\pi} \ln \frac{M_t}{M_{t0}} \right) - \frac{3}{5} \frac{\Delta_{s^2}^{top}}{\alpha(M_Z)}, \\ \frac{1}{\alpha_2(M_Z)} &= s^2(M_Z) \left( \frac{1}{\alpha(M_Z)} + \frac{8}{9\pi} \ln \frac{M_t}{M_{t0}} \right) + \frac{\Delta_{s^2}^{top}}{\alpha(M_Z)}, \\ \frac{1}{\alpha_3(M_Z)} &= \frac{1}{\alpha_s(M_Z)} + \frac{1}{3\pi} \ln \frac{M_t}{M_Z}, \end{aligned} \quad (4.1)$$

where  $\Delta_{s^2}^{top} \approx -0.92 \times 10^{-7} \text{GeV}^{-2} (M_t^2 - M_{t0}^2)$ <sup>[42]</sup> and accounts for the quadratic top mass dependence of  $\sin^2 \theta_W(M_Z) \equiv s^2(M_Z)$  in Ref. 40. Below  $M_Z$  the “true” decoupled QED coupling is related to  $\alpha(M_Z)$  via

$$\frac{1}{\alpha^-(M_Z)} = \frac{1}{\alpha(M_Z)} - \frac{8}{9\pi} \ln \frac{M_{t0}}{M_Z} - \frac{1}{6\pi} (1 + 21 \ln \frac{M_Z}{M_W}). \quad (4.2)$$

We also incorporate the mass thresholds of Ref. 13 to determine the relation between the running fermion masses defined in the effective  $SU(3) \times U(1)$  low energy theory and those above  $M_Z$ . The effect of these thresholds is quite small given the smallness of  $\alpha_2(M_Z) \approx 0.03$  and the Yukawa couplings of the light fermions. However these results did not account for a heavy top quark. Essentially the only modification of the results is the matching function for the bottom quark mass. By properly integrating out the charged Nambu-Goldstone bosons in Feynman gauge one obtains a dependence on the SM top Yukawa coupling,  $y_t^{SM}$  ( $y_i^{SM}(\mu) = m_i(\mu)/v$

where  $v = 174.104$  GeV and  $i$  runs over all SM fermions). The general result for all massive fermions lighter than the top quark is<sup>[13]</sup>

$$m_i^{low}(\mu) = m_i^{SM}(\mu)(1 + \Delta_{m_i}^{SM}) , \quad (4.3)$$

where

$$\Delta_{m_i}^{SM} = \frac{\alpha_2(\mu)}{8\pi c^2} \left( \left( -\frac{3}{4}(g_V^i)^2 + \frac{5}{4}(g_A^i)^2 \right) \left( \ln \frac{M_Z}{\mu} - \frac{1}{4} \right) + c^2 \left( \ln \frac{M_W}{\mu} - \frac{1}{4} \right) \right) , \quad (4.4)$$

for all but the bottom quark mass and  $c = \cos \theta_W$ . Here  $g_{V,A}^i = 2(g_L^i \pm g_R^i)$ , where  $g_{L,R}^i = T_{3L,R}^i - s^2 Q^i$  and  $T_{3L,R}^i$  and  $Q^i$  are the third component of weak isospin and the electric charge, respectively, for a given handedness of the  $i^{\text{th}}$  fermion. For the different quark and lepton charge sectors one has

$$\begin{aligned} g_A^\nu &= 1, & g_V^\nu &= 1, \\ g_A^e &= -1, & g_V^e &= -1 + 4s^2, \\ g_A^u &= 1, & g_V^u &= 1 - \frac{8}{3}s^2, \\ g_A^d &= -1, & g_V^d &= -1 + \frac{4}{3}s^2. \end{aligned} \quad (4.5)$$

For the case of the bottom mass one obtains

$$\begin{aligned} \Delta_b^{SM} &= \frac{\alpha_2(\mu)}{8\pi c^2} \left( \left( -\frac{3}{4}g_V^{d2} + \frac{5}{4} \right) \left( \ln \frac{M_Z}{\mu} - \frac{1}{4} \right) + c^2 |V_{tb}|^2 F_2(M_W^2, M_t^2) \right) \\ &\quad - \frac{(y_t^{SM})^2(\mu)}{16\pi^2} |V_{tb}|^2 \left( F_1(M_W^2, M_t^2) - \frac{1}{4} F_2(M_W^2, M_t^2) \right) , \end{aligned} \quad (4.6)$$

where the CKM matrix element  $|V_{tb}| \approx 1$  and  $F_{1,2}$  are defined in Appendix B. The term proportional to  $y_t^{SM}$  is dominant. For pole masses  $M_t$  up to 200 GeV this effect corresponds to a shift of  $m_b(M_Z)$  downwards by at most 0.6% from its value below  $M_Z$ .

The pole masses for the heavier quarks,  $M_q(q = c, b, t)$ , are determined by finding a consistent solution to the three loop relation

$$M_q = m_q(M_q) \left( 1 + \frac{4}{3} \frac{\alpha_s(M_q)}{\pi} + K_q \left( \frac{\alpha_s(M_q)}{\pi} \right)^2 \right), \quad (4.7)$$

where

$$K_q = 16.11 - 1.04 \sum_{M_i < M_q} \left( 1 - \frac{M_i}{M_q} \right), \quad (4.8)$$

with  $K_c = 13.3$  and  $K_b = 12.4$ .<sup>[43]</sup> In this analysis we will take the pole mass  $M_b$  in the range from 4.7 to 5.3 GeV. Using the three loop running of the strong coupling,  $\alpha_s$ ,<sup>1</sup> we find  $m_b(M_b) = 4.06, 4.24, 4.43, 4.61 \pm 0.08$  GeV and  $m_b(M_Z) = 2.81, 2.96, 3.11, 3.26 \pm 0.16$  GeV for  $M_b = 4.7, 4.9, 5.1, 5.3$  GeV, respectively, and we have included the uncertainty for the strong coupling  $\alpha_s(M_Z) = 0.120 \pm 0.007$ . The pole mass for the  $\tau$  lepton is given experimentally by  $M_\tau = 1.7771 \pm 0.0005$  GeV,<sup>[45]</sup> which, using the QED relation between the pole and running masses gives  $m_\tau(M_Z) = 1.7476 \pm 0.0006$  just below the electroweak threshold. With the loop effects of  $W$  and  $Z$  bosons included as in Eq. (4.4) one has  $m_\tau^+(M_Z) = 1.7494 \pm 0.0006$  just above the threshold.

The supersymmetric threshold is a potentially more important correction to to RG evolution of the couplings. It is sensitive to the details of the sparticle spectrum and in the case of the Yukawa coupling thresholds has quite different effects in different regions of parameter space. We shall first review the gauge thresholds and then give a simplified form for the Yukawa thresholds. The exact Yukawa coupling matching functions for the MSSM in the case of one light Higgs doublet are given in Appendix A.

The exact form of the matching functions for the gauge couplings at  $M_{SUSY}$  is well known. We will parametrize the gauge thresholds in terms of three mass

---

<sup>1</sup> We also include two loop QCD threshold effects<sup>[44]</sup> which, however, are negligible in the mass range of interest.

scales,<sup>[8]</sup>  $M_i$ . The general result for the gauge threshold matching conditions is

$$\frac{1}{\alpha_i^-(\mu)} = \frac{1}{\alpha_i^+(\mu)} - \Delta_i^{SU5Y}(\mu) - \Delta_i^{DR} , \quad (4.9)$$

where  $\alpha_i^\pm$  denotes the gauge couplings just above/below  $M_{SU5Y}$ . We convert from  $\overline{\text{MS}}$  to  $\overline{\text{DR}}$  couplings above  $M_{SU5Y}$  with the conversion factor given by  $\Delta_i^{DR} = -C_2(G_i)/12\pi$ , where the quadratic Casimir  $C_2(G)$  is  $N$  for  $SU(N)$  and 0 for  $U(1)$  groups. The matching functions are

$$\Delta_i^{SU5Y}(\mu) = \frac{1}{2\pi} \sum_p b_i^{(p)} \ln \frac{M_p}{\mu} , \quad (4.10)$$

where  $p$  runs over all sparticles integrated out near  $\mu \approx M_{SU5Y}$ . Here  $b_i^{(p)}$  is the contribution of sparticle  $p$  to the one loop coefficient  $b_i = (\frac{33}{5}, 1, -3)$ , ( $i = 1, 2, 3$ ) of the  $\beta$  function for  $g_i$  in the MSSM,

$$\beta_{g_i} = \frac{dg_i}{dt} = \frac{b_i}{16\pi^2} g_i^3 , \quad (4.11)$$

where  $t = \ln \mu$ . The cumulative effect of these thresholds can be parametrized in terms of mass scales  $M_i$  via

$$\Delta_i^{SU5Y}(\mu) = \frac{1}{2\pi} (b_i - b_i^{SM}) \ln \frac{M_i}{\mu} , \quad (4.12)$$

where  $b_i^{SM} = (\frac{41}{10}, -\frac{19}{6}, -7)$  are the corresponding coefficients in the SM and  $b_i - b_i^{SM} = (\frac{5}{2}, \frac{25}{6}, 4)$ . To get some idea of the dependence of the  $M_i$  on the sparticle spectrum we compute them for the case of separate degeneracies among squarks, sleptons, gauginos, higgsinos, and heavy Higgs particles:

$$\begin{aligned} M_1 &= m_{\tilde{\ell}}^{\frac{9}{25}} m_{\tilde{q}}^{\frac{11}{25}} m_{\tilde{H}}^{\frac{4}{25}} m_H^{\frac{1}{25}} , \\ M_2 &= m_{\tilde{\ell}}^{\frac{3}{25}} m_{\tilde{q}}^{\frac{9}{25}} m_{\tilde{H}}^{\frac{4}{25}} m_{\tilde{W}}^{\frac{8}{25}} m_H^{\frac{1}{25}} , \\ M_3 &= m_{\tilde{q}}^{\frac{1}{2}} m_{\tilde{g}}^{\frac{1}{2}} . \end{aligned} \quad (4.13)$$

The complete Yukawa thresholds at  $M_{SU5Y}$  are quite complicated, however we can give some indication of their form and estimate their effects. The most

tractable form useful for making estimates occurs in the limit of small gaugino-Higgsino mixing (see Eqs. (A.30)-(A32)) and is given by

$$\begin{aligned}
y_t^{SM}(\mu) &= y_t(\mu) \sin \beta (1 + \Delta_{y_t}^{SUSY}) , \\
y_b^{SM}(\mu) &= y_b(\mu) \cos \beta (1 + \Delta_{y_b}^{SUSY}) , \\
y_\tau^{SM}(\mu) &= y_\tau(\mu) \cos \beta (1 + \Delta_{y_\tau}^{SUSY}) ,
\end{aligned} \tag{4.14}$$

where

$$\begin{aligned}
16\pi^2 \Delta_{y_\tau}^{SUSY} &\simeq \frac{1}{4} y_\tau^2 \left( F_2(m_{\tilde{\nu}_\tau}^2, m_{\tilde{H}^\pm}^2) + \sum_i F_2(m_{\tilde{\tau}_i}^2, m_{\tilde{H}^0}^2) + \sin^2 \beta F_2(m_{\tilde{H}^\pm}^2, 0) \right) \\
&+ \frac{1}{2} g_2^2 \left( \mu_H \mathcal{M}_2 \tan \beta \sum_i (G_2(m_{\tilde{\tau}_i}^2, m_{\tilde{H}^0}^2, m_{\tilde{W}^3}^2) (O_{i1}^T)^2 \right. \\
&\quad \left. + G_2(m_{\tilde{\nu}_\tau}^2, m_{\tilde{H}^\pm}^2, m_{\tilde{W}^3}^2)) \right. \\
&\quad \left. - 2t^2 \mathcal{M}_1 (\mu_H \tan \beta + A_\tau) \sum_{i,j} G_2(m_{\tilde{B}}^2, m_{\tilde{\tau}_i}^2, m_{\tilde{\tau}_j}^2) (P'_{ij}(\tau))^2 \right) ,
\end{aligned} \tag{4.15}$$

$$\begin{aligned}
16\pi^2 \Delta_{y_b}^{SUSY} &\simeq \frac{8}{3} g_3^2 \left( -2m_{\tilde{g}} (\mu_H \tan \beta + A_b) \sum_{i,j} G_2(m_{\tilde{g}}^2, m_{\tilde{b}_i}^2, m_{\tilde{b}_j}^2) (P'_{ij}(b))^2 \right. \\
&\quad \left. + \frac{1}{4} \sum_i F_2(m_{\tilde{b}_i}^2, m_{\tilde{g}}^2) \right) \\
&+ y_t^2 \left( -2\mu_H \tan \beta \sum_{i,j} (m_t G_2(m_{\tilde{H}^\pm}^2, m_{\tilde{t}_i}^2, m_{\tilde{t}_j}^2) P'_{ij}(t) P_{ij}(t) \right. \\
&\quad \left. + (\mu_H \cot \beta + A_t) G_2(m_{\tilde{H}^\pm}^2, m_{\tilde{t}_i}^2, m_{\tilde{t}_j}^2) (P'_{ij}(t))^2 \right. \\
&\quad \left. + \frac{1}{4} \left( \sum_i F_2(m_{\tilde{t}_i}^2, m_{\tilde{H}^\pm}^2) (O_{i2}^t)^2 + \cos^2 \beta F_2(m_{\tilde{H}^\pm}^2, m_{\tilde{t}_i}^2) \right) \right) \tag{4.16} \\
&+ \frac{1}{4} y_b^2 \left( \sum_i F_2(m_{\tilde{t}_i}^2, m_{\tilde{H}^\pm}^2) (O_{i1}^t)^2 + \sum_i F_2(m_{\tilde{b}_i}^2, m_{\tilde{H}^0}^2) \right. \\
&\quad \left. + \sin^2 \beta F_2(m_{\tilde{H}^\pm}^2, m_{\tilde{t}_i}^2) \right) \\
&+ \frac{1}{2} g_2^2 \left( \mu_H \mathcal{M}_2 \tan \beta \sum_i (G_2(m_{\tilde{b}_i}^2, m_{\tilde{H}^0}^2, m_{\tilde{W}^3}^2) (O_{i1}^b)^2 \right. \\
&\quad \left. + G_2(m_{\tilde{t}_i}^2, m_{\tilde{H}^\pm}^2, m_{\tilde{W}^3}^2) (O_{i1}^t)^2 \right) ,
\end{aligned}$$

$$\begin{aligned}
16\pi^2 \Delta_{y_t}^{SUSY} \simeq & \frac{8}{3} g_3^2 \left( -2m_{\tilde{g}} \sum_{i,j} \left( m_t G_2(m_{\tilde{g}}^2, m_{\tilde{t}_i}^2, m_{\tilde{t}_j}^2) P'_{ij}(t) P_{ij}(t) \right. \right. \\
& + (\mu_H \cot \beta + A_t) G_2(m_{\tilde{g}}^2, m_{\tilde{t}_i}^2, m_{\tilde{t}_j}^2) (P'_{ij}(t))^2 \\
& \left. \left. + \frac{1}{4} \sum_i F_2(m_{\tilde{t}_i}^2, m_{\tilde{g}}^2) \right) \right. \\
& + \frac{1}{4} y_t^2 \left( \sum_i F_2(m_{\tilde{b}_i}^2, m_{\tilde{H}^\pm}^2) (O_{i1}^b)^2 + \sum_i F_2(m_{\tilde{t}_i}^2, m_{\tilde{H}^0}^2) \right. \\
& \left. \left. + \cos^2 \beta F_2(m_{\tilde{H}^\pm}^2, m_b^2) \right) \right. \\
& \left. + \frac{1}{4} y_b^2 \left( \sum_i F_2(m_{\tilde{b}_i}^2, m_{\tilde{H}^\pm}^2) (O_{i2}^b)^2 + \sin^2 \beta F_2(m_{\tilde{H}^\pm}^2, m_b^2) \right) \right), \tag{4.17}
\end{aligned}$$

where  $t = \tan \theta_W$ ,  $\mu_H$  is the supersymmetric Higgs mass parameter defined in Eq. (A.1) and  $A_{t,b,\tau}$  and  $\mathcal{M}_{1,2}$  are the soft supersymmetry breaking parameters defined in Eqs. (A.2). All parameters as well as the function  $F_2$  have an implicit dependence on the renormalization scale ( $\sim M_{SUSY}$ ) The function  $G_2$  is positive and is defined in Appendix B. The  $P$  matrices involve products of the squark and slepton mixing matrices  $O^{t,b,\tau}$  and are defined in Eqs. (A.3) and (A.22). Note that all terms proportional to the products  $PP'$  drop out in the limit of no squark or slepton mixing. To put these into perhaps more conventional notation in terms of the left-right squark and slepton mixing angles  $\theta_t$ ,  $\theta_b$  and  $\theta_\tau$  defined as in Eq. (A.3), use the general relations

$$\begin{aligned}
\sum_{i,j} G_2(m^2, m_{\tilde{q}_i}^2, m_{\tilde{q}_j}^2) P'_{ij}{}^2 &= \frac{1}{4} \sin^2 2\theta_q \left( G_2(m^2, m_{\tilde{q}_1}^2, m_{\tilde{q}_1}^2) + G_2(m^2, m_{\tilde{q}_2}^2, m_{\tilde{q}_2}^2) \right) \\
&+ \frac{1}{2} \cos^2 2\theta_q G_2(m^2, m_{\tilde{q}_1}^2, m_{\tilde{q}_2}^2), \tag{4.18} \\
\sum_{i,j} G_2(m^2, m_{\tilde{q}_i}^2, m_{\tilde{q}_j}^2) P'_{ij} P_{ij} &= \frac{1}{2} \sin 2\theta_q \left( G_2(m^2, m_{\tilde{q}_1}^2, m_{\tilde{q}_1}^2) - G_2(m^2, m_{\tilde{q}_2}^2, m_{\tilde{q}_2}^2) \right),
\end{aligned}$$

where  $q = t, b, \tau$ . The explicit form of these angles in terms of the superpotential and soft supersymmetry breaking parameters of Eqs. (A.1-2) can be found in Ref. 6, for example.

For small  $\tan\beta$  one may further neglect squark and slepton mixing except for the stop mixing effects. In this case the gluino contributions to the quark wavefunction renormalization and to the vertex diagrams of Fig. 1 give the dominant effect. Note that for  $\mu_H < 0$  one typically finds larger stop squark mixing, so that the threshold effect in  $y_t$  should be largest in that case.

At large  $\tan\beta$ , where the corrections to  $y_b$  and  $y_\tau$  tend to be more significant, the sbottom and stau mixing must be included. In this case enhancements proportional to  $\tan\beta$  occur from vertex graphs containing gluinos, charginos and neutralinos. The gluino contribution from Fig. 1 dominates the correction to  $y_b$  for large  $\tan\beta$ . The chargino and neutralino contributions of Fig. 2 are also large in this regime. Depending on the relative signs of  $\mu_H$  and  $A_t$ , the part of the finite diagram of Fig. 2 proportional to  $\mu_H A_t y_t^2 \tan\beta$  can either enhance or decrease the gluino contribution. The divergent wino exchange graph tends to depress the gluino contribution slightly. The enhanced  $y_\tau$  vertex corrections come from the order  $g_2^2 \tan\beta$  contributions of Fig. 3. In this case the bino exchange graph can be important due to the maximal hypercharge of the leptons. It is opposite in sign to wino and Higgsino vertex contributions. In analyzing the possible large  $\tan\beta$  enhancements, it is important to note that the sign of most of the relevant vertex contributions is controlled by the sign of  $\mu_H$  (or  $\mu_H$  and  $A_t$ ) and the various large contributions can appear with opposite sign. In addition, if we take  $M_{SUSY} \simeq M_Z$  then<sup>1</sup> the wavefunction renormalization contributions tend to be positive. In light of these facts a complete analysis is required. We will discuss the numerical significance of these thresholds in Section 7.

---

<sup>1</sup> The choice of  $M_{SUSY}$  is not important when the full threshold corrections are included since they incorporate the effects of one loop running between different effective supersymmetry scales.

## 5. Semi-Analytic Unification Analysis

We outline a semi-analytic analysis of gauge and Yukawa coupling unification. In particular, we discuss the solutions for  $M_{GUT}$ ,  $M_{H_3}$ , and  $m_t(M_Z)$  obtained when the  $\beta$  functions for the gauge and Yukawa couplings are integrated at the two and one loop level respectively. For the gauge couplings we must approximate the two loop Yukawa coupling effects and for the Yukawa couplings we can give only approximate solutions to the one loop  $\beta$  functions. We then look at the effect of the one loop threshold matching functions on these solutions. This of course can only give some idea of the dependencies of these masses on other parameters since a full analysis with one loop thresholds requires integration of the two loop  $\beta$  functions. The full numerical analysis will be given in Section 7.

We use the condition of gauge coupling unification to determine part of the GUT scale spectrum from deviations from the naive unification condition. Threshold conditions at the GUT scale relate the mismatch of the gauge couplings to masses of superheavy particles. At the two loop level we shall consider the scenario, earlier considered in Ref. 33, in which one predicts  $M_{H_3}$ ,  $M_{GUT} = (M_V^2 M_\Sigma)^{\frac{1}{3}}$  and the coupling constant at the GUT scale,  $\alpha_G$ , for fixed  $\alpha$ ,  $\sin^2 \theta_W$  and  $\alpha_s$  at  $M_Z$ . This scenario, which at one loop essentially reduces to determining the effective scale  $M_{SUSY}$  rather than  $M_{H_3}$ , is sensitive to the large  $\alpha_s$  error bars as well as boundary corrections at  $M_Z$  and  $M_{SUSY}$ , particularly since  $M_{H_3}$  itself only appears in threshold matching functions.

We also consider the implication of the Yukawa coupling thresholds derived in Sections 3 and 4 to the minimal SU(5) prediction  $y_b(M_{GUT}) = y_\tau(M_{GUT})$ . One may either fix  $M_t$  to predict the pole mass  $M_b$  (or the running mass  $m_b(M_Z)$ ) or use the accepted range of allowed  $M_b$  values to predict  $M_t$  (or  $m_t(M_Z)$ ). In the former case the threshold corrections are straightforward to estimate and constitute a significant correction to  $M_b$  which should be included into the analysis of Ref. 8 (These Yukawa corrections essentially belong to their correction parameter  $\rho_F$ ). In the latter case the analysis is more difficult and must be done numerically,

however we will see how both the gauge and Yukawa coupling thresholds filter into a semi-analytic expression for  $m_t(M_Z)$ .

In the first approximation  $M_{GUT}$ ,  $M_{H_3}$  and  $\alpha_G$  are determined entirely by gauge coupling unification. They depend on  $M_t$  only through two loop effects in the gauge running and through threshold effects, primarily at the weak scale. The solutions to the two loop gauge coupling  $\beta$  functions generalizing Eq. (4.11) are

$$\frac{1}{\alpha_i(M_Z)} = \frac{1}{\alpha_G} + \frac{(b_i^{SM} - b_i)}{2\pi} \ln \frac{M_{SUSY}}{M_Z} + \frac{b_i}{2\pi} \ln \frac{M_{GUT}}{M_Z} + \theta_i - \Delta_i, \quad (5.1)$$

where  $\Delta_i = \Delta_i^{SM} + \Delta_i^{SUSY} + \Delta_i^{GUT}$  and the  $\theta_i$  are the two loop contributions, including the effects of the top Yukawa coupling. By utilizing the threshold corrections given in Eqs. (3.12), (3.13), (4.1), (4.9) and (4.12), one obtains the solutions

$$\begin{aligned} t_G &= \ln \frac{M_{GUT}}{M_Z} = t_G^0 + \Delta_{t_G}, \\ t_H &= \ln \frac{M_{H_3}}{M_Z} = t_H^0 + \Delta_{t_H}, \\ \frac{1}{\alpha_G} &= \frac{1}{\alpha_G^0} + \Delta_{\alpha_G}, \end{aligned} \quad (5.2)$$

where the naive one loop results are

$$\begin{aligned} t_G^0 &= \frac{\pi}{6} \left( \frac{1 - 2s^2}{\alpha} - \frac{2}{3} \frac{1}{\alpha_s} \right) - \frac{2}{9} \ln \frac{M_{SUSY}}{M_Z}, \\ t_H^0 &= \frac{\pi}{2} \left( \frac{-1 + 6s^2}{\alpha} - \frac{10}{3\alpha_s} \right) + \frac{5}{6} \ln \frac{M_{SUSY}}{M_Z}, \\ \frac{1}{\alpha_G^0} &= \frac{-1 + 14s^2}{12\alpha} + \frac{1}{18\alpha_s} + \frac{79}{36\pi} \ln \frac{M_{SUSY}}{M_Z}, \end{aligned} \quad (5.3)$$

and the threshold and two loop correction terms are

$$\begin{aligned} \Delta_{t_G} &= -\frac{2}{9} \ln \frac{U_{SUSY}}{M_{SUSY}} + \delta_{t_G}^{SM} + \delta_{t_G}^{\overline{DR}} - \frac{\pi}{18} (5\theta_1 - 3\theta_2 - 2\theta_3), \\ \Delta_{t_H} &= \frac{5}{6} \ln \frac{V_{SUSY}}{M_{SUSY}} + \delta_{t_H}^{SM} - \frac{5\pi}{6} (-\theta_1 + 3\theta_2 - 2\theta_3), \\ \Delta_{\alpha_G} &= \frac{79}{36\pi} \ln \frac{W_{SUSY}}{M_{SUSY}} + \delta_{\alpha_G}^{SM} + \delta_{\alpha_G}^{\overline{DR}} + \delta_{\alpha_G}^{GUT} + \frac{1}{36} (-5\theta_1 + 39\theta_2 + 2\theta_3), \end{aligned} \quad (5.4)$$

where  $s = \sin \theta_W$ ,  $\delta_{t_G}^{\overline{DR}} = \frac{1}{18}$  and  $\delta_{\alpha_G}^{\overline{DR}} = -\frac{7}{36\pi}$ . We will use superscript 0's to denote

the one loop results which use a naive step approximation to the thresholds. In the above all low scale parameters are implicitly evaluated at  $M_Z$ . Note that the two loop contribution of the top Yukawa drops out of the solution for  $M_{GUT}$  while if we estimate constant  $y_t \approx 1$  then this effect changes  $t_H$  by of order  $\frac{1}{8\pi^2} y_t^2 t_G \approx 0.4$  and  $1/\alpha_G$  by  $\frac{3}{16\pi^3} y_t^2 t_G \approx 0.2$ , respectively.

The weak scale threshold corrections are

$$\begin{aligned}
\delta_{t_G}^{SM} &= \delta_{t_G}^{top;s^2} + \delta_{t_G}^{top;\alpha} + \delta_{t_G}^{top;\alpha_s} \\
&= -\frac{\pi}{3} \frac{\Delta_{s^2}^{top}}{\alpha} + \frac{4}{27} (1 - 2s^2) \ln \frac{M_t}{M_{t0}} - \frac{1}{27} \ln \frac{M_t}{M_Z} , \\
\delta_{t_H}^{SM} &= \delta_{t_H}^{top;s^2} + \delta_{t_H}^{top;\alpha} + \delta_{t_H}^{top;\alpha_s} \\
&= 3\pi \frac{\Delta_{s^2}^{top}}{\alpha} + \frac{4}{9} (-1 + 6s^2) \ln \frac{M_t}{M_{t0}} - \frac{5}{9} \ln \frac{M_t}{M_Z} , \\
\delta_{\alpha_G^{-1}}^{SM} &= \delta_{\alpha_G^{-1}}^{top;s^2} + \delta_{\alpha_G^{-1}}^{top;\alpha} + \delta_{\alpha_G^{-1}}^{top;\alpha_s} \\
&= \frac{7}{6} \frac{\Delta_{s^2}^{top}}{\alpha} + \frac{2}{27\pi} (-1 + 14s^2) \ln \frac{M_t}{M_{t0}} + \frac{1}{54\pi} \ln \frac{M_t}{M_Z} .
\end{aligned} \tag{5.5}$$

The residual GUT threshold due to the undetermined value of  $M_V$  is

$$\delta_{\alpha_G^{-1}}^{GUT} = -\frac{5}{\pi} \ln \frac{M_V}{M_{GUT}} = -\frac{5}{3\pi} \ln \frac{M_V}{M_\Sigma} . \tag{5.6}$$

The three effective scales replacing the naive scale  $M_{SUSY}$  are

$$\begin{aligned}
U_{SUSY} &= M_1^{-\frac{25}{16}} M_2^{\frac{25}{16}} M_3 \simeq \left( \frac{m_{\tilde{q}}}{m_{\tilde{\ell}}} \right)^{\frac{3}{8}} m_{\tilde{W}}^{\frac{1}{2}} m_{\tilde{g}}^{\frac{1}{2}} , \\
V_{SUSY} &= M_1^{-\frac{5}{4}} M_2^{\frac{25}{4}} M_3^{-4} \simeq \left( \frac{m_{\tilde{\ell}}}{m_{\tilde{q}}} \right)^{\frac{3}{10}} \left( \frac{m_{\tilde{W}}}{m_{\tilde{g}}} \right)^2 m_{\tilde{H}}^{\frac{1}{5}} m_{\tilde{H}}^{\frac{4}{5}} , \\
W_{SUSY} &= M_1^{-\frac{25}{316}} M_2^{\frac{325}{316}} M_3^{\frac{4}{79}} \simeq \left( \frac{m_{\tilde{\ell}}}{m_{\tilde{q}}} \right)^{\frac{15}{158}} m_{\tilde{q}}^{\frac{36}{79}} m_{\tilde{W}}^{\frac{26}{79}} m_{\tilde{H}}^{\frac{12}{79}} m_{\tilde{H}}^{\frac{3}{79}} m_{\tilde{g}}^{\frac{2}{79}} .
\end{aligned} \tag{5.7}$$

We can approximate a range for these effective scales in the context of the canonical soft breaking of supersymmetry induced from a hidden sector of  $N=1$  supergravity. In this case there is a common  $SU(5)$  invariant gaugino mass  $M_{\frac{1}{2}}$ , a common soft

supersymmetry breaking scalar mass  $M_0$  and a common trilinear scalar coupling  $A$  (see Eq. (A.2)) at  $M_{GUT}$ . Then there is a simple one loop relation between the gaugino masses:

$$\frac{m_{\tilde{W}}}{m_{\tilde{g}}} = \frac{\alpha_2(M_{SUSY})}{\alpha_3(M_{SUSY})} \approx 0.28 . \quad (5.8)$$

Assuming  $m_{\tilde{\ell}} \simeq m_{\tilde{q}}$  we obtain the approximate relations

$$U_{SUSY} \approx 0.53 m_{\tilde{g}} , \quad V_{SUSY} \approx 0.08 m_H^{\frac{1}{5}} m_{\tilde{H}}^{\frac{4}{5}} , \quad W_{SUSY} \approx m_{\tilde{q}}^{\frac{1}{2}} m_{\tilde{W}}^{\frac{1}{3}} m_{\tilde{H}}^{\frac{1}{6}} . \quad (5.9)$$

Alternatively, in the no-scale supergravity case ( $M_0 = A = 0$ ) one has  $m_{\tilde{q}} \simeq m_{\tilde{g}} \simeq 3m_{\tilde{W}} \simeq 3m_{\tilde{\ell}}$ . We then have instead the approximate relations

$$U_{SUSY} \approx 0.80 m_{\tilde{g}} , \quad V_{SUSY} \approx 0.06 m_H^{\frac{1}{5}} m_{\tilde{H}}^{\frac{4}{5}} , \quad W_{SUSY} \approx 0.70 m_{\tilde{g}}^{\frac{5}{6}} m_{\tilde{H}}^{\frac{1}{6}} . \quad (5.10)$$

As pointed out in Ref. 33, the supersymmetric threshold corrections to  $M_{GUT}$  depend mainly on the wino and gluino masses while  $M_{H_3}$  is most sensitive to the Higgsino mass. The corrections to  $\alpha_G$  depend mainly on  $M_2$  and are most sensitive to the squark masses. If we allow a range of 100 – 1000 GeV for  $m_H$  and  $m_{\tilde{H}}$  while the gluino mass is taken to range between 120 – 1000 GeV,<sup>1</sup> then for degenerate squarks and sleptons  $64 \lesssim U_{SUSY} \lesssim 530$  GeV and  $8 \lesssim V_{SUSY} \lesssim 80$  GeV, and bear little relation to the naive  $M_Z \lesssim M_{SUSY} \lesssim 1$  TeV. We also take  $100 \lesssim W_{SUSY} \sim M_2 \lesssim 700$  GeV in this case. Note that the approximate upper limit on the sparticle masses of 1 TeV is the generic order of magnitude expectation if supersymmetry is to avoid introducing a new low scale hierarchy problem. In the no-scale case the corresponding limits are  $96 \lesssim U_{SUSY} \lesssim 800$  GeV,  $6 \lesssim V_{SUSY} \lesssim 60$  GeV, and  $73 \lesssim W_{SUSY} \sim M_2 \lesssim 630$  GeV.

---

<sup>1</sup> The lower limit on the gluino mass is near the experimental lower bound<sup>[46]</sup> if the light gluino window is closed.

Before turning to the  $M_t$  solution we give an estimate of the relative importance of the different corrections to  $t_G$  and  $t_H$ . The relevant low energy parameters are<sup>[40,47]</sup>

$$\begin{aligned}
M_Z &= 91.187 \pm 0.007 \text{ GeV} , \\
\alpha^{-1}(M_Z) &= 127.9 \pm 0.1 , \\
\alpha_s(M_Z) &= 0.120 \pm 0.007 , \\
s_0^2 &= 0.2324 \pm 0.0003 ,
\end{aligned}
\tag{5.11}$$

where, as in Ref. 41, we denote by  $s_0$  the sine of the Weinberg angle for a central value of  $M_{t0} = 143$  GeV with the quadratic top mass uncertainty removed and treated as a threshold correction as discussed in the previous section. The current best fit value of  $\alpha_s$  from LEP and all collider and neutrino experiments is  $\alpha_s = 0.120 \pm 0.006 \pm 0.002$ <sup>[47]</sup> where the second set of error bars corresponds to a SM Higgs mass in the range  $60 < m_h < 1000$  GeV and we have included a conservative error in (5.11).

For central values of the parameters the one loop solutions are  $t_G^0 = 32.9$  corresponding to  $M_{GUT}^0 = 1.83 \times 10^{16}$  GeV and  $1/\alpha_G^0 = 24.5$  for  $M_{SUSY} = M_Z$ . We should note that the one loop solution,  $M_{H_3}^0$  given in Eq. (5.2), is only a definition and is related to the scenario in which the effective scale  $M_{SUSY}$  is determined by the requirement of gauge coupling unification. We may write

$$\begin{aligned}
t_{HX} = \ln \frac{M_{H_3}}{M_{GUT}} &= \ln \frac{M_{H_3}^0}{M_{GUT}^0} + \frac{19}{18} \ln \frac{T_{SUSY}}{M_{SUSY}} \\
&+ \frac{2\pi}{9} (5\theta_1 - 12\theta_2 + 7\theta_3) + \delta_{t_{HX}}^{SM} + \delta_{t_{HX}}^{\overline{DR}} ,
\end{aligned}
\tag{5.12}$$

where

$$\ln \frac{M_{H_3}^0}{M_{GUT}^0} = \frac{19}{18} \ln \frac{M_{SUSY}}{M_{SUSY}^0} = -\frac{2\pi}{9} \left( \frac{3(1-5s^2)}{\alpha} + \frac{7}{\alpha_s} \right) + \frac{19}{18} \ln \frac{M_{SUSY}}{M_Z} , \tag{5.13}$$

and  $M_{SUSY}^0$ , the naive one loop value required for gauge unification, is 79.2, 7.3, 0.9 GeV for  $\alpha_s(M_Z) = 0.113, 0.120, 0.127$ , respectively. The scale  $T_{SUSY} =$

$M_1^{-\frac{25}{19}} M_2^{\frac{100}{19}} M_3^{-\frac{56}{19}}$ , using the notation of Ref. 48. For  $M_{SUSY} = M_Z$  this gives  $M_{H_3}^0 \approx 2.6 \times 10^{17}$  GeV for  $\alpha_s(M_Z) = 0.120$ , however,  $M_{H_3}$  can only be reliably determined at the two loop level.

Next we quantify the correction terms to these naive estimates. The current experimental limit on the top quark mass from fits to electroweak data is  $M_t = 164_{-17-21}^{+16+18}$  GeV,<sup>[47]</sup> where the central value is for a Higgs mass of 300 GeV and the second set of error bars corresponds to  $60 < m_h < 1000$  GeV. In the MSSM a range  $50 < m_h < 150$  GeV is more appropriate, giving  $M_t = 143_{-19-8}^{+17+6}$  GeV.<sup>[42]</sup> The current lower limit from the  $D\emptyset$  experiment is  $M_t > 131$  GeV (95% C.L.).<sup>[49]</sup> We will allow  $M_t$  to range from 130 to 200 GeV, and obtain the following ranges for the top dependent electroweak corrections:

$$\begin{aligned}
\delta_{t_G}^{top;s^2} &= (-0.04, 0.24) & \delta_{t_G}^{top;\alpha} &= (-0.008, 0.03) & \delta_{t_G}^{top;\alpha_s} &= (-0.013, -0.03) , \\
\delta_{t_H}^{top;s^2} &= (.39, -2.2) & \delta_{t_H}^{top;\alpha} &= (-0.02, 0.06) & \delta_{t_H}^{top;\alpha_s} &= (-0.20, -0.44) , \\
\delta_{\alpha_G^{-1}}^{top;s^2} &= (0.05, -0.27) & \delta_{\alpha_G^{-1}}^{top;\alpha} &= (-0.005, 0.02) & \delta_{\alpha_G^{-1}}^{top;\alpha_s} &= (0.002, 0.005) ,
\end{aligned} \tag{5.14}$$

where the first(second) entries are for the lower(upper) limit for  $M_t$ . The influences of corrections from thresholds, two loop terms and the experimental error bars in (5.11) are summarized in Table 1. The top dependent thresholds in (5.14) are summed together with  $\overline{DR}$  conversion factors in the SM threshold entries for the above range of  $M_t$  values. The MSSM threshold entries include the supersymmetric threshold as well as the effect of running SM parameters from  $M_Z$  to  $M_{SUSY}$  for the previously mentioned ranges taken for  $U_{SUSY}$ ,  $V_{SUSY}$  and  $W_{SUSY}$ . The upper range corresponds to the degenerate squark-slepton case while the lower entry is for the no-scale case. The  $\alpha_s$  error bar entries are given first for the lower, then the upper limit on  $\alpha_s$ . The percent deviations given are relative to the naive one loop predictions given above. We see that  $M_{H_3}$  decreases with increasing  $M_t$  and increases with increasing  $\alpha_s$  and Higgsino mass ( $V_{SUSY}$ ). The effective GUT scale increases with increasing  $M_t$  and  $\alpha_s$  and decreases with increasing gluino mass

( $U_{SUSY}$ ). The magnitude of the effect on  $M_{GUT}$  due to each of these parameters is comparable, ranging up to 40%.

Correction	Parameter Variations			% Deviations		
	$\delta_{t_G}$	$\delta_{t_H}$	$\delta\alpha_G^{-1}$	$M_{GUT}$	$M_{H_3}$	$\frac{1}{\alpha_G}$
SM (top) threshold	(+0.008, +0.35)	(+.06, -3.0)	(-0.03, -0.36)	(0.8, 41)	(6, -95)	(-0.1, -1.5)
MSSM threshold	(+0.08, -0.39) (-0.01, -0.48)	(-2.0, -.11) (-2.3, -.35)	(+0.07, +1.6) (-0.17, +1.5)	( 8, -32) (-1, -38)	(-86, -10) (-90, -30)	( 0.3, 6.5) (-0.7, 6.1)
$s_0^2$ error bar	$\pm 0.04$	$\pm 0.36$	$\pm 0.05$	$\pm 4$	(-30, 43)	$\pm 0.2$
$\alpha$ error bar	$\pm 0.03$	$\pm 0.06$	$\pm 0.02$	$\pm 3$	$\pm 6$	$\pm 0.1$
$\alpha_s$ error bar	(-0.19, +0.17)	(-2.8, +2.5)	(+0.03, -0.03)	(-17, 18.5)	(-94, +1120)	$\pm 0.1$
two loop ( $y_t = 0$ )	0.18	-3.8	1.1	20	-98	4.4
two loop ( $y_t$ only)	0	0.4	0.2	0	49	1

Table 1. Corrections to  $M_{GUT}$ ,  $M_{H_3}$  and  $1/\alpha_G$ .

Note that the  $\Delta_{s_2}^{top}$  correction dominates the SM threshold effects and, as expected, the ‘‘correction’’ terms for  $M_{H_3}$  can be large. The  $\alpha_s$  error bar correction is the largest, changing  $M_{H_3}$  over three orders of magnitude. The MSSM threshold correction to  $M_{H_3}$  was included in the analysis of Ref. 33, but the top dependent SM threshold was not discussed. These two effects can be comparable in magnitude, with the SM effects changing  $M_{H_3}$  by up to two orders of magnitude, corresponding to a change in the proton decay lifetime of four orders of magnitude. Clearly, when we also solve for  $M_t$  from the condition of Yukawa unification, the solution for  $M_{H_3}$  will be substantially correlated with the  $M_t$  solution. The tendency to predict large values of  $M_t$  means that the effect of the SM threshold will generally be to depress  $M_{H_3}$ . As we shall see in Section 6, the opposite is true for the lower bound on  $M_{H_3}$  from proton decay. The combination of these results may be useful in strengthening proton decay constraints on the parameter space.<sup>[50]</sup>

We next turn to the Yukawa unification predictions for either  $M_t$  or  $m_b(M_Z)$ . We discuss both cases with emphasis on the former. The one loop  $\beta$  functions

for the Yukawa couplings are not solvable analytically, however we shall give some semi-analytic solutions. The one loop Yukawa  $\beta$  functions for the third generation in the MSSM are

$$\beta_{y_\alpha} = \frac{dy_\alpha}{dt} = \frac{y_\alpha}{16\pi^2}(-c_{\alpha i}g_i^2 + b_{\alpha\beta}y_\beta^2), \quad (5.15)$$

where  $\alpha = (t, b, \tau)$  and  $b_{\alpha\beta}$  and  $c_{\alpha i}$  are given by the matrices

$$\begin{pmatrix} 6 & 1 & 0 \\ 1 & 6 & 1 \\ 0 & 3 & 4 \end{pmatrix} \text{ and } \begin{pmatrix} \frac{13}{15} & 3 & \frac{16}{3} \\ \frac{7}{15} & 3 & \frac{16}{3} \\ \frac{9}{5} & 3 & 0 \end{pmatrix}, \quad (5.16)$$

respectively. The analogous matrices in the SM,  $b_{\alpha\beta}^{SM}$  and  $c_{\alpha i}^{SM}$ , are given by

$$\begin{pmatrix} \frac{9}{2} & \frac{3}{2} & 1 \\ \frac{3}{2} & \frac{9}{2} & 1 \\ 3 & 3 & \frac{9}{2} \end{pmatrix} \text{ and } \begin{pmatrix} \frac{17}{20} & \frac{9}{4} & 8 \\ \frac{1}{4} & \frac{9}{4} & 8 \\ \frac{9}{4} & \frac{9}{4} & 0 \end{pmatrix}, \quad (5.17)$$

respectively. At one loop, in the naive step approximation, the SM Yukawa couplings are matched to those in the MSSM at  $M_{SUSY}$  via  $y_t = y_t^{SM}/\sin\beta$ ,  $y_b = y_b^{SM}/\cos\beta$  and  $y_\tau = y_\tau^{SM}/\cos\beta$ , where  $\tan\beta = \frac{v_2}{v_1}$  is the ratio of the VEVs of the two Higgs doublets  $H_1$  and  $H_2$  in the MSSM (see Appendix A). Using Eqs. (5.15), the one loop solution for  $m_b/m_\tau$  at  $M_Z$  can be written as

$$\frac{m_b^0(M_Z)}{m_\tau^0(M_Z)} = A_{b/\tau}^{0SM} A_{b/\tau}^0 B_t^{0SM - \frac{3}{2}} B_b^{0SM \frac{3}{2}} B_\tau^{0SM - \frac{7}{2}} B_t^0 \left(\frac{B_b^0}{B_\tau^0}\right)^3, \quad (5.18)$$

where

$$\begin{aligned} A_{b/\tau}^{0SM} &= \left(\frac{\alpha_1^0(M_{SUSY})}{\alpha_1^0(M_Z)}\right)^{-\frac{10}{41}} \left(\frac{\alpha_3^0(M_{SUSY})}{\alpha_3^0(M_Z)}\right)^{-\frac{4}{7}}, \\ A_{b/\tau}^0 &= \left(\frac{\alpha_G^0}{\alpha_1^0(M_{SUSY})}\right)^{-\frac{10}{99}} \left(\frac{\alpha_G^0}{\alpha_3^0(M_{SUSY})}\right)^{-\frac{8}{9}}, \end{aligned} \quad (5.19)$$

and

$$\begin{aligned}
B_\alpha^{0SM}(M_Z, M_{SUSY}) &= \exp\left(-\frac{1}{16\pi^2} \int_{t_z}^{t_s} dt (y_\alpha^{0SM})^2\right), \\
B_\alpha^0(M_{SUSY}, M_{GUT}^0) &= \exp\left(-\frac{1}{16\pi^2} \int_{t_s}^{t_G^0} dt (y_\alpha^0)^2\right).
\end{aligned} \tag{5.20}$$

Here the parameters  $t_s = \ln \frac{M_{SUSY}}{M_Z}$ ,  $t_z = 1$  and  $t_G^0$  is given in Eq. (5.3). On the other hand the full two loop solution including the Yukawa thresholds of Sections 3 and 4 is

$$\begin{aligned}
\frac{m_b(M_Z)}{m_\tau(M_Z)} &= A_{b/\tau}^{SM} A_{b/\tau} B_t^{SM-\frac{3}{2}} B_b^{SM\frac{3}{2}} B_\tau^{SM-\frac{7}{2}} B_t \left(\frac{B_b}{B_\tau}\right)^3 \Theta_{b/\tau} \\
&\times (1 + \Delta_{b/\tau}^{SM} + \Delta_{b/\tau}^{SUSY} + \Delta_{b/\tau}^{GUT}),
\end{aligned} \tag{5.21}$$

where

$$\begin{aligned}
A_{b/\tau}^{SM} &= \left(\frac{\alpha_1^-(M_{SUSY})}{\alpha_1^+(M_Z)}\right)^{-\frac{10}{41}} \left(\frac{\alpha_3^-(M_{SUSY})}{\alpha_3^+(M_Z)}\right)^{-\frac{4}{7}}, \\
A_{b/\tau} &= \left(\frac{\alpha_1^-(M_{GUT})}{\alpha_1^+(M_{SUSY})}\right)^{-\frac{10}{99}} \left(\frac{\alpha_3^-(M_{GUT})}{\alpha_3^+(M_{SUSY})}\right)^{-\frac{8}{9}},
\end{aligned} \tag{5.22}$$

and

$$\begin{aligned}
B_\alpha^{SM}(M_Z^+, M_{SUSY}^-) &= \exp\left(-\frac{1}{16\pi^2} \int_{t_z^+}^{t_s^-} dt (y_\alpha^{SM})^2\right), \\
B_\alpha(M_{SUSY}^+, M_{GUT}^-) &= \exp\left(-\frac{1}{16\pi^2} \int_{t_s^+}^{t_G^-} dt (y_\alpha)^2\right).
\end{aligned} \tag{5.23}$$

The thresholds corrections  $\Delta_{b/\tau}$  are contained in Eqs. (3.11), (4.6) and (4.15) - (4.17). The two loop corrections are contained in  $\Theta_{b/\tau}$  which we will take to be unity in this section. The  $\pm$  superscripts indicate parameters just above/below the scale at which they are evaluated, *i.e.* on either side of the threshold boundary. We call the threshold corrections  $\Delta_{b/\tau}$  in (5.21) the direct threshold corrections. There

are also indirect threshold corrections which arise in rewriting the the quantities in (5.22) and (5.23) in terms of the naive one loop results. The discontinuities in the other parameters at the threshold boundaries indirectly filter into the result for  $m_b/m_\tau$ . These indirect threshold effects will primarily involve the gauge coupling thresholds.

For the indirect threshold effects in the  $A_{b/\tau}$  parameters we find

$$\begin{aligned} A_{b/\tau}^{SM} &= A_{b/\tau}^0 (1 + \Delta_{b/\tau}^{\alpha SM}) , \\ A_{b/\tau} &= A_{b/\tau}^0 (1 + \Delta_{b/\tau}^\alpha) , \end{aligned} \quad (5.24)$$

where

$$\begin{aligned} 1 + \Delta_{b/\tau}^{\alpha SM} &= \left( \frac{1 + \alpha_1^0(M_Z)\Delta_1^{SM}}{1 + \alpha_1^0(M_{SUSY})\Delta_1^{SM}} \right)^{-\frac{10}{41}} \left( \frac{1 + \alpha_s^0(M_Z)\Delta_3^{SM}}{1 + \alpha_3^0(M_{SUSY})\Delta_3^{SM}} \right)^{-\frac{4}{7}} , \\ 1 + \Delta_{b/\tau}^\alpha &= \left( \frac{1 + \alpha_1^0(M_{SUSY})(\Delta_1^{SM} + \Delta_1^{SUSY})}{1 + \alpha_G^0(\Delta_{\alpha_G} - \Delta_1^{GUT}(M_{GUT}))} \right)^{-\frac{10}{99}} \\ &\quad \times \left( \frac{1 + \alpha_3^0(M_{SUSY})(\Delta_3^{SM} + \Delta_3^{SUSY} + \Delta_3^{DR})}{1 + \alpha_G^0(\Delta_{\alpha_G} - \Delta_3^{GUT}(M_{GUT}))} \right)^{-\frac{8}{9}} . \end{aligned} \quad (5.25)$$

Later we will also need

$$A_t^{SM} = A_t^0 (1 + \Delta_t^{\alpha SM}) , \quad (5.26)$$

where

$$A_t^0 = \left( \frac{\alpha_1^0(M_{SUSY})}{\alpha_1^0(M_Z)} \right)^{\frac{17}{164}} \left( \frac{\alpha_2^0(M_{SUSY})}{\alpha_2^0(M_Z)} \right)^{-\frac{27}{76}} \left( \frac{\alpha_3^0(M_{SUSY})}{\alpha_3^0(M_Z)} \right)^{-\frac{4}{7}} , \quad (5.27)$$

and

$$\begin{aligned} 1 + \Delta_t^{\alpha SM} &= \left( \frac{1 + \alpha_1^0(M_Z)\Delta_1^{SM}}{1 + \alpha_1^0(M_{SUSY})\Delta_1^{SM}} \right)^{\frac{17}{164}} \left( \frac{1 + \alpha_2^0(M_Z)\Delta_1^{SM}}{1 + \alpha_2^0(M_{SUSY})\Delta_1^{SM}} \right)^{-\frac{27}{76}} \\ &\quad \times \left( \frac{1 + \alpha_3^0(M_Z)\Delta_1^{SM}}{1 + \alpha_3^0(M_{SUSY})\Delta_1^{SM}} \right)^{-\frac{4}{7}} . \end{aligned} \quad (5.28)$$

The threshold correction to  $\alpha_G$  is given in Eq. (5.4). In the expressions for  $\Delta_i^{GUT}$  of Eq. (3.13) we shall insert the one loop expressions for  $\ln M_{H_3}/M_{GUT}$  given in

Eq. (5.13), consistent with the scenario considered here. Note that terms proportional to  $\ln M_V/M_{GUT}$  cancel in the differences  $\Delta_{\alpha_G} - \Delta_i^{GUT}$  so that these threshold corrections are computable given the sparticle spectrum. In all cases we find that  $\Delta_{b/\tau}^{\alpha SM}$  and  $\Delta_t^{\alpha SM}$  are negligible ( $\lesssim 0.1\%$  for  $M_{SUSY}$  up to 1 TeV) due to the absence of large logarithms.

The indirect threshold corrections to the  $B$  parameters are primarily of second order compared to the direct thresholds in Eq. (5.21) and are more difficult to estimate analytically. However, one can account simply for the threshold effects in  $t_G$  given in Eq. (5.4). We may write

$$B_\alpha \approx B_\alpha^0 \left( 1 - \frac{1}{16\pi^2} \Delta_{t_G} \bar{y}_\alpha^2 \right), \quad (5.29)$$

although the full corrections should be computed numerically. The threshold corrections to the  $B^{SM}$  can be neglected. We can now rewrite Eq. (5.21) in terms of the naive one loop result

$$\begin{aligned} \frac{m_b(M_Z)}{m_\tau(M_Z)} &\approx \frac{m_b^0(M_Z)}{m_\tau^0(M_Z)} \Theta_{b/\tau} (1 + \Delta_{b/\tau}^{SM} + \Delta_{b/\tau}^{SUSY} + \Delta_{b/\tau}^{GUT} \\ &\quad + \Delta_{b/\tau}^{\alpha SM} + \Delta_{b/\tau}^\alpha - \frac{1}{16\pi^2} \Delta_{t_G} (\bar{y}_t^2 + 3\bar{y}_b^2 - 3\bar{y}_\tau^2)). \end{aligned} \quad (5.30)$$

This may be used to determine  $m_b(M_Z)$  using the Yukawa unification condition. However it is important to note that such a solution will be sensitive to potentially large threshold corrections both at  $M_{SUSY}$  and  $M_{GUT}$ , the former occurring for large  $\tan \beta$  and the latter occurring for large allowed splittings  $M_V \gg M_\Sigma$  or  $M_{H_3} \gg M_{GUT}$  and large  $\bar{y}_t$  (see Sections 3 and 4). We shall discuss these corrections further in Section 7.

We focus instead on using Eq. (5.21) to solve for  $m_t(M_Z)$ . Here we use a good approximate analytic solution for  $y_t$  for small to moderate  $\tan \beta$  (see also Ref. 51).

$$B_t(M_{SUSY}^+, M_{GUT}^-) \simeq (1 - y_t^2(M_{SUSY}^+) K_t(M_{SUSY}^+, M_{GUT}^-))^{\frac{1}{12}}, \quad (5.31)$$

where

$$K_t(M_{SUSY}^+, M_{GUT}^-) = \frac{3}{4\pi^2} \int_{t_s^+}^{t_G^-} dt A_t^{-2}(t_s, t) , \quad (5.32)$$

and

$$A_t(t_s^+, t_G^-) = \left( \frac{\alpha_1^-(M_{GUT})}{\alpha_1^+(M_{SUSY})} \right)^{\frac{13}{198}} \left( \frac{\alpha_2^-(M_{GUT})}{\alpha_2^+(M_{SUSY})} \right)^{\frac{3}{2}} \left( \frac{\alpha_3^-(M_{GUT})}{\alpha_3^+(M_{SUSY})} \right)^{-\frac{8}{9}} . \quad (5.33)$$

We then solve (5.21) for  $y_t(M_Z)$  using  $B_t = k(\frac{B_t}{B_b})^3$  where  $k = k^0(1 - \delta k)$  and

$$\begin{aligned} k^0 &= \frac{m_b(M_Z)}{m_\tau(M_Z)} (A_{b/\tau}^{0SM} A_{b/\tau}^0)^{-1} B_t^{0SM \frac{3}{2}} B_b^{0SM - \frac{3}{2}} B_\tau^{0SM \frac{7}{2}} , \\ \delta k &\simeq \Delta_{b/\tau}^{SM} + \Delta_{b/\tau}^{SUSY} + \Delta_{b/\tau}^{GUT} + \Delta_{b/\tau}^{\alpha SM} + \Delta_{b/\tau}^\alpha . \end{aligned} \quad (5.34)$$

The solution for  $m_t(M_Z)$  is

$$\begin{aligned} m_t(M_Z) &= m_t^0(M_Z) \left( 1 + \Delta_{y_t}^{SUSY} + \Delta_t^{\alpha SM} - \frac{1}{2} \Delta_{K_t} \right. \\ &\quad \left. + C(\delta k + 3(\Delta_{B_b} - \Delta_{B_\tau})) \right) , \end{aligned} \quad (5.35)$$

where

$$m_t^0(M_Z) = v \sin \beta A_t^{0SM} B_t^{0SM \frac{9}{2}} B_b^{0SM \frac{3}{2}} B_\tau^{0SM} \frac{\sqrt{1 - (k^0)^{12} \left( \frac{B_\tau^0}{B_b^0} \right)^{36}}}{\sqrt{K_t^0}} , \quad (5.36)$$

$v = 174.104$  GeV and we have inserted the appropriate threshold corrections to  $y_t$ .

The factor  $C$  is given by

$$C = \frac{6(k^0)^{12} \left( \frac{B_\tau^0}{B_b^0} \right)^{36}}{1 - (k^0)^{12} \left( \frac{B_\tau^0}{B_b^0} \right)^{36}} . \quad (5.37)$$

Also, we have introduced a threshold correction factor  $\Delta_{K_t}$ , defined by  $K_t = K_t^0(1 + \Delta_{K_t})$ , which must be determined numerically.

Next we evaluate some of the parameters appearing in Eq. (5.35). In particular we estimate the corrections arising from the gauge coupling thresholds. We will evaluate the Yukawa thresholds from supersymmetric particles of the MSSM and SUSY-SU(5) in the numerical section to follow. Table 2 gives values for the corrections to  $y_b/y_\tau$  and  $K_t$  from gauge coupling thresholds which affect  $M_{GUT}$  and  $\alpha_G$ . Results are given for  $\tan\beta = 1.5$  for explicit two loop  $M_t$  solutions. The results are insensitive to  $M_t$  and  $\tan\beta$  (a two loop effect in the gauge coupling evolution). The gauge coupling sparticle spectrum parameters are taken to be  $M_1 = 368$  GeV,  $M_2 = 256$  GeV and  $M_3 = 375$  GeV.

$M_{SUSY}$	$M_t$	$\Delta_{b/\tau}^\alpha$	$\Delta_{K_t}$
91.2	157.4	-0.06	-0.03
500	173.9	0.02	0.003

Table 2. Corrections to  $M_t$  from Gauge Coupling Thresholds in the MSSM ( $\alpha_s(M_Z) = 0.120$ ,  $M_b = 4.9$  GeV,  $\tan\beta = 1.5$ ).

The correction factors  $\Delta_{K_t}$  are for central values  $K_t^0 = 0.77, 0.85$  for  $M_{SUSY} = M_Z, 500$  GeV, respectively. The correction term  $\Delta_{B_b} - \Delta_{B_\tau}$  in Eq. (5.35) is negligible except for large  $\tan\beta$  in which case it has a value of  $-0.01$  for  $M_{SUSY} = M_Z$ . For low  $\tan\beta$  we also find  $m_t^0(M_Z) = (195.7 \text{ GeV}) \sin\beta$ , consistent with the infrared quasi-fixed point solution<sup>[52,53]</sup> for  $m_t$ . This behaviour is modified for larger  $\tan\beta$  since the factor of  $B_\tau^0/B_b^0$  is proportional to  $\exp(\sec^2\beta)$ . For low  $\tan\beta$  the fixed point solution implies that this factor is very close to 1. Thus the factor  $C$  multiplying the  $y_b/y_\tau$  threshold corrections in Eq. (5.35) is determined by  $k^0$  only. For the  $M_{SUSY} = M_Z$  and  $\tan\beta = 1.5$  case in Table 2 we find  $k^0 = 0.72$  and  $C = 0.12$ . Hence we see explicitly how the fixed point solution inhibits the influence of potentially large GUT or MSSM threshold corrections to  $y_b/y_\tau$  on the  $M_t$  solution. In this sense the solution for  $m_t(M_Z)$  tends to be more robust than the alternative  $m_b(M_Z)$  solution entertained by some authors. Of course, away

from the fixed point  $B_\tau^0/B_b^0$  tends to be larger than 1, and the factor  $C$  need not be small. Still, for moderate values of  $\tan\beta$ , one finds  $C \lesssim 0.3$ , and to the extent that the approximation of Eq. (5.31) is still valid, the robustness of the  $M_t$  solution is maintained except for extremely large  $\tan\beta$ .

## 6. GUT Scale Constraints

In order to extract any meaningful information concerning the parameter space we must impose some constraints on the superheavy sector beyond that of unification. Proton decay is the strongest constraint on the Higgsino color triplet mass due to the dimension 5 operators which it induces.<sup>[54]</sup> A recent thorough analysis by the authors of Ref. 33 suggests that a conservative lower bound is

$$M_{H_3} \geq 5.3 \times 10^{15} \text{ GeV} . \quad (6.1)$$

This corresponds to extreme limits on the superparticles, *i.e.* heavy squarks of order 1 TeV in mass and a maximal ratio of squark to charged wino masses, low  $\tan\beta$  and a top mass around 100 GeV. The proton lifetime for the expected dominant decay mode  $p \rightarrow K^+ \bar{\nu}_\mu$  is given by<sup>[33]</sup>

$$\begin{aligned} \tau(p \rightarrow K^+ \bar{\nu}_\mu) = 6.9 \times 10^{31} \text{ yr} & \left| \frac{0.003 \text{ GeV}^3}{\beta_n} \frac{0.67}{A_s} \frac{\sin 2\beta}{1 + y^{tK}} \frac{M_{H_3}}{10^{17} \text{ GeV}} \right. \\ & \left. \times \frac{\text{TeV}^{-1}}{m_{\tilde{W}}(G_2(m_{\tilde{W}}^2, m_{\tilde{u}}^2, m_{\tilde{d}}^2) + G_2(m_{\tilde{W}}^2, m_{\tilde{u}}^2, m_{\tilde{e}}^2))} \right|^2 , \end{aligned} \quad (6.2)$$

where  $\beta_n$  is the relevant nuclear matrix element and lies between 0.003 and 0.03  $\text{GeV}^3$ . The parameter  $y^{tK}$  gives the ratio of the third to the second family contributions. Since it involves undetermined complex phases from CKM matrix elements one must allow for possible cancellations between different families. A conservative value of  $|1 + y^{tK}| \gtrsim 0.4$  can be taken to get conservative limits on  $M_{H_3}$ .

The quantity  $A_s$  is a short-distance factor incorporating the anomalous dimensions of the important dimension 5 operators as well as the renormalization of the strange and charm masses from  $M_Z$  to  $M_{GUT}$ . The current experimental limit is  $\tau(p \rightarrow K^+ \bar{\nu}_\mu) \gtrsim 1 \times 10^{32}$  yr,<sup>[55]</sup> implying that the squared factor in (6.2) must be  $\gtrsim O(1)$ .

We would like to note that the limit (6.1) can be substantially strengthened when combined with sparticle spectrum predictions and the large  $M_t$  solutions required by bottom-tau Yukawa unification. Note that  $A_s$  is enhanced by up to a factor of 3 when such large values of  $y_t$  are included in the running charm Yukawa coupling, decreasing the predicted lifetime by nearly an order of magnitude. In particular, we have an additional motivation to compute  $M_{H_3}$  rather than  $\alpha_s(M_Z)$  as a gauge unification scenario. By determining  $M_{H_3}$  for each sparticle spectrum determined by one's favorite set of theoretical criterion, *e.g.* universal soft SUSY breaking, radiative electroweak breaking, *etc.*, one can immediately apply strengthened and correlated limits from proton decay to this spectrum. The well-known figure of merit is typically the factor  $R \equiv m_{\tilde{q}}^2 / (m_{\tilde{W}^\pm} \times 1 \text{ TeV})$ , where  $m_{\tilde{q}}$  is a first generation squark mass. This factor obtains a lower bound from proton decay, while typical sparticle spectra generated with the standard theoretical assumptions require  $R \lesssim 25$  ( $\lesssim 4$  in the no-scale case assuming  $m_{\tilde{q}} \gtrsim 120$  GeV) for sparticle masses below 1 TeV. Even more of the parameter space of the MSSM can be excluded by this procedure.<sup>[50]</sup> For the present analysis however, we will consider the conservative limit of Eq. (6.1).

One may also bound the adjoint and color triplet Higgs masses from above by the requirement that the superpotential couplings  $\lambda_{1,2}$  be perturbative ( $< 2\sqrt{\pi}$ ) below the Planck scale.<sup>[1,33]</sup> Of course, this is purely theoretical prejudice as there may indeed be new physics between  $M_{GUT}$  and  $M_{Planck} \simeq 1.2 \times 10^{19}$  GeV. We therefore use the perturbativity constraint only to give an indication of a realistic GUT spectrum and not a strict requirement. We do not impose fine tuning constraints which require that these couplings are not too small<sup>[1]</sup> as such small couplings in the superpotential are technically (though not aesthetically) natural due to the

nonrenormalization theorem.<sup>[38]</sup>

In the one loop approximation the GUT scale renormalization group equations for the Yukawa-like couplings, taking into account only third generation effects, are

$$\begin{aligned}
\beta_g &= -\frac{3}{16\pi^2}g^3, \\
\beta_{\lambda_1} &= \frac{1}{16\pi^2}\lambda_1\left(\frac{63}{5}\lambda_1^2 + 3\lambda_2^2 - 30g^2\right), \\
\beta_{\lambda_2} &= \frac{1}{16\pi^2}\lambda_2\left(\frac{21}{5}\lambda_1^2 + \frac{53}{5}\lambda_2^2 - \frac{98}{5}g^2 + 3y_t^2 + 4y_b^2\right), \\
\beta_{y_t} &= \frac{1}{16\pi^2}y_t\left(\frac{24}{5}\lambda_2^2 + 9y_t^2 + 4y_b^2 - \frac{96}{5}g^2\right), \\
\beta_{y_b} &= \frac{1}{16\pi^2}y_b\left(\frac{24}{5}\lambda_2^2 + 3y_t^2 + 10y_b^2 - \frac{84}{5}g^2\right),
\end{aligned} \tag{6.3}$$

where we have corrected an error in the  $\beta_{y_t}$  of Ref. 33. Using the minimal SU(5) relations

$$\frac{M_{H_3}}{M_V} = \frac{\lambda_2}{g}, \quad \frac{M_\Sigma}{M_V} = \frac{2\lambda_1}{g}, \tag{6.4}$$

we find the following results for one loop perturbativity up to  $M_{Planck}/\sqrt{8\pi}$  for  $M_{GUT} = 2 \times 10^{16}$  GeV and  $\alpha_G = 1/24.5$ :

$$M_{H_3} \lesssim 1.9M_V, \quad M_\Sigma \lesssim 3.8M_V. \tag{6.5}$$

If we require perturbativity up to  $10^{17}$  GeV instead, then the factors becomes 2.7 and 5.3, respectively. The limits are obtained for each Yukawa coupling by taking all other Yukawa couplings to zero in its  $\beta$  function. The same constraints applied to the ordinary Yukawa couplings gives  $y_t(M_{GUT}) \lesssim 1.5(2.1)$  and  $y_b(M_{GUT}) \lesssim 1.4(2.0)$ , where the values in parenthesis correspond to perturbativity up to  $10^{17}$  GeV. However in the analysis below we choose to be somewhat inconsistent by requiring only that these couplings remain perturbative up to  $M_{GUT}$ .

## 7. Full Renormalization Group Analysis

A complete two loop numerical analysis is necessary to properly determine the influence of threshold effects on the solutions for  $M_t$ ,  $M_{H_3}$  and  $M_{GUT}$ . We will consider the effect of turning on and off various thresholds as well as the effect of varying various parameters appearing in the threshold formulae.

From Table 1 we saw that  $M_{H_3}$  decreases with  $m_t$  and  $\alpha$  and increases with  $s^2$ ,  $\alpha_s$  and  $V_{SUSY}(m_{\tilde{H}})$  while  $M_{GUT}$  increases with  $m_t$  and  $\alpha_s$  and decreases with  $s^2$ ,  $\alpha$  and  $U_{SUSY}(m_{\tilde{W}}, m_{\tilde{g}})$ . Just considering gauge unification for the moment, we can quantify these dependencies numerically, incorporating all the gauge coupling threshold corrections. We numerically integrate the relevant two loop  $\beta$  functions (see Refs. 13, 56 and 57 and references therein) and use a modified globally convergent nonlinear Newton method to find the solutions for  $M_{H_3}$  and  $M_{GUT}$  consistent with the mismatch of the gauge couplings at  $M_{GUT}$ . The results are indicated in Figs. 4-7, and highlight the various dependencies mentioned above. In all the figures we indicate the dominant effect of the uncertainty in  $\alpha_s(M_Z)$  as well as the influence of large and small  $\tan\beta$  for central values of  $\sin\theta_W(M_Z)$  and  $\alpha(M_Z)$ . In Fig. 4 we depict the logarithmic dependence of  $M_{GUT}$  on the gluino mass for  $120 \text{ GeV} \leq m_{\tilde{g}} \leq 1 \text{ TeV}$  for fixed  $M_t = 165.4 \text{ GeV}$ . For fixed  $\alpha_s$  we see that the variation of  $M_{GUT}$  over the entire range corresponds approximately to a 50% deviation. Similarly, Fig. 5 shows the variation of  $M_{GUT}$  with  $M_t$  for  $130 \text{ GeV} \leq m_t(M_Z) \leq 200 \text{ GeV}$  for fixed  $m_{\tilde{g}} = 400 \text{ GeV}$ . Here the rise in  $M_{GUT}$  is determined by the quadratic dependence of  $\sin\theta_W$  on  $M_t$  and gives a 20-30% deviation over the entire range of  $M_t$ . Note that the curves cut off at different values of  $M_t$  corresponding to the nonperturbative limit of  $y_t$ .

The logarithmic variation of  $M_{H_3}$  with  $V_{SUSY} \simeq .08m_{\tilde{H}}$  is shown in Fig. 6 for  $100 \text{ GeV} \leq m_{\tilde{H}} \leq 1 \text{ TeV}$  and  $M_t = 165.4 \text{ GeV}$ . Note that only in the case of large values of  $\alpha_s$  do we obtain consistency with even the most conservative proton decay bound,  $M_{H_3} > 10^{15.7} \text{ GeV}$ . Here we get an order of magnitude change in  $M_{H_3}$  over the range of  $V_{SUSY}$ . The more complicated dependence of  $M_{H_3}$  with  $M_t$

for  $130 \text{ GeV} \leq m_t(M_Z) \leq 200 \text{ GeV}$  is given in Fig. 7 for fixed  $V_{SUSY} = 45 \text{ GeV}$ . The initial fall of  $M_{H_3}$  with  $M_t$  is due to the electroweak threshold while its rise for large  $M_t$  is due to the effect of large  $y_t$  on the two loop gauge  $\beta$  functions. The variations in  $M_{H_3}$  are on the order of 30%.

Before imposing the condition of Yukawa unification, gauge unification constrains the solutions for  $M_{GUT}$  and  $M_{H_3}$ . For  $M_t$  between 130 and 200 GeV and  $0.5 \lesssim \tan \beta \lesssim 60$  we find the ranges

$$\begin{aligned} 1.0(0.96) \times 10^{16} < M_{GUT} < 3.9(3.7) \times 10^{16} \text{ GeV} , \\ 1.7(1.2) \times 10^{13} < M_{H_3} < 1.6(0.9) \times 10^{17} \text{ GeV} , \end{aligned} \tag{7.1}$$

for the case of approximately degenerate squarks and sleptons, with the no-scale limits given in parentheses. These results are comparable with those of Ref. 33. Note that the lower limit on  $M_{GUT}$  and the upper limit on  $M_{H_3}$  will be sensitive to the restricted range of values of  $M_t$  which result from Yukawa unification. The application of the most conservative proton decay bound from the previous section can be translated into a lower bound on the strong coupling constant. By tuning the remaining parameters so that  $M_{H_3}$  is as large as possible we find

$$\alpha_s(M_Z) \gtrsim 0.118 (0.119) , \tag{7.2}$$

where again the limit in parenthesis corresponds to the no-scale case.

To get some idea of the size of the GUT scale Yukawa coupling threshold corrections, we combine the renormalization group constraints with the perturbativity constraints of Section 6. The perturbativity constraints of Eq. (6.5) together with Eq. (7.1) imply

$$\begin{aligned} M_V > 7.0(6.1) \times 10^{15} \text{ GeV} , \\ M_\Sigma < 0.9(1.2) \times 10^{17} \text{ GeV} , \end{aligned}$$

where the two values correspond to perturbativity up to  $M_{Planck}/\sqrt{8\pi} = 2.4 \times 10^{18} \text{ GeV}$  and  $10^{17} \text{ GeV}$ , respectively. If we further assume that no superheavy masses

lie above the relevant Planck mass scale, we find in addition

$$\frac{M_V}{M_\Sigma} \lesssim 1.2 \times 10^7 . \quad (7.3)$$

Although this may appear to be an extreme choice there is nothing to rule it out phenomenologically, in fact such a case was considered recently<sup>[58]</sup> where the fine-tuning of  $\lambda_1$  is used to solve the Polonyi problem.<sup>[59]</sup> What we regard as a fine-tuning of parameters may indeed be fixed by some not as yet not fully understood quantum gravitational model. In any case, supersymmetry insures that any tuning of superpotential parameters is at least technically natural as they are multiplicatively renormalized. From Eqs. (3.11), (5.34) and (5.35) we see that such a large splitting tends to increase the top mass prediction. In many cases no perturbative solution can be found, however, away from the infrared quasi-fixed point of  $y_t$ , sizable enhancements of the predictions can occur. In Fig. 8 we plot the  $M_t$  solution *vs.*  $\tan \beta$  for various values of the ratio  $M_V/M_\Sigma$  for  $M_b = 5.2$  GeV,  $\alpha_s(M_Z) = 0.120$  and  $M_{SUSY} = M_Z$ . The largest deviation from the naive case is a 15% increase in  $M_t$  and corresponds to  $\Delta_{b/\tau}^{GUT} \simeq 0.1$ . The sparticle spectrum parameters are fixed at  $m_{\tilde{g}} = M_3 = 1$  TeV and  $V_{SUSY} = 80$  GeV. The typical GUT masses are then  $M_{GUT} = 10^{16.1 \pm 0.1}$  GeV and  $M_{H_3} = 10^{15.7 \pm 0.4}$  GeV for these solutions. We also plot the bound from the nonperturbative limit on  $y_t$ , indicating that for this particular example, one is not in the domain of attraction of the fixed point.

The GUT scale matching function for  $y_b/y_\tau$  of Eq. (3.11) can also be negative for large  $y_t$  and  $M_{H_3}$ . We set  $M_V/M_\Sigma = 0.3$ , near the minimum required by the perturbativity argument. In Fig. 9 we give an example for this case for  $M_b = 4.9$  GeV,  $\alpha_s(M_Z) = 0.127$  and  $M_{SUSY} = M_Z$ . Using the same set of sparticle spectrum parameters as in the previous figure, we obtain GUT masses in the ranges  $M_{GUT} = 10^{16.2 \pm 0.1}$  GeV and  $M_{H_3} = 10^{16.8 \pm 0.3}$  GeV. The deviations here are smaller:  $\Delta_{b/\tau}^{GUT} \simeq -0.02$  since  $M_{H_3}$  cannot be larger than  $M_{GUT}$  by more than an order of magnitude. The important thing to note is that the lack of knowledge of the GUT scale spectrum does not preclude extracting reliable predictions for  $M_t$

over much of the parameter space and the uncertainties in these predictions can be reasonably estimated. In regions where predictions are not robust, *i.e.* away from the attraction of the infrared fixed point for  $y_t$ , one must worry about 10 - 20% effects in the minimal model.

For completeness we also depict the most significant uncertainty in the  $M_t$  solution: the error bars on  $\alpha_s$  and  $M_b$ . Fig. 10 shows the  $M_t$  *vs.*  $\tan\beta$  contours for different  $\alpha_s$  for the generic case  $M_V = M_\Sigma$ ,  $M_b = 4.9$  GeV and sparticle spectrum parameters  $m_{\tilde{g}} = 400$  GeV,  $V_{SUSY} = 35$  GeV and  $M_3 = 375$  GeV. In Fig. 11 we show these contours for different  $M_b$  ranging from 4.7 to 5.3 GeV for  $\alpha_s(M_Z) = 0.120$  and the same remaining inputs as in Fig. 10. Note that for small  $M_b$  the curves are cut off due to the lack of a perturbative solution for  $M_t$  for intermediate values of  $\tan\beta$ . Clearly, in the absence of additional theoretical cuts such as proton decay or radiative electroweak symmetry breaking there remains a large parameter space. Even if one imposes the restricted  $M_t$  limits from fits to electroweak data, one can find solutions for all regions of  $\tan\beta$ , at least for larger  $M_b$ . A better determination of  $M_b$  could eliminate the intermediate  $\tan\beta$  solutions, although this subject is fraught with theoretical uncertainties.

Next we turn to a discussion of the Yukawa threshold corrections in the MSSM. Using the approximate matching functions of Eq. (4.15) - (4.17) we incorporate  $M_t$  into the numerical routine together with  $M_{GUT}$  and  $M_{H_3}$  and compute the threshold effects on the top mass solution for representative sparticle spectra consistent with universal soft supersymmetry breaking parameters at the GUT scale as well as radiative electroweak symmetry breaking.<sup>[6]</sup> We also consider the low, intermediate and high  $\tan\beta$  cases separately. Table 3 gives the effect of the threshold corrections for low  $\tan\beta = 1.47$  and some sample soft breaking parameters including the generic no-scale case. We also consider both signs of  $\mu_H$  and take  $A = 0$  throughout.

$M_0$	$M_{\frac{1}{2}}$	$\mu_H$	$\Delta_{y_t}^{SUSY}$	$\Delta_{y_b}^{SUSY}$	$\Delta_{y_\tau}^{SUSY}$	$M_t$ (naive)	$M_t$
100	140	+375	0.02	0.006	-0.006	164.1	167.6
100	140	-375	0.03	0.03	-0.01	164.1	170.5
0	150	+353	0.02	0.007	-0.007	164.2	167.8
0	200	-466	0.07	0.04	-0.01	163.0	175.4

Table 3. Low  $\tan\beta$  Threshold Corrections to  $M_t$  in the MSSM  
( $\tan\beta = 1.47$ ,  $\alpha_s(M_Z) = 0.120$ ,  $M_b = 4.8$  GeV,  $A = 0$  )

All masses in the tables are in GeV. Note that the increased stop squark splitting in the case of  $\mu_H < 0$  increases the  $y_t$  corrections. The SUSY thresholds increase the top mass prediction relative to the naive result which includes only the gauge coupling thresholds. The dominant effect arises from the gluino-induced vertex corrections of Fig. 1 (for  $\mu_H < 0$ ) and the gluino contribution to the top quark wavefunction renormalization. These are also the dominant contributions to the  $y_b$  threshold, although for  $\mu_H > 0$  the gluino-induced vertex and wavefunction renormalization contributions almost cancel, while they add constructively for  $\mu_H < 0$ . Since  $y_t$  is near the fixed point in this region, the order 5% corrections to  $y_b/y_\tau$  translate into a negligible effect on the  $M_t$  solution as discussed in Section 5.

For intermediate and high  $\tan\beta$  the bottom and  $\tau$  Yukawa corrections become more important. For intermediate  $\tan\beta = 15$  and  $M_{\frac{1}{2}} = 100$  GeV, Table 4 summarizes the typical threshold effects.

$M_0$	$\mu_H$	$\Delta_{y_t}^{SUSY}$	$\Delta_{y_b}^{SUSY}$	$\Delta_{y_\tau}^{SUSY}$	$M_t$ (naive)	$M_t$
100	164	0.01	-0.1	0.025	194.5	178.3
200	316	0.03	-0.03	0.025	190.3	187.5
300	462	0.035	-0.01	0.02	187.3	188.7

Table 4. Intermediate  $\tan\beta$  Threshold Corrections to  $M_t$  in the MSSM ( $\tan\beta = 15$ ,  $\alpha_s(M_Z) = 0.118$ ,  $M_b = 4.9$  GeV,  $M_{\frac{1}{2}} = 100$  GeV,  $A = 0$  )

It is interesting to see the source of the enhanced  $y_b$  and  $y_\tau$  corrections. For  $M_0 = 100$  GeV the gluino induced vertex of Fig. 1 contributes  $-0.13$ , while the chargino induced vertices of Fig. 2 with a stop squark internal lines contribute  $0.0175$ . Accounting for other small corrections leaves a 10% effect. On the other hand for  $M_0 = 300$  GeV and correspondingly larger squark and slepton masses, many contributions come into play. Now the chargino contributions add to  $0.03$ , the gluino vertex correction is  $-0.09$  and the total wavefunction renormalization contribution is  $0.03$ . Accounting for heavy Higgs effects and the neutralino contributions leaves a net 1% effect in  $y_b$ . Clearly a complete analysis is important even for intermediate values of  $\tan\beta$ . The dominant corrections to  $y_\tau$  come from the neutral and charged wino induced graphs of Fig. 3.

For larger  $\tan\beta = 40$  and  $M_{\frac{1}{2}} = 100$  GeV, we give typical threshold effects in Table 5.

$M_{\frac{1}{2}}$	$\mu_H$	$\Delta_{y_t}^{SUSY}$	$\Delta_{y_b}^{SUSY}$	$\Delta_{y_\tau}^{SUSY}$	$M_t$ (naive)	$M_t$
200	205	0.04	-0.035	0.04	177.6	154.5
400	450	0.05	-0.045	0.06	169.0	78.2
600	660	0.055	-0.03	0.065	162.3	45.2

Table 5. Large  $\tan\beta$  Threshold Corrections to  $M_t$  in the MSSM ( $\tan\beta = 40$ ,  $\alpha_s(M_Z) = 0.118$ ,  $M_b = 4.9$  GeV,  $M_0 = 400$  GeV,  $A = 0$  )

Here the heavier spectrum chosen enhances all the wavefunction renormalization contributions and the gluino vertex contributions to  $y_b$  approach 20%. For the positive  $\mu_H$  chosen however, this is partially cancelled as described in the intermediate  $\tan\beta$  case. Even so, the effect on  $M_t$  is dramatic. Here one is far from the attraction of the infrared fixed point. The typically large  $M_t$  predictions in SUSY-GUTs normally arise because the QCD running of  $y_b$  typically places it below  $y_\tau$  at  $M_{GUT}$ . A large top Yukawa coupling counters this behaviour. However, here the large, order 10%, threshold correction increases  $y_b$  relative to  $y_\tau$  at

$M_{GUT}$  and smaller values of  $M_t$  are required. In fact, for some spectra the situation becomes unstable in the sense that no positive  $y_t$  can be found such that the  $y_b(M_{GUT}) = y_\tau(M_{GUT})$  unification occurs.

Finally, we use the results of Section 5 to estimate the contribution of the gauge coupling thresholds to the  $M_t$  solution which are already incorporated in the “naive” solution in the above tables. Using Eq. (5.24) we find the ranges  $\Delta_{b/\tau}^\alpha \approx (-0.014, -0.03)$ ,  $(-0.03, -0.045)$ ,  $(-0.044, -0.084)$  for the data of Tables 3, 4 and 5, respectively. In the intermediate and high  $\tan\beta$  regions this effect supplements the other potentially large negative Yukawa corrections to  $y_b/y_\tau$ . There is also a threshold correction to  $K_t$  of Eq. (5.32) given by  $\Delta_{K_t} \approx -0.02$  for the data of Tables 3 and 4 and in the range  $\approx (-0.025, -0.046)$  for Table 5. The corresponding fractional correction to  $M_t$  is  $-\frac{1}{2}\Delta_{K_t}$  and enhances the generally positive direct Yukawa threshold correction to  $y_t$ . The generic features of the analytic solutions are born out, at least in the low  $\tan\beta$  region where they are valid. In particular, the gauge and Yukawa corrections to  $y_b/y_\tau$  both at  $M_{SUSY}$  and  $M_{GUT}$  do not directly feed into the  $M_t$  solution. They are multiplied by a factor,  $C$  of Eq. (5.37), which for the data of Table 3 is  $C \approx 0.1$ . The fact that the corrections to  $M_t$  are dominated by the direct threshold correction  $\Delta_{y_t}^{SUSY}$  for low  $\tan\beta$  confirms this expectation.

## 8. Conclusions

We have given a complete treatment of Yukawa coupling threshold corrections in the MSSM and minimal SUSY-SU(5). We have applied these as well as the gauge coupling thresholds to both approximate one loop analytic and consistent two loop numerical solutions for the superheavy masses  $M_{GUT}$  and  $M_{H_3}$  and the top quark mass,  $M_t$  in the context of gauge and Yukawa unification in SUSY-SU(5). We have highlighted the sensitivities of these solutions to the low scale parameters. The effective GUT scale was the most constrained and variations of  $\alpha_s(M_Z)$ ,  $M_t$  and the gluino mass led to of order 40% deviations in  $M_{GUT}$ .

We have also found limits on the colored Higgs triplet superfield mass,  $M_{H_3}$ , from an RG analysis of unification. This approach avoids ad hoc assumptions about the degeneracies of the superheavy particles. We displayed the sensitivities of  $M_{H_3}$  on  $\alpha_s(M_Z)$ ,  $M_t$ ,  $\tan\beta$  and the Higgsino masses which are much larger than for  $M_{GUT}$ . Using these results we found that a conservative analysis of the proton decay bound could be translated into a lower bound on the strong coupling,  $\alpha_s(M_Z) \gtrsim 0.118$  for any sparticle spectrum with masses less than order 1 TeV. We also concluded that  $M_{H_3}$  must be lighter than  $2 \times 10^{17}$  GeV. This in turn limits the size of GUT scale corrections to  $y_b/y_\tau$  so that these effects cannot produce too large a decrease in the solution for  $M_t$ . We found also that away from the attractive region of the infrared quasi-fixed point of the top Yukawa coupling, there can be significant positive corrections to  $M_t$  if there is a substantial allowed splitting of the superheavy vector and adjoint scalar masses,  $M_V \gg M_\Sigma$ . This typically occurs for larger values of  $M_b$ , while for smaller values no perturbative solution can be found. For low  $\tan\beta$  these corrections to  $y_b/y_\tau$  have different effects on the two alternative solutions,  $M_t$  for fixed  $M_b$  or  $m_b(M_Z)$  for fixed  $M_t$ . In the former case the corrections are suppressed, while in the latter they feed directly into the uncertainty for  $m_b(M_Z)$ .

We have given a detailed calculation of the Yukawa corrections in the MSSM and analyzed their effect on the  $M_t$  solution for various regions of  $\tan\beta$  and representative sparticle spectra. We have shown, both analytically and numerically, the robustness of this solution for low  $\tan\beta$ , where the dominant corrections come from gluino-induced effects. For larger  $\tan\beta$  we discussed the importance of the complete calculation to determining the potentially large corrections to  $y_b$  and  $y_\tau$ . These corrections were particularly sensitive to the signs of  $\mu_H$  and  $A_t$ . For all  $\tan\beta$  we described the enhancing effect of stop squark mixing on  $M_t$  for both signs of  $\mu_H$ .

We emphasized the effect of the  $\alpha_s$  and  $M_b$  error bars on  $M_t$ , by far the dominant uncertainty. With strong bounds from proton decay in the context of canonical supergravity induced soft supersymmetry breaking, this parameter space

can be cut substantially. A critical analysis of the theoretical uncertainty in  $M_b$  would also help reduce the parameter space, particularly the intermediate  $\tan\beta$  region, which is still allowed if one accepts larger values of  $M_b \sim 5.2$  GeV. Intermediate values of  $\tan\beta$  must also be reconsidered when the supersymmetric Yukawa thresholds are included as these can reduce  $M_t$  by 10%. We will discuss these issues and perform a more complete analysis of the MSSM and GUT Yukawa thresholds under more specific assumptions for the sparticle spectrum in a future work.<sup>[50]</sup>

## ACKNOWLEDGEMENTS

The author would like to thank Vernon Barger and Pierre Ramond for useful comments on earlier drafts of the manuscript. He would also like to thank Paul Ohmann for sharing some of his sparticle spectrum data. He is also grateful for the hospitality of the IFT at the University of Florida where part of this work was completed. This research was supported in part by the University of Wisconsin Research Committee with funds granted by the Wisconsin Alumni Research Foundation and in part by the U. S. Department of Energy under contract no. DE-AC02-76ER00881.

## APPENDIX A: Yukawa Threshold Corrections in the MSSM

Below we give the complete supersymmetry breaking threshold corrections to third generation Yukawa couplings in the MSSM in the case in which intergenerational mixing is negligible in the squark and slepton mass matrices. The relevant factors as in Eq. (2.10) are the finite parts of the one loop wavefunction renormalizations for the third generation fermions and the light SM Higgs and the Yukawa vertex corrections involving heavy sparticles. We give results for the scenario in which there is only one light Higgs below the scale at which the threshold conditions are applied.

First we give some notation and conventions. Our conventions closely follow those of Refs. 60 and 61 which the reader should consult for more details. We define our superpotential in the MSSM as

$$P = \epsilon_{ij}(Y_d \hat{H}_1^i \hat{Q}^j \hat{D} + Y_e \hat{H}_1^i \hat{L}^j \hat{E} + Y_u \hat{H}_2^j \hat{Q}^i \hat{U} + \mu_H \hat{H}_1^i \hat{H}_2^j), \quad (\text{A.1})$$

where the hats denote superfields,  $\epsilon_{12} = -\epsilon_{21} = 1$  and  $Y_{u,d,e}$  are the conventional Yukawa matrices, with  $y_t$ ,  $y_b$  and  $y_\tau$  the respective diagonal elements for the third family. The superfields  $Q$ ,  $U$ ,  $D$ ,  $L$  and  $E$  have the hypercharge assignments of the corresponding quarks and leptons. The Higgs superfields  $H_{1,2}$  have hypercharge  $y = -1, +1$  and their scalar components acquire vacuum expectation values  $\langle H_1^1 \rangle = v_1/\sqrt{2}$  and  $\langle H_2^2 \rangle = v_2/\sqrt{2}$ , respectively. A general set of soft supersymmetry breaking parameters is introduced without explicit regard to their origin. These include soft trilinear scalar couplings mimicking those of the superpotential as well as explicit mass terms for the gauginos, squarks, sleptons and Higgs fields.

$$\begin{aligned} V_{\text{soft}} &= -\epsilon_{ij}(Y_d A_d H_1^i \tilde{Q}^j \tilde{D} + Y_e A_e H_1^i \tilde{L}^j \tilde{E} + Y_u A_u H_2^j \tilde{Q}^i \tilde{U} + \mu_H B H_1^i H_2^j), \\ \mathcal{L}_{\text{soft}}^{\text{mass}} &= \frac{1}{2} \mathcal{M}_1 \bar{\lambda}_B \lambda_B + \frac{1}{2} \mathcal{M}_2 \bar{\lambda}_W^i \lambda_W^i + \frac{1}{2} \mathcal{M}_3 \bar{\lambda}_g^A \lambda_g^A \\ &\quad - m_Q^2 \tilde{Q}^{i*} \tilde{Q}^i - m_U^2 \tilde{U}^* \tilde{U} - m_D^2 \tilde{D}^* \tilde{D} \\ &\quad - m_L^2 \tilde{L}^{i*} \tilde{L}^i - m_E^2 \tilde{E}^* \tilde{E} - m_{H_1}^2 \tilde{H}_1^{i*} \tilde{H}_1^i - m_{H_2}^2 \tilde{H}_2^{i*} \tilde{H}_2^i, \end{aligned} \quad (\text{A.2})$$

where we denote superpartners of ordinary particles with a tilde, and  $\lambda$  is used to denote the Majorana gaugino fields. We also define squark and slepton fields with the same charge conventions as their partners:  $\tilde{Q} = (\tilde{u}_L, \tilde{d}_L)$ ,  $\tilde{U} = \tilde{u}_R^*$ ,  $\tilde{D} = \tilde{d}_R^*$ ,  $\tilde{Q} = (\tilde{\nu}_L, \tilde{e}_L)$  and  $\tilde{E} = \tilde{e}_R^*$ .

The threshold corrections will in general involve squark and slepton mixing matrices for the third generation. For example, denoting the stop squark mass eigentates as  $\tilde{t}_{1,2}$ , we can relate them to weak eigenstates  $\tilde{t}_{L,R}$  by an orthogonal matrix  $O^t$  such that  $O^t M_t^2 O^{tT} = \bar{M}_t^2$  where  $\bar{M}_t^2$  is diagonal and

$$\begin{pmatrix} \tilde{t}_1 \\ \tilde{t}_2 \end{pmatrix} = \begin{pmatrix} \cos \theta_t & \sin \theta_t \\ -\sin \theta_t & \cos \theta_t \end{pmatrix} \begin{pmatrix} \tilde{t}_L \\ \tilde{t}_R \end{pmatrix} = O^t \begin{pmatrix} \tilde{t}_L \\ \tilde{t}_R \end{pmatrix}. \quad (\text{A.3})$$

We define  $O^b$  and  $O^\tau$  similarly. The neutralino mass matrix is diagonalized by the unitary matrix  $Z$  such that  $Z^* M_{\chi^0} Z^{-1} = \bar{M}_{\chi^0}$  and relates the weak bino, wino and Higgsino eigenstates to the mass eigenstate Majorana fields  $\chi_i^0$  via

$$\begin{aligned} -i\lambda_B &= Z_{i1}^* \chi_i^0, & -i\lambda_W^3 &= Z_{i2}^* \chi_i^0, \\ \tilde{H}_1^1 &= Z_{i3}^* \chi_i^0, & \tilde{H}_2^2 &= Z_{i4}^* \chi_i^0. \end{aligned} \quad (\text{A.4})$$

The upper index on the Higgsino fields is an  $SU(2)_L$  index. Finally we define the unitary mixing matrices for the charginos by  $U^* M_{\chi^\pm} V^{-1} = \bar{M}_{\chi^\pm}$  where the charged Higgsino and wino are related to the Dirac mass eigenstates  $\chi_{Di}^T = (\chi_i^+, \bar{\chi}_i^-)$  via

$$\tilde{H}_2^1 = V_{i2}^* \chi_i^+, \quad \tilde{H}_1^2 = U_{i2}^* \chi_i^-, \quad -i\lambda_W^+ = V_{i1}^* \chi_i^+, \quad -i\lambda_W^- = U_{i1}^* \chi_i^-. \quad (\text{A.5})$$

Explicit forms for the mass and mixing matrices can be found in Refs. 6, 61, and 62.

We first give the finite parts of the wavefunction renormalization of the top and bottom quark and  $\tau$  lepton due to loops involving squarks, sleptons, gluinos, neutralinos, charginos, and the heavy Higgs doublet involving the charged Higgs,  $H^\pm$ , the pseudoscalar  $A$  and the heavy scalar  $H^0$ . We sum the coefficients of  $\not{\partial} P_{L,R}$

in the effective action obtained by integrating out these fields and find (using the notation of Section 2) for the top quark,

$$\begin{aligned}
\bar{K}_{t(L+R)} = & -\frac{1}{32\pi^2} \left( \frac{8}{3} g_3^2 \sum_i F_2(m_{t_i}^2, m_g^2) \right. \\
& + y_b^2 \left( \sum_{i,j} F_2(m_{b_i}^2, m_{\chi_j^\pm}^2) (O_{i2}^b)^2 |U_{j2}|^2 + F_2(m_{H^\pm}^2, m_b^2) \sin^2 \beta \right) \\
& + y_t^2 \left( \sum_{i,j} F_2(m_{b_i}^2, m_{\chi_j^\pm}^2) (O_{i1}^b)^2 |V_{j2}|^2 + \sum_{i,j} F_2(m_{t_i}^2, m_{\chi_j^0}^2) |Z_{j4}|^2 \right. \\
& \quad \left. + \cos^2 \beta (F_2(m_{H^\pm}^2, m_b^2) + \frac{1}{2} (F_2(m_{H^0}^2, m_t^2) - F_2(m_A^2, m_t^2))) \right) \\
& + g_2^2 \left( \sum_{i,j} F_2(m_{b_i}^2, m_{\chi_j^\pm}^2) (O_{i1}^b)^2 |U_{j1}|^2 \right. \\
& \quad + \frac{1}{2} \sum_{i,j} F_2(m_{t_i}^2, m_{\chi_j^0}^2) ((O_{i1}^t)^2 |Z_{j2} + \frac{1}{3} Z_{j1} t|^2 \\
& \quad \left. + \frac{16}{9} (O_{i2}^t)^2 |Z_{j1}|^2 t^2) \right) \\
& - g_2 y_b \left( 2 \sum_{i,j} F_2(m_{b_i}^2, m_{\chi_j^\pm}^2) O_{i1}^b O_{i2}^b \text{Re}(U_{j1} U_{j2}^*) \right) \\
& \left. + g_2 y_t \left( \sqrt{2} \sum_{i,j} F_2(m_{t_i}^2, m_{\chi_j^0}^2) O_{i1}^t O_{i2}^t \text{Re}((Z_{j2} - Z_{j1} t) Z_{j4}^*) \right) \right), \tag{A.6}
\end{aligned}$$

and for the bottom quark,

$$\begin{aligned}
\bar{K}_{b(L+R)} = & -\frac{1}{32\pi^2} \left( \frac{8}{3} g_3^2 \sum_i F_2(m_{b_i}^2, m_g^2) \right. \\
& + y_t^2 \left( \sum_{i,j} F_2(m_{t_i}^2, m_{\chi_j^\pm}^2) (O_{i2}^t)^2 |V_{j2}|^2 + F_2(m_{H^\pm}^2, m_t^2) \cos^2 \beta \right) \\
& + y_b^2 \left( \sum_{i,j} F_2(m_{b_i}^2, m_{\chi_j^\pm}^2) (O_{i1}^t)^2 |U_{j2}|^2 + \sum_{i,j} F_2(m_{b_i}^2, m_{\chi_j^0}^2) |Z_{j3}|^2 \right. \\
& \quad \left. + \sin^2 \beta (F_2(m_{H^\pm}^2, m_t^2) + \frac{1}{2} (F_2(m_{H^0}^2, m_b^2) - F_2(m_A^2, m_b^2))) \right) \\
& + g_2^2 \left( \sum_{i,j} F_2(m_{t_i}^2, m_{\chi_j^\pm}^2) (O_{i1}^t)^2 |V_{j1}|^2 \right. \\
& \quad + \frac{1}{2} \sum_{i,j} F_2(m_{b_i}^2, m_{\chi_j^0}^2) ((O_{i1}^b)^2 |Z_{j2} - \frac{1}{3} Z_{j1} t|^2 \\
& \quad \left. + \frac{4}{9} (O_{i2}^b)^2 |Z_{j1}|^2 t^2) \right) \\
& - g_2 y_t \left( 2 \sum_{i,j} F_2(m_{t_i}^2, m_{\chi_j^\pm}^2) O_{i1}^t O_{i2}^t \text{Re}(V_{j1} V_{j2}^*) \right) \\
& \left. - g_2 y_b \left( \sqrt{2} \sum_{i,j} F_2(m_{b_i}^2, m_{\chi_j^0}^2) O_{i1}^b O_{i2}^b \text{Re}((Z_{j2} - Z_{j1} t) Z_{j3}^*) \right) \right), \tag{A.7}
\end{aligned}$$

where  $F_2$  is defined in Appendix B and  $t = \tan \theta_W$ . The result for the  $\tau$  lepton is

$$\begin{aligned}
\bar{K}_{\tau(L+R)} = & -\frac{1}{32\pi^2} \left( y_\tau^2 \left( \sum_j F_2(m_{\nu_\tau}^2, m_{\chi_j^\pm}^2) |U_{j2}|^2 + \sum_{i,j} F_2(m_{\tau_i}^2, m_{\chi_j^0}^2) |Z_{j3}|^2 \right. \right. \\
& \left. \left. + \sin^2 \beta (F_2(m_{H^\pm}^2, 0) + \frac{1}{2} (F_2(m_{H^0}^2, m_\tau^2) - F_2(m_A^2, m_\tau^2))) \right) \right) \\
& + g_2^2 \left( \sum_i F_2(m_{\nu_\tau}^2, m_{\chi_i^\pm}^2) |V_{i1}|^2 \right. \\
& \quad + \frac{1}{2} \sum_{i,j} F_2(m_{\tau_i}^2, m_{\chi_j^0}^2) ((O_{i1}^\tau)^2 |Z_{j2} + Z_{j1} t|^2 \\
& \quad \left. + 4(O_{i2}^\tau)^2 |Z_{j1}|^2 t^2) \right) \\
& - g_2 y_\tau \left( \sqrt{2} \sum_{i,j} F_2(m_{\tau_i}^2, m_{\chi_j^0}^2) O_{i1}^\tau O_{i2}^\tau \text{Re}((Z_{j2} - Z_{j1} t) Z_{j3}^*) \right) \Big), \tag{A.8}
\end{aligned}$$

where  $\bar{K}_{\alpha(L+R)} = \bar{K}_{\alpha L} + \bar{K}_{\alpha R}$ .

The neutral Higgs wavefunction renormalization contributions arise from chargino and neutralino loop diagrams in general giving matrix contributions so that,

$$\bar{Z}_H = \begin{pmatrix} 1 + \bar{K}_{H_0} & \bar{K}_{hH} \\ \bar{K}_{hH} & 1 + \bar{K}_{h_0} \end{pmatrix}, \quad (\text{A.9})$$

where

$$\begin{aligned} \bar{K}_{h_0} &= \frac{g_2^2}{16\pi^2} \left( \frac{1}{6}(3+t^2) + \sum_{i,j} (|A''_{ij}|^2 F_3(m_{\chi_i^0}, m_{\chi_j^0}) \right. \\ &\quad \left. + 2|A_{ij}|^2 F_3(m_{\chi_i^\pm}, m_{\chi_j^\pm})) \right), \\ \bar{K}_{H_0} &= \frac{g_2^2}{16\pi^2} \left( \frac{1}{6}(3+t^2) + \sum_{i,j} (|B''_{ij}|^2 F_3(m_{\chi_i^0}, m_{\chi_j^0}) \right. \\ &\quad \left. + 2|B_{ij}|^2 F_3(m_{\chi_i^\pm}, m_{\chi_j^\pm})) \right), \\ \bar{K}_{hH} &= -\frac{g_2^2}{16\pi^2} \left( \sum_{i,j} (\text{Re}(A''_{ij} B''_{ij}^*) F_3(m_{\chi_i^0}, m_{\chi_j^0}) \right. \\ &\quad \left. + 2\text{Re}(A_{ij} B_{ij}^*) F_3(m_{\chi_i^\pm}, m_{\chi_j^\pm})) \right), \end{aligned} \quad (\text{A.10})$$

and where

$$\begin{aligned} A''_{ij} &= -Q''_{ij} \cos\beta + S''_{ij} \sin\beta, & A_{ij} &= -Q_{ij} \cos\beta - S_{ij} \sin\beta, \\ B''_{ij} &= Q''_{ij} \sin\beta + S''_{ij} \cos\beta, & B_{ij} &= -Q_{ij} \sin\beta + S_{ij} \cos\beta, \end{aligned} \quad (\text{A.11})$$

with<sup>[60]</sup>

$$\begin{aligned} Q_{ij} &= \frac{1}{\sqrt{2}} V_{i1} U_{j2}, & S_{ij} &= \frac{1}{\sqrt{2}} V_{i2} U_{j1}, \\ Q''_{ij} &= \frac{1}{2} [Z_{i3} (Z_{j2} - Z_{j1} t) + (i \leftrightarrow j)] \epsilon_i, \\ S''_{ij} &= \frac{1}{2} [Z_{i4} (Z_{j2} - Z_{j1} t) + (i \leftrightarrow j)] \epsilon_i. \end{aligned}$$

The factor  $\epsilon_i = \pm 1$  is introduced<sup>[63]</sup> to insure positive mass neutralino eigenstates. When  $Z$  is defined without regard to the positivity of the mass eigenvalues, the

elements of the matrix  $\bar{M}_{\chi^0}$  are  $\epsilon_i m_{\chi_i^0}$  ( $i = 1, \dots, 4$ ). The function  $F_3$  is given in Appendix B. In general the matrix  $\bar{Z}_H$  must be diagonalized,  $\bar{Z}_H^d = O_h \bar{Z}_H O_h^T$ , giving an effective light Higgs field:

$$h_0^{eff} = (\bar{Z}_H^d)^{\frac{1}{2}} ((O_h)_{21} H_0 + (O_h)_{22} h_0) . \quad (\text{A.12})$$

This results in a threshold correction to the neutral Higgs mixing angle  $\alpha$  of Ref. 60. However, in the limit of small gaugino-Higgsino mixing considered later, these off-diagonal contributions vanish.

We next give the one particle irreducible Yukawa vertex corrections. These contributions involve more complicated functions of the squark, slepton, neutralino and chargino mixing angles although many of them simplify in certain approximations for the sparticle mass matrices. The greatest simplifications occur in the limit of no squark and slepton mixing and vanishing mixing between the bino, neutral wino and the Higgsinos. Except for the case of large  $\tan \beta$  one would expect small L-R mixing in the sbottom and stau mass matrices. However due to the large top Yukawa coupling the mixing can be substantial. Also the lack of mixing in the neutralino sector is expected if the bino and neutral wino masses are dominated by their soft-breaking masses and if the Higgsino masses are determined by the parameter  $\mu_H$  in the superpotential. This approximation is certainly appropriate to the case of radiatively induced electroweak symmetry breaking near the low  $\tan \beta$  fixed point<sup>[6,64]</sup> and works reasonably well for larger  $\tan \beta$ . We quote the entire results as well as the simplified results in the limit of small gaugino-Higgsino mixing. Note these terms can give rise to substantial enhancements of the threshold corrections proportional to ratios of sparticle masses to  $m_b$  or  $m_\tau$  if the mixing and mass-splitting between neutralinos or same generation squarks and sleptons is large.

The finite Yukawa corrections are denoted  $\bar{K}_\alpha^Y = \delta y_\alpha / y_\alpha$  as in Section 2. We separately give the results for Higgs, neutralino, chargino and gluino corrections.

For the  $h_0\bar{t}t$  vertex we obtain

$$\bar{K}_t^Y = \bar{K}_t^Y(\text{Higgs}) + \bar{K}_t^Y(\chi^0) + \bar{K}_t^Y(\chi^\pm) + \bar{K}_t^Y(\tilde{g}) , \quad (\text{A.13})$$

where the separate contributions are

$$\begin{aligned} \bar{K}_t^Y(\text{Higgs}) = & \frac{\cos^2\beta}{16\pi^2} \left( \frac{1}{2}y_t^2 \left( F_1(m_t^2, m_{H_0}^2) - F_1(m_t^2, m_A^2) \right. \right. \\ & + M_Z^2(-(\cos^2 2\beta - 2\sin^2 2\beta)G_2(m_{H_0}^2, m_{H_0}^2, m_t^2) \\ & + 12\sin^2\beta \cos 2\beta G_2(m_{H_0}^2, m_{h_0}^2, m_t^2) \\ & + \cos^2 2\beta G_2(m_A^2, m_A^2, m_t^2) \\ & \left. \left. + 4\cos 2\beta \sin^2\beta G_2(m_A^2, m_Z^2, m_t^2) \right) \right) \\ & + y_b^2 \left( F_1(m_b^2, m_{H^\pm}^2) \right. \\ & + M_Z^2((2c^2 - \cos^2 2\beta)G_2(m_{H^\pm}^2, m_{H^\pm}^2, m_b^2) \\ & \left. \left. + 2\cos^2 2\beta G_2(m_{H^\pm}^2, m_W^2, m_b^2) \right) \right) , \end{aligned} \quad (\text{A.14})$$

$$\begin{aligned} \bar{K}_t^Y(\chi^0) = & \frac{1}{16\pi^2} \left( -g_2^2 \frac{1+t^2}{4} - \sqrt{2}g_2 \sum_{i,j,k} \left( G_1(m_{\tilde{t}_i}^2, m_{\chi_j^0}^2, m_{\chi_k^0}^2) N_{ijk}^{LR}(t) \right. \right. \\ & \left. \left. + m_{\chi_j^0} m_{\chi_k^0} G_2(m_{\tilde{t}_i}^2, m_{\chi_j^0}^2, m_{\chi_k^0}^2) N_{ijk}^{RL}(t) \right) \right. \\ & \left. + 2m_t \sum_{i,j,k} m_{\chi_i^0} G_2(m_{\chi_i^0}^2, m_{\tilde{t}_j}^2, m_{\tilde{t}_k}^2) \bar{N}_{ijk}(t) \right) , \end{aligned} \quad (\text{A.15})$$

$$\begin{aligned} \bar{K}_t^Y(\chi^\pm) = & \frac{1}{16\pi^2} \left( \frac{-g_2^2}{2} - \sqrt{2}g_2 \sum_{i,j,k} \left( G_1(m_{\tilde{b}_i}^2, m_{\chi_j^\pm}^2, m_{\chi_k^\pm}^2) C_{ijk}^{LR}(t) \right. \right. \\ & \left. \left. + m_{\chi_j^\pm} m_{\chi_k^\pm} G_2(m_{\tilde{b}_i}^2, m_{\chi_j^\pm}^2, m_{\chi_k^\pm}^2) C_{ijk}^{RL}(t) \right) \right. \\ & \left. + 2m_b \sum_{i,j,k} m_{\chi_i^\pm} G_2(m_{\chi_i^\pm}^2, m_{\tilde{b}_j}^2, m_{\tilde{b}_k}^2) \bar{C}_{ijk}(t) \right) , \end{aligned} \quad (\text{A.16})$$

$$\bar{K}_t^Y(\tilde{g}) = \frac{1}{16\pi^2} \left( -\frac{16}{3} g_3^2 m_t m_{\tilde{g}} \sum_{i,j} G_2(m_{\tilde{g}}^2, m_{\tilde{t}_i}^2, m_{\tilde{t}_j}^2) \bar{G}_{ij}(t) \right), \quad (\text{A.17})$$

and where the functions  $F_i$  and  $G_i$  are defined in Appendix B. The quantities  $N_{ijk}^{LR}(t)$ ,  $N_{ijk}^{RL}(t)$  and  $\bar{N}_{ijk}(t)$  in the neutralino contribution are

$$\begin{aligned} N_{ijk}^{LR}(t) &= y_t N_{ijk}^1(t) + g_2 N_{ijk}^2(t) + g_2 \left(\frac{g_2}{y_t}\right) N_{ijk}^3(t), \\ N_{ijk}^{RL}(t) &= y_t \tilde{N}_{ijk}^1(t) + g_2 \tilde{N}_{ijk}^2(t) + g_2 \left(\frac{g_2}{y_t}\right) \tilde{N}_{ijk}^3(t), \\ \bar{N}_{ijk}(t) &= y_t^2 \bar{N}_{ijk}^1(t) + y_t g_2 \bar{N}_{ijk}^2(t) + g_2^2 \bar{N}_{ijk}^3(t) \\ &\quad + g_2^2 \left(\frac{g_2}{y_t}\right) \bar{N}_{ijk}^4(t) + g_2^2 \left(\frac{g_2}{y_t}\right)^2 \bar{N}_{ijk}^5(t), \end{aligned} \quad (\text{A.18})$$

where

$$\begin{aligned} N_{ijk}^1(t) &= \text{Re}[T_{Lik}^{0*}(t) T_{Rij}^0(t) (-Q''_{jk} \cot \beta + S''_{jk})], \\ N_{ijk}^2(t) &= -\text{Re}[(R_{Lik}^{0*}(t) T_{Rij}^0(t) + T_{Lik}^{0*}(t) R_{Rij}^0(t)) \\ &\quad \times (-Q''_{jk} \cot \beta + S''_{jk})], \\ N_{ijk}^3(t) &= \text{Re}[R_{Lik}^{0*}(t) R_{Rij}^0(t) (-Q''_{jk} \cot \beta + S''_{jk})], \end{aligned} \quad (\text{A.19})$$

and

$$\begin{aligned} \bar{N}_{ijk}^1(t) &= \text{Re}[T_{Lki}^{0*}(t) T_{Rji}^0(t) (P_{jk}(t) + P'_{jk}(t) \left(\frac{\mu_H \cot \beta + A_t}{m_t}\right))], \\ \bar{N}_{ijk}^2(t) &= -\text{Re}[(R_{Lki}^{0*}(t) T_{Rji}^0(t) + T_{Lki}^{0*}(t) R_{Rji}^0(t)) \\ &\quad \times (P_{jk}(t) + P'_{jk}(t) \left(\frac{\mu_H \cot \beta + A_t}{m_t}\right))], \\ \bar{N}_{ijk}^3(t) &= \frac{1}{c^2} (\cot^2 \beta - 1) \text{Re}[T_{Lki}^{0*}(t) T_{Rji}^0(t) P''_{jk}(t)] \\ &\quad + \text{Re}[R_{Lki}^{0*}(t) R_{Rji}^0(t) (P_{jk}(t) + P'_{jk}(t) \left(\frac{\mu_H \cot \beta + A_t}{m_t}\right))], \\ \bar{N}_{ijk}^4(t) &= -\frac{1}{c^2} (\cot^2 \beta - 1) \text{Re}[(R_{Lki}^{0*}(t) T_{Rji}^0(t) + T_{Lki}^{0*}(t) R_{Rji}^0(t)) P''_{jk}(t)], \\ \bar{N}_{ijk}^5(t) &= \frac{1}{c^2} (\cot^2 \beta - 1) \text{Re}[R_{Lki}^{0*}(t) R_{Rji}^0(t) P''_{jk}(t)]. \end{aligned} \quad (\text{A.20})$$

The quantities  $\tilde{N}_{ijk}(t)$  are obtained by interchanging the  $L$  and  $R$  subscripts in (A.19). The matrices  $R$  and  $T$  involve products of squark and neutralino mixing

matrices while the  $P$  matrices involve products of squark mixing matrices only. They are defined by

$$\begin{aligned}
R_{Lij}^0(f) &= \sqrt{2}O_{i1}^f((T_{3f} - e_f)tZ_{j1}^* - T_{3f}Z_{j2}^*) , \\
R_{Rij}^0(f) &= \sqrt{2}O_{i2}^f e_f t Z_{j1} \epsilon_j , \\
T_{Lij}^0(f) &= O_{i2}^f Z_{j(3)}^* , \\
T_{Rij}^0(f) &= O_{i1}^f Z_{j(3)} \epsilon_j ,
\end{aligned} \tag{A.21}$$

and

$$\begin{aligned}
P_{ij}(f) &= O_{i1}^f O_{j1}^f + O_{i2}^f O_{j2}^f , \\
P'_{ij}(f) &= \frac{1}{2}(O_{i1}^f O_{j2}^f + O_{i2}^f O_{j1}^f) , \\
P''_{ij}(f) &= O_{i1}^f O_{j1}^f (T_{3f} - e_f s^2) + O_{i2}^f O_{j2}^f e_f s^2 ,
\end{aligned} \tag{A.22}$$

where  $f = (t, b, \tau)$  with charge  $e_f$  and weak isospin  $T_{3f}$ . In  $T_{L,R}^0$  the  $\binom{4}{3}$  indices correspond to  $f = \binom{t}{b, \tau}$ . For the sneutrino case there is no  $\tilde{\nu}_{\tau R}$  so one must make the replacements  $P_{\nu\tau} = 1$ ,  $P'_{\nu\tau} = 0$  and  $P''_{\nu\tau} = \frac{1}{2}$ . In all these quantities  $c = \cos \theta_W$  and  $s$  and  $t$  are the sine and tangent, respectively.

The quantities  $C_{ijk}^{LR}(t)$ ,  $C_{ijk}^{RL}(t)$  and  $\bar{C}_{ijk}(t)$  in the chargino contribution are

$$\begin{aligned}
C_{ijk}^{LR}(t) &= y_b C_{ijk}^1(t) + g_2 C_{ijk}^2(t) , \\
C_{ijk}^{RL}(t) &= y_b \tilde{C}_{ijk}^1(t) + g_2 \tilde{C}_{ijk}^2(t) , \\
\bar{C}_{ijk}(t) &= y_b^2 \bar{C}_{ijk}^1(t) + y_b g_2 \bar{C}_{ijk}^2(t) \\
&\quad + g_2^2 \bar{C}_{ijk}^3(t) + g_2^2 \left(\frac{g_2}{y_b}\right) \bar{C}_{ijk}^4(t) ,
\end{aligned} \tag{A.23}$$

where

$$\begin{aligned}
C_{ijk}^1(t) &= \text{Re}[T_{Lik}^{\pm*}(t)T_{Rij}^{\pm}(t)(Q_{jk}^* \cot \beta + S_{jk}^*)] , \\
C_{ijk}^2(t) &= \text{Re}[R_{Lik}^{\pm*}(t)T_{Rij}^{\pm}(t)(Q_{jk}^* \cot \beta + S_{jk}^*)] , \\
\tilde{C}_{ijk}^1(t) &= \text{Re}[T_{Lik}^{\pm*}(t)T_{Rij}^{\pm}(t)(Q_{kj} \cot \beta + S_{kj})] , \\
\tilde{C}_{ijk}^2(t) &= \text{Re}[R_{Lik}^{\pm*}(t)T_{Rij}^{\pm}(t)(Q_{kj} \cot \beta + S_{kj})] ,
\end{aligned} \tag{A.24}$$

and

$$\begin{aligned}
\overline{C}_{ijk}^1(t) &= \cot \beta \operatorname{Re}[T_{Lki}^{\pm*}(t)T_{Rji}^{\pm}(t)(P_{jk}(b) + P'_{jk}(b)(\frac{\mu_H \tan \beta + A_b}{m_b}))], \\
\overline{C}_{ijk}^2(t) &= -\cot \beta \operatorname{Re}[R_{Lki}^{\pm*}(t)T_{Rji}^{\pm}(t)(P_{jk}(b) + P'_{jk}(b)(\frac{\mu_H \tan \beta + A_b}{m_b}))], \quad (\text{A.25}) \\
\overline{C}_{ijk}^3(t) &= \cot 2\beta \operatorname{Re}[T_{Lki}^{\pm*}(t)T_{Rji}^{\pm}(t)P''_{jk}(b)], \\
\overline{C}_{ijk}^4(t) &= -\cot 2\beta \operatorname{Re}[R_{Lki}^{\pm*}(t)T_{Rji}^{\pm}(t)P''_{jk}(b)].
\end{aligned}$$

The matrices  $R^{\pm}$  and  $T^{\pm}$  involve products of squark and chargino mixing matrices

$$\begin{aligned}
R_{Lij}^{\pm}(t) &= O_{i1}^b U_{j1}^*, & T_{Lij}^{\pm}(t) &= O_{i2}^b U_{j2}^*, & T_{Rij}^{\pm}(t) &= O_{i1}^b V_{j2}, \\
R_{Lij}^{\pm}(b) &= O_{i1}^t V_{j1}^*, & T_{Lij}^{\pm}(b) &= O_{i2}^t V_{j2}^*, & T_{Rij}^{\pm}(b) &= O_{i1}^t U_{j2}, \quad (\text{A.26}) \\
R_{Li}^{\pm}(\tau) &= V_{i1}^*, & T_{Li}^{\pm}(\tau) &= 0, & T_{Ri}^{\pm}(\tau) &= U_{i2}.
\end{aligned}$$

Finally the gluino contribution depends on  $\overline{G}_{ij}(t)$ , defined by

$$\begin{aligned}
\overline{G}_{ij}(t) &= P'_{ij}(t) \left( P_{ij}(t) + P'_{ij}(t) \left( \frac{\mu_H \cot \beta + A_t}{m_t} \right) \right) \\
&\quad + \frac{g^2 \cot^2 \beta - 1}{y_t^2 2c^2} P'_{ij}(t) P''_{ij}(t). \quad (\text{A.27})
\end{aligned}$$

The finite corrections to the  $h_0 \bar{b}b$  vertex are obtained from those for the top vertex with the following substitutions. First interchange  $b \leftrightarrow t$  and  $\cos \beta \leftrightarrow \sin \beta$  everywhere in Eqs. (A.14) - (A.17) and in the definitions of  $N^i$ ,  $C^i$  (and their  $L \leftrightarrow R$  counterparts),  $\overline{N}^i$ ,  $\overline{C}^i$  and  $\overline{G}$ . Then in the  $N^i$ , substitute  $-Q'' \leftrightarrow S''$  and in the  $C^i$  substitute  $Q_{jk} \rightarrow S_{kj}$ ,  $S_{jk} \rightarrow Q_{kj}$ . Also in  $\overline{N}_{ijk}^{3,4,5}(b)$  and  $\overline{G}_{ij}(b)$  one must change the signs of the terms with  $\tan^2 \beta - 1$  factors and one must change the overall signs of  $\overline{C}_{ijk}^{3,4}(b)$ . The finite corrections to the  $h_0 \bar{\tau}\tau$  vertex are obtained from those for the bottom vertex by substituting  $b \rightarrow \tau$ ,  $y_t, m_t \rightarrow 0$  and  $t \rightarrow \nu_{\tau}$  everywhere (omitting the appropriate sums). The charged Higgs and gluino contributions vanish in this vertex, while the only chargino contributions come from wino induced contributions involving  $g_2^2 C^2$  and  $g_2^2 \overline{C}^4$ .

We may now construct the threshold matching functions for the third generation Yukawa couplings. Using the results of Section 2,

$$\begin{aligned} y_t^{SM}(\mu) &= y_t(\mu) \sin \beta (1 + \Delta_{y_t}^{SUSY}) , \\ y_b^{SM}(\mu) &= y_b(\mu) \cos \beta (1 + \Delta_{y_b}^{SUSY}) , \\ y_\tau^{SM}(\mu) &= y_\tau(\mu) \cos \beta (1 + \Delta_{y_\tau}^{SUSY}) , \end{aligned} \tag{A.28}$$

where

$$\Delta_{y_\alpha}^{SUSY} = \bar{K}_\alpha^Y - \frac{1}{2}(\bar{K}_{\alpha L} + \bar{K}_{\alpha R} + \bar{K}_{h_0}) . \tag{A.29}$$

The explicit form for the complete matching functions is rather unwieldy however simplified forms can be constructed in certain limits. For example, in the low to intermediate  $\tan \beta$  range it is appropriate to include order  $y_t^2$  and  $g_3^2$  effects as the dominant contribution. We shall consider a particular limit in which the neutralino and chargino mass matrices have a definite form, determined by assuming values for the Higgs potential parameter  $\mu_H$  and the gaugino masses  $\mathcal{M}_{1,2}$  which are significantly larger than  $M_Z$ . The the neutralino mass matrix has the approximate form

$$M_{\chi^0} \approx \begin{pmatrix} \mathcal{M}_1 & 0 & 0 & 0 \\ 0 & \mathcal{M}_2 & 0 & 0 \\ 0 & 0 & 0 & \mu_H \\ 0 & 0 & \mu_H & 0 \end{pmatrix} , \tag{A.30}$$

so that  $Z_{ij} = \delta_{ij}$ ,  $Z_{i3} = Z_{i4} = 0$  and  $Z_{i+2,j+2} = Z_{2ij}$ , where

$$Z_2 = \frac{1}{\sqrt{2}} \begin{pmatrix} 1 & 1 \\ 1 & -1 \end{pmatrix} . \tag{A.31}$$

Due to the appearance of a negative Majorana mass eigenvalue we have  $\epsilon_3 = -\epsilon_4 = \text{sgn}(\mu_H)$  (note also  $\epsilon_{1,2} = 1$ ). The chargino mass matrix is approximately diagonal,

$$M_{\chi^\pm} \approx \begin{pmatrix} \mathcal{M}_2 & 0 \\ 0 & -\mu_H \end{pmatrix} , \tag{A.32}$$

with  $U_{ij} \approx \delta_{ij}$  and  $V \approx \text{diag}(1, -\text{sgn}(\mu_H))$ , where  $\text{sgn}(\mu_H) = \mu_H/|\mu_H|$ . Thus in this limit the neutralino eigenstates are the bino, neutral wino and a Dirac Higgsino

with masses  $m_{\tilde{B}} \approx \mathcal{M}_1$ ,  $m_{\tilde{W}_3} \approx \mathcal{M}_2$  and  $m_{\tilde{H}^0} \approx |\mu_H|$ . The chargino eigenstates are just the charged wino and Higgsino with masses  $m_W \approx \mathcal{M}_2$  and  $m_{\tilde{H}^\pm} \approx |\mu_H|$ .

In this limit, the explicit form of the vertex corrections can be obtained using simplified forms of the  $N^i$ ,  $\tilde{N}^i$ ,  $\bar{N}^i$ ,  $C^i$ ,  $\tilde{C}^i$  and  $\bar{C}^i$ . For the neutralino contributions we have

$$\begin{aligned}
\sum_{j=3,4} N_{ijk}^2(t) &= \frac{1}{2\sqrt{2}} \left( (O_{i1}^t)^2 \delta_{k2} + \frac{t^2}{3} \delta_{k1} (-(O_{i1}^t)^2 + 4(O_{i2}^t)^2) \right), \\
\sum_{j=3,4} N_{ijk}^2(b) &= \frac{1}{2\sqrt{2}} \left( (O_{i1}^b)^2 \delta_{k2} + \frac{t^2}{3} \delta_{k1} ((O_{i1}^b)^2 + 2(O_{i2}^b)^2) \right), \\
\sum_{j=3,4} N_{ijk}^2(\tau) &= \frac{1}{2\sqrt{2}} \left( (O_{i1}^\tau)^2 \delta_{k2} + t^2 \delta_{k1} (-(O_{i1}^\tau)^2 + 2(O_{i2}^\tau)^2) \right), \\
\bar{N}_{ijk}^3(t) &= -\frac{2}{9} t^2 \delta_{i1} P'_{jk}(t) \left( P_{jk}(t) + P'_{jk}(t) \left( \frac{\mu_H \cot \beta + A_t}{m_t} \right) \right), \\
\bar{N}_{ijk}^3(b) &= \frac{1}{9} t^2 \delta_{i1} P'_{jk}(b) \left( P_{jk}(b) + P'_{jk}(b) \left( \frac{\mu_H \tan \beta + A_b}{m_b} \right) \right), \\
\bar{N}_{ijk}^3(\tau) &= -t^2 \delta_{i1} P'_{jk}(\tau) \left( P_{jk}(\tau) + P'_{jk}(\tau) \left( \frac{\mu_H \tan \beta + A_\tau}{m_\tau} \right) \right).
\end{aligned} \tag{A.33}$$

The simplified chargino contributions can be obtained using

$$\begin{aligned}
C_{ijk}^2(t) &= \frac{1}{\sqrt{2}} (O_{i1}^b)^2 \delta_{k1} \delta_{j2}, \\
C_{ijk}^2(b) &= \frac{1}{\sqrt{2}} (O_{i1}^t)^2 \delta_{k1} \delta_{j2}, \\
C_{ijk}^2(\tau) &= \frac{1}{\sqrt{2}} \delta_{k1} \delta_{j2}, \\
\bar{C}_{ijk}^1(t) &= -\text{sgn}(\mu_H) \delta_{i2} \cot \beta P'_{jk}(b) \left( P_{jk}(b) + P'_{jk}(b) \left( \frac{\mu_H \tan \beta + A_b}{m_b} \right) \right), \\
\bar{C}_{ijk}^1(b) &= -\text{sgn}(\mu_H) \delta_{i2} \tan \beta P'_{jk}(t) \left( P_{jk}(t) + P'_{jk}(t) \left( \frac{\mu_H \cot \beta + A_t}{m_t} \right) \right), \\
\bar{C}_{ijk}^3(t) &= -\text{sgn}(\mu_H) \delta_{i2} \cot 2\beta P'_{jk}(b) P''_{jk}(b), \\
\bar{C}_{ijk}^3(b) &= -\text{sgn}(\mu_H) \delta_{i2} \cot 2\beta P'_{jk}(t) P''_{jk}(t).
\end{aligned} \tag{A.34}$$

The contributions of  $\tilde{N}^2$  and  $\tilde{C}^2$  are determined by multiplying the results for  $N^2$  and  $C^2$  by  $-\text{sgn}(\mu_H) \cot \beta$  for the top case and by  $-\text{sgn}(\mu_H) \tan \beta$  for the bottom,

$\tau$  cases. The other neutralino and chargino contributions vanish in this limit. The wavefunction renormalization contributions also simplify in an obvious way; in particular, the terms proportional to  $g_2 y_\alpha$  vanish in this limit.

Below we give the dominant contributions to the matching functions and ignore those contributions of less than 1% to the Yukawa couplings. Some of the  $y_b$  and  $y_\tau$  corrections will be suppressed in the low  $\tan\beta$  region while receiving large enhancements for high  $\tan\beta$ . The converse is true for the corrections to  $y_t$ . The gluino contributions dominate the top and bottom Yukawa corrections. For large  $\tan\beta$  the finite vertex contributions from graphs with chargino and neutralino exchange are enhanced for the bottom and  $\tau$  cases and give large contributions. For high(low)  $\tan\beta$  the finite parts of wavefunction renormalization contributions depending on  $y_t(y_b, y_\tau)$  can be important as well. The matching functions are

$$\begin{aligned}
16\pi^2 \Delta_{y_t}^{SUSY} \simeq & \frac{8}{3} g_3^2 \left( -2m_{\tilde{g}} \sum_{i,j} \left( m_t G_2(m_{\tilde{g}}^2, m_{\tilde{t}_i}^2, m_{\tilde{t}_j}^2) P'_{ij}(t) P_{ij}(t) \right. \right. \\
& + (\mu_H \cot\beta + A_t) G_2(m_{\tilde{g}}^2, m_{\tilde{t}_i}^2, m_{\tilde{t}_j}^2) (P'_{ij}(t))^2 \\
& \left. \left. + \frac{1}{4} \sum_i F_2(m_{\tilde{t}_i}^2, m_{\tilde{g}}^2) \right) \right. \\
& + \frac{1}{4} y_t^2 \left( \sum_i F_2(m_{\tilde{b}_i}^2, m_{\tilde{H}^\pm}^2) (O_{i1}^b)^2 + \sum_i F_2(m_{\tilde{t}_i}^2, m_{\tilde{H}^0}^2) \right. \\
& \left. \left. + \cos^2\beta F_2(m_{\tilde{H}^\pm}^2, m_b^2) \right) \right. \\
& \left. + \frac{1}{4} y_b^2 \left( \sum_i F_2(m_{\tilde{b}_i}^2, m_{\tilde{H}^\pm}^2) (O_{i2}^b)^2 + \sin^2\beta F_2(m_{\tilde{H}^\pm}^2, m_b^2) \right) \right), \tag{A.35}
\end{aligned}$$

$$\begin{aligned}
16\pi^2 \Delta_{y_b}^{SUSY} &\simeq \frac{8}{3} g_3^2 \left( -2m_{\tilde{g}}(\mu_H \tan \beta + A_b) \sum_{i,j} G_2(m_{\tilde{g}}^2, m_{\tilde{b}_i}^2, m_{\tilde{b}_j}^2) (P'_{ij}(b))^2 \right. \\
&\quad \left. + \frac{1}{4} \sum_i F_2(m_{\tilde{b}_i}^2, m_{\tilde{g}}^2) \right) \\
&\quad + y_t^2 \left( -2\mu_H \tan \beta \sum_{i,j} \left( m_t G_2(m_{\tilde{H}^\pm}^2, m_{\tilde{t}_i}^2, m_{\tilde{t}_j}^2) P'_{ij}(t) P_{ij}(t) \right. \right. \\
&\quad \left. \left. + (\mu_H \cot \beta + A_t) G_2(m_{\tilde{H}^\pm}^2, m_{\tilde{t}_i}^2, m_{\tilde{t}_j}^2) (P'_{ij}(t))^2 \right) \right. \\
&\quad \left. + \frac{1}{4} \left( \sum_i F_2(m_{\tilde{t}_i}^2, m_{\tilde{H}^\pm}^2) (O_{i2}^t)^2 + \cos^2 \beta F_2(m_{\tilde{H}^\pm}^2, m_t^2) \right) \right) \quad (\text{A.36}) \\
&\quad + \frac{1}{4} y_b^2 \left( \sum_i F_2(m_{\tilde{t}_i}^2, m_{\tilde{H}^\pm}^2) (O_{i1}^t)^2 + \sum_i F_2(m_{\tilde{b}_i}^2, m_{\tilde{H}^0}^2) \right. \\
&\quad \left. + \sin^2 \beta F_2(m_{\tilde{H}^\pm}^2, m_t^2) \right) \\
&\quad + \frac{1}{2} g_2^2 \left( \mu_H \mathcal{M}_2 \tan \beta \sum_i \left( G_2(m_{\tilde{b}_i}^2, m_{\tilde{H}^0}^2, m_{\tilde{W}^3}^2) (O_{i1}^b)^2 \right. \right. \\
&\quad \left. \left. + G_2(m_{\tilde{t}_i}^2, m_{\tilde{H}^\pm}^2, m_{\tilde{W}^-}^2) (O_{i1}^t)^2 \right) \right),
\end{aligned}$$

$$\begin{aligned}
16\pi^2 \Delta_{y_\tau}^{SUSY} &\simeq \frac{1}{4} y_\tau^2 \left( F_2(m_{\tilde{\nu}_\tau}^2, m_{\tilde{H}^\pm}^2) + \sum_i F_2(m_{\tilde{\tau}_i}^2, m_{\tilde{H}^0}^2) + \sin^2 \beta F_2(m_{\tilde{H}^\pm}^2, 0) \right) \\
&\quad + \frac{1}{2} g_2^2 \left( \mu_H \mathcal{M}_2 \tan \beta \sum_i \left( G_2(m_{\tilde{\tau}_i}^2, m_{\tilde{H}^0}^2, m_{\tilde{W}^3}^2) (O_{i1}^\tau)^2 \right. \right. \\
&\quad \left. \left. + G_2(m_{\tilde{\nu}_\tau}^2, m_{\tilde{H}^\pm}^2, m_{\tilde{W}^-}^2) \right) \right. \\
&\quad \left. - 2t^2 \mathcal{M}_1 (\mu_H \tan \beta + A_\tau) \sum_{i,j} G_2(m_{\tilde{B}}^2, m_{\tilde{\tau}_i}^2, m_{\tilde{\tau}_j}^2) (P'_{ij}(\tau))^2 \right), \quad (\text{A.37})
\end{aligned}$$

where we have used Eqs. (A.30) - (A.32).

## APPENDIX B: Function Definitions

In the appendix we define the various functions arising from parameter integrals in the evaluation of the finite parts of one loop diagrams. The functions  $F_i$  and  $G_i$  come from two and three point functions, respectively. The  $F_i$  are

$$\begin{aligned}
 F_1(M_A^2, M_B^2) &= \int_0^1 d\alpha \ln\left(\frac{M_A^2\alpha + M_B^2(1-\alpha)}{\mu^2}\right) \\
 &= \frac{1}{M_A^2 - M_B^2} \left( M_A^2 \ln \frac{M_A^2}{\mu^2} - M_B^2 \ln \frac{M_B^2}{\mu^2} \right) - 1, \\
 F_2(M_A^2, M_B^2) &= 2 \int_0^1 d\alpha \alpha \ln\left(\frac{M_A^2\alpha + M_B^2(1-\alpha)}{\mu^2}\right) \\
 &= \frac{1}{(M_A^2 - M_B^2)^2} \left( (M_A^4 - 2M_A^2 M_B^2) \ln \frac{M_A^2}{\mu^2} + M_B^4 \ln \frac{M_B^2}{\mu^2} \right) \\
 &\quad + \frac{M_B^2}{M_A^2 - M_B^2} - \frac{1}{2}, \\
 F_3(M_A^2, M_B^2) &= 6 \int_0^1 d\alpha \alpha(1-\alpha) \ln\left(\frac{M_A^2\alpha + M_B^2(1-\alpha)}{\mu^2}\right) \\
 &= \frac{1}{(M_A^2 - M_B^2)^3} \left( M_A^4(M_A^2 - 3M_B^2) \ln \frac{M_A^2}{\mu^2} \right. \\
 &\quad \left. - M_B^4(M_B^2 - 3M_A^2) \ln \frac{M_B^2}{\mu^2} \right) + \frac{2M_A^2 M_B^2}{(M_A^2 - M_B^2)^2} - \frac{5}{6}.
 \end{aligned} \tag{B.1}$$

Both  $F_1$  and  $F_3$  are symmetric. The explicit forms of the functions for the limits  $M_A \gg (\ll) M_B$  are

$$\begin{aligned}
 F_1(M_A^2, 0) &= \ln \frac{M_A^2}{\mu^2} - 1, \\
 F_2(M_A^2, 0) &= \ln \frac{M_A^2}{\mu^2} - \frac{1}{2}, \quad F_2(0, M_A^2) = \ln \frac{M_A^2}{\mu^2} - \frac{3}{2}, \\
 F_3(M_A^2, 0) &= \ln \frac{M_A^2}{\mu^2} - \frac{5}{6},
 \end{aligned} \tag{B.2}$$

and for  $M_A = M_B$ ,  $F_i = \ln M_A^2/\mu^2$ . The  $G_i$  are

$$\begin{aligned}
G_1(M_A^2, M_B^2, M_C^2) &= 2 \int_0^1 d\alpha \int_0^{1-\alpha} d\beta \ln \left( \frac{M_A^2 \alpha + M_B^2 \beta + M_C^2 (1 - \alpha - \beta)}{\mu^2} \right) \\
&= \frac{M_A^4}{(M_A^2 - M_B^2)(M_A^2 - M_C^2)} \left( \ln \frac{M_A^2}{\mu^2} - \frac{1}{2} \right) \\
&\quad + (A \leftrightarrow B) + (A \leftrightarrow C) - 1, \tag{B.3} \\
G_2(M_A^2, M_B^2, M_C^2) &= \int_0^1 d\alpha \int_0^{1-\alpha} d\beta \frac{1}{M_A^2 \alpha + M_B^2 \beta + M_C^2 (1 - \alpha - \beta)} \\
&= \frac{1}{M_A^2 - M_B^2} \left( \frac{M_A^2}{M_A^2 - M_C^2} \ln \frac{M_A^2}{M_C^2} - \frac{M_B^2}{M_B^2 - M_C^2} \ln \frac{M_B^2}{M_C^2} \right).
\end{aligned}$$

We also consider the limits below

$$\begin{aligned}
G_1(M_A^2, M_B^2, M_C^2) &= \begin{cases} \frac{2M_A^2}{M_A^2 - M_C^2} \left( \ln \frac{M_A^2}{\mu^2} - \frac{1}{2} \right) - 1 \\ \quad + \frac{M_C^4}{(M_A^2 - M_C^2)^2} \left( \ln \frac{M_C^2}{\mu^2} - \frac{1}{2} \right) & M_A = M_B \\ \left( \ln \frac{M_A^2}{\mu^2} - \frac{1}{2} \right) & M_A = M_B \gg M_C \\ \frac{M_A^2 \ln \frac{M_A^2}{\mu^2} - M_B^2 \ln \frac{M_B^2}{\mu^2}}{M_A^2 - M_B^2} - \frac{3}{2} & M_A, M_B \gg M_C \\ \ln \frac{M_A^2}{\mu^2} - \frac{3}{2} & M_A \gg M_B, M_C \end{cases} \tag{B.4} \\
G_2(M_A^2, M_B^2, M_C^2) &= \begin{cases} \frac{M_C^2}{(M_A^2 - M_C^2)^2} \ln \frac{M_C^2}{M_A^2} + \frac{1}{M_A^2 - M_C^2} & M_A = M_B \\ \frac{1}{M_A^2} & M_A = M_B \gg M_C \\ \frac{1}{M_A^2 - M_B^2} \ln \frac{M_A^2}{M_B^2} & M_A, M_B \gg M_C, \end{cases}
\end{aligned}$$

where we have included the particular cases that occur in the threshold corrections.

## REFERENCES

1. R. Arnowitt and P. Nath, *Phys. Rev. Lett.* **69** (1992) 725; *Phys. Lett.* **289B** (1992) 368.
2. G. G. Ross and R. G. Roberts, *Nucl. Phys.* **B377** (1992) 571.
3. S. Kelley, J. L. Lopez, D. V. Nanopoulos, H. Pois and K. Yuan *Nucl. Phys.* **B398** (1993) 3.
4. M. Olechowski and S. Pokorski, *Nucl. Phys.* **B404** (1993) 590.
5. P. Ramond, Talk presented at the International Workshop on Recent Advances in the Superworld, Woodlands, TX, Institute for Fundamental Theory preprint UFIFT-HEP-93-13 (Apr. 1993); D. J. Castaño, E. J. Piard and P. Ramond, UFIFT-HEP-93-18 (Aug. 1993).
6. V. Barger, M. S. Berger and P. Ohmann, U. Wisconsin preprint MAD/PH/801 (Nov. 1993).
7. G. L. Kane, C. Kolda, L. Roszkowski and J. D. Wells, U. Michigan preprint UM-TH-93-24 (hep-ph/9312272).
8. P. Langacker and N. Polonsky, University of Pennsylvania preprint, UPR-0556T, May 1993.
9. L. Hall, R. Rattazzi and U. Sarid, Lawrence Berkeley Lab preprint, LBL-333997 (hep-ph/9306309) (June 1993).
10. R. Hempfling, DESY preprint, DESY-93-092 (Jul. 1993).
11. W. A. Bardeen, M. Carena, S. Pokorski and C. E. M. Wagner, Max Planck Institute preprint, MPI-PH-93-103 (Feb. 1994).
12. H. E. Haber and R. Hempfling, *Phys. Rev.* **D48** (1993) 4280; R. Hempfling, DESY preprint, DESY-93-012 (Feb. 1993).
13. H. Arason, D. Castaño, B. Keszthelyi, S. Mikaelian, E. Piard, P. Ramond and B. D. Wright, *Phys. Rev.* **D46** (1992) 3945.

14. J. Oliensis and M. Fishler, *Phys. Rev.* **D28** (1983) 194.
15. S. Dimopoulos, L. J. Hall and S. Raby, *Phys. Rev. Lett.* **68** (1992) 1984;  
*Phys. Rev.* **D45** (1992) 4195.
16. V. Barger, M. S. Berger, T. Han and M. Zralek, *Phys. Rev. Lett.* **68** (1992) 3394.
17. H. Arason, D. J. Castaño, E. J. Piard and P. Ramond, *Phys. Rev.* **D47** (1993) 232.
18. P. Ramond, R. G. Roberts and G. G. Ross, *Nucl. Phys.* **B406** (1993) 19.
19. G. Anderson, S. Dimopoulos, L. J. Hall, S. Raby and G. D. Starkman, Lawrence Berkeley Lab preprint, LBL-33531 (Aug. 1993).
20. A. Masiero, D. V. Nanopoulos, K. Tamvakis and T. Yanagida, *Phys. Lett.* **115B** (1982) 380.
21. T. W. Appelquist and J. Carrazone, *Phys. Rev.* **D11** (1975) 2856.
22. S. Weinberg, *Phys. Lett.* **91B** (1980) 51.
23. L. Hall, *Nucl. Phys.* **B178** (1981) 75.
24. B. A. Ovrut and H. J. Schnitzer, *Phys. Rev.* **D21** (1980) 3369;  
*Phys. Rev.* **D22** (1980) 2518; *Nucl. Phys.* **B179** (1981) 381;  
*Phys. Lett.* **100B** (1981) 403; *Nucl. Phys.* **B184** (1981) 109.
25. B. Wright and B. Keszthelyi, in preparation.
26. H. Arason, D. Castaño, B. Keszthelyi, S. Mikaelian, E. Piard, P. Ramond and B. D. Wright, *Phys. Rev. Lett.* **67** (1991) 2933.
27. S. Kelly, J. L. Lopez and D. V. Nanopoulos, *Phys. Lett.* **274B** (1992) 387.
28. B. Ananthanarayan, G. Lazarides and Q. Shafi, *Phys. Rev.* **D44** (1991) 1613.
29. A. Givon, L. Hall and U. Sarid, *Phys. Lett.* **271B** (1991) 138.
30. M. B. Einhorn and D. R. T. Jones, *Nucl. Phys.* **B196** (1982) 475.

31. I. Antoniadis, C. Kounnas and K. Tamvakis, *Phys. Lett.* **119B** (1982) 377.
32. K. Hagiwara and Y. Yamada, *Phys. Rev. Lett.* **70** (1993) 709; Y. Yamada, *Z. Phys.* **C60** (1993) 83.
33. J. Hisano, H. Murayama and T. Yanagida, *Nucl. Phys.* **B402** (1993) 46; *Phys. Rev. Lett.* **69** (1992) 1014.
34. B. Ovrut and J. Wess, *Phys. Rev.* **D25** (1982) 409.
35. P. Binétruy, P. Sorba and R. Stora, *Phys. Lett.* **129B** (1983) 85.
36. M. T. Grisaru, W. Siegel and M. Roček, *Nucl. Phys.* **B159** (1979) 429.
37. W. Siegel, *Phys. Lett.* **84B** (1979) 193, *Phys. Lett.* **94B** (1980) 37, D. M. Capper, D. R. T. Jones and P. van Nieuwenhuizen, *Nucl. Phys.* **B167** (1980) 479.
38. J. Wess and B. Zumino, *Phys. Lett.* **49B** (1974) 52; J. Iliopoulos and B. Zumino, *Nucl. Phys.* **B76** (1974) 310; S. Ferrara, J. Iliopoulos and B. Zumino, *Nucl. Phys.* **B77** (1974) 413; B. Zumino, *Nucl. Phys.* **B89** (1975) 535; S. Ferrara and O. Piguet, *Nucl. Phys.* **B93** (1975) 261.
39. L. J. Hall and U. Sarid, *Phys. Rev. Lett.* **70** (1993) 2673.
40. G. Degrassi, S. Fanchiotti and A. Sirlin, *Nucl. Phys.* **B351** (1991) 49.
41. P. Langacker and N. Polonsky, *Phys. Rev.* **D47** (1993) 4028.
42. P. Langacker and N. Polonsky, University of Pennsylvania preprint, UPR-0594T (Feb. 1994).
43. N. Gray, D. J. Broadhurst, W. Grafe, and K. Schilcher, *Z. Phys.* **C48** (1990) 673.
44. W. Bernreuther and W. Wetzel, *Nucl. Phys.* **B197** (1982) 228.
45. H. Marsiske, Talk presented at the Second Workshop on Tau Lepton Physics, Ohio State University, Sept 1992, SLAC preprint SLAC-PUB-5977 (Oct. 1992)

46. F. M. Borzumati, DESY preprint 93-090 (1993).
47. The LEP Collaborations ALEPH, DELPHI, L3, OPAL and the LEP Electroweak Working Group, CERN preprint, CERN/PPE/93-157 (Aug. 1993).
48. M. Carena, S. Pokorski and C. E. M. Wagner, *Nucl. Phys.* **B406** (1993) 59.
49. The DØ Collaboration, S. Abachi *et al.*, FERMILAB preprint, FERMILAB Pub-94/004-E (Jan. 1994).
50. V. Barger, M. S. Berger, P. Ohmann and B. Wright, in preparation.
51. S. G. Naculich, *Phys. Rev.* **D48** (1993) 5293.
52. V. Barger, M. S. Berger and P. Ohmann, *Phys. Rev.* **D47** (1993) 2038;  
V. Barger, M. S. Berger, P. Ohmann and R. J. Phillips, *Phys. Lett.* **314B** (1993) 351.
53. M. Carena, M. Olechowski, S. Pokorski and C. E. M. Wagner, *Phys. Lett.* **320B** (1994) 110.
54. S. Weinberg, *Phys. Rev.* **D26** (1982) 287; N. Sakai and T. Yanagida, *Nucl. Phys.* **B197** (1982) 533; S. Dimopoulos, S. Raby and F. Wilczek, *Phys. Lett.* **112B** (1982) 133; J. Ellis, D. V. Nanopoulos and S. Rudaz, *Nucl. Phys.* **B202** (1982) 43; S. Chadha and M. Daniels, *Nucl. Phys.* **B229** (1983) 105; B. A. Campbell, J. Ellis and D. V. Nanopoulos, *Phys. Lett.* **141B** (1984) 229; R. Arnowitt, A. H. Chamseddine and P. Nath, *Phys. Lett.* **156B** (1985) 215, *Phys. Rev.* **D32** (1985) 2348.
55. Kamiokande Collaboration, K. S. Hirata, *et al.*, *Phys. Lett.* **220B** (1989) 308.
56. M. E. Machacek and M. T. Vaughn, *Nucl. Phys.* **B222** (1983) 83;  
*Nucl. Phys.* **B236** (1984) 221; *Nucl. Phys.* **B249** (1985) 70.
57. V. Barger, M. S. Berger and P. Ohmann, *Phys. Rev.* **D47** (191993) 1093.
58. T. Moroi and T. Yanagida, Tohoku University preprint, TU-455 (Mar. 1994).

59. G. D. Coughlan, N. Fischler, E. W. Kolb, S. Raby and G. G. Ross, *Phys. Lett.* **131B** (1983) 59.
60. J. F. Gunion, H. E. Haber, G. L. Kane and S. Dawson, “The Higgs Hunter’s Guide,” Addison-Wesley (1990).
61. H. Haber and G. Kane, *Phys. Reports* **C117** (1985) 75.
62. J. Rosiek, *Phys. Rev.* **D41** (1990) 3464.
63. J. F. Gunion and H. E. Haber, *Nucl. Phys.* **B272** (1986) 1.
64. M. Carena, M. Olechowski, S. Pokorski and C. E. M. Wagner, CERN preprint, CERN-TH.7060/93 (Oct. 1993).

## FIGURE CAPTIONS

- 1) Vertex diagrams contributing to dominant gluino induced threshold corrections to  $y_t$  and  $y_b$ .
- 2) Vertex diagrams involving squarks, Higgsinos and winos giving the dominant contributions to  $y_b$  threshold correction which are enhanced in the large  $\tan\beta$  region.
- 3) Vertex diagrams involving sleptons, Higgsinos and gauginos giving the dominant contributions to  $y_\tau$  threshold correction which are enhanced in the large  $\tan\beta$  region. The bino exchange diagram can be important due to the large hypercharge of the  $\tau$  lepton.
- 4) Variation of  $M_{GUT}$  with gluino mass for  $120 \text{ GeV} \leq m_{\tilde{g}} \leq 1 \text{ TeV}$  and central values of  $\sin\theta_W(M_Z)$  and  $\alpha(M_Z)$ . Contours are given for the allowed range of  $\alpha_s(M_Z)$  and two values of  $\tan\beta$  for fixed  $M_t = 165.4 \text{ GeV}$ .
- 5) Variation of  $M_{GUT}$  with  $M_t$  for  $130 \text{ GeV} \leq m_t(M_Z) \leq 200 \text{ GeV}$  and central values of  $\sin\theta_W(M_Z)$  and  $\alpha(M_Z)$ . Contours are given for the allowed range of  $\alpha_s(M_Z)$  and two values of  $\tan\beta$  for fixed  $m_{\tilde{g}} = 400 \text{ GeV}$ .
- 6) Variation of  $M_{H_3}$  with  $V_{SUSY} \simeq .08m_{\tilde{H}}$  for  $100 \text{ GeV} \leq m_{\tilde{H}} \leq 1 \text{ TeV}$  and central values of  $\sin\theta_W(M_Z)$  and  $\alpha(M_Z)$ . Contours are given for the allowed range of  $\alpha_s(M_Z)$  and two values of  $\tan\beta$  for fixed  $M_t = 165.4 \text{ GeV}$ .
- 7) Variation of  $M_{H_3}$  with  $M_t$  for  $130 \text{ GeV} \leq m_t(M_Z) \leq 200 \text{ GeV}$  and central values of  $\sin\theta_W(M_Z)$  and  $\alpha(M_Z)$ . Contours are given for the allowed range of  $\alpha_s(M_Z)$  and two values of  $\tan\beta$  for fixed  $V_{SUSY} = 45 \text{ GeV}$ . Note that the initial fall of  $M_{H_3}$  with  $M_t$  is due to the electroweak threshold while its rise for large  $M_t$  is due to the effect of large  $y_t$  on the two loop gauge  $\beta$  functions.
- 8) The dependence of the  $M_t$  solution on  $\tan\beta$  showing the effect of a large splitting of  $M_V$  and  $M_\Sigma$  for  $M_b = 5.2 \text{ GeV}$ ,  $\alpha_s(M_Z) = 0.120$  and  $M_{SUSY} = M_Z$ . The sparticle spectrum parameters are fixed at  $m_{\tilde{g}} = M_3 = 1 \text{ TeV}$  and  $V_{SUSY} = 80 \text{ GeV}$ . The typical GUT masses are then  $M_{GUT} = 10^{16.1 \pm 0.1} \text{ GeV}$

and  $M_{H_3} = 10^{15.7 \pm 0.4}$  GeV for these solutions. We also indicate the bound from the nonperturbative limit on  $y_t$ .

- 9) The dependence of the  $M_t$  solution on  $\tan\beta$  showing the effect of a splitting of  $M_{H_3}$  above  $M_{GUT}$  for  $M_b = 4.9$  GeV,  $\alpha_s(M_Z) = 0.127$  and  $M_{SUSY} = M_Z$ . The sparticle spectrum parameters are fixed at  $m_{\tilde{g}} = M_3 = 1$  TeV and  $V_{SUSY} = 80$  GeV. The typical GUT masses are then  $M_{GUT} = 10^{16.2 \pm 0.1}$  GeV and  $M_{H_3} = 10^{16.8 \pm 0.3}$  GeV for these solutions. We again indicate the bound from the nonperturbative limit on  $y_t$ .
- 10) The dependence of the  $M_t$  solution from Yukawa unification on  $\tan\beta$  for the allowed range of  $\alpha_s(M_Z)$  for  $M_b = 4.9$  GeV and  $M_{SUSY} = M_Z$ . We give the solutions with and without GUT scale Yukawa thresholds for the generic case  $M_V = M_\Sigma$ .
- 11) The dependence of the  $M_t$  solution on  $\tan\beta$  for bottom pole masses in the range  $4.7 \text{ GeV} \leq M_b \leq 5.3 \text{ GeV}$  for  $\alpha_s(M_Z) = 0.120$  and  $M_{SUSY} = M_Z$ . Again, the solutions with and without GUT scale Yukawa thresholds correspond to the generic case  $M_V = M_\Sigma$ . The curves for  $M_b = 4.7$  and  $4.8$  GeV with GUT thresholds are cut off due to the absence of perturbative solutions.

This figure "fig1-1.png" is available in "png" format from:

<http://arxiv.org/ps/hep-ph/9404217v2>

This figure "fig1-2.png" is available in "png" format from:

<http://arxiv.org/ps/hep-ph/9404217v2>

This figure "fig1-3.png" is available in "png" format from:

<http://arxiv.org/ps/hep-ph/9404217v2>

This figure "fig1-4.png" is available in "png" format from:

<http://arxiv.org/ps/hep-ph/9404217v2>

This figure "fig1-5.png" is available in "png" format from:

<http://arxiv.org/ps/hep-ph/9404217v2>

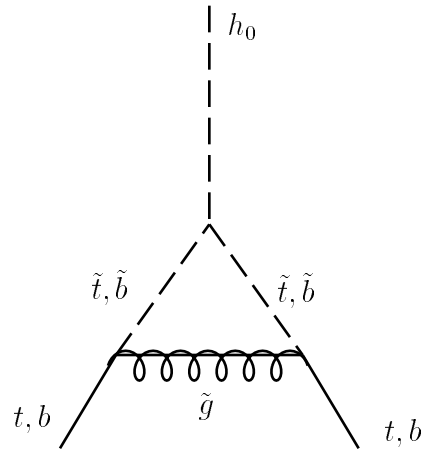


Figure 1

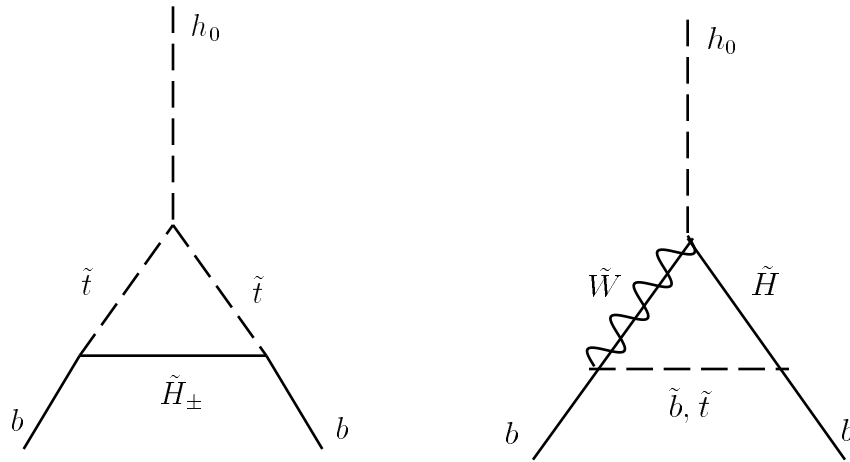


Figure 2

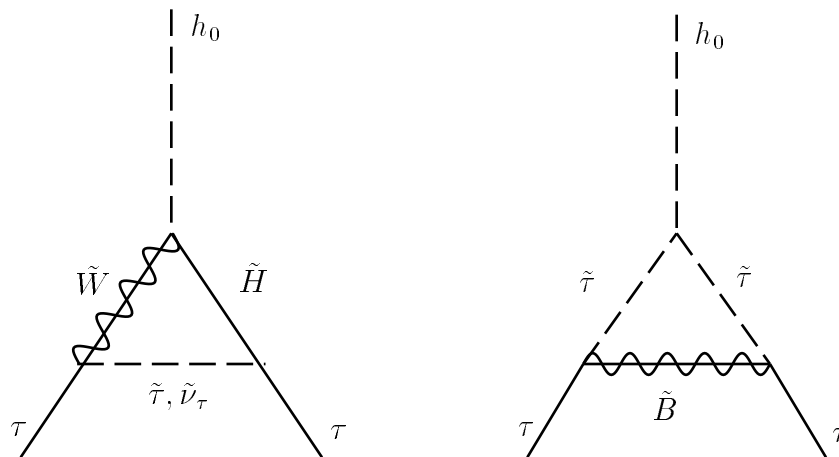


Figure 3



Figure 4

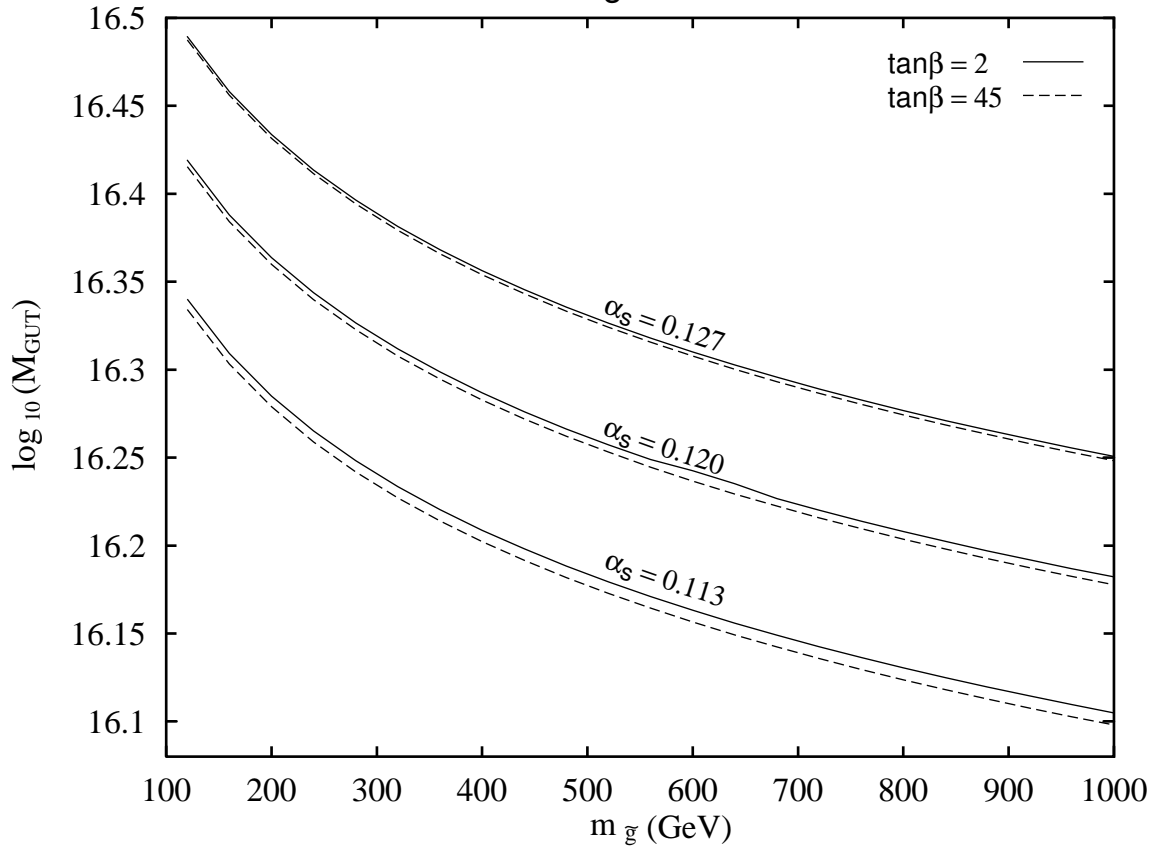


Figure 5

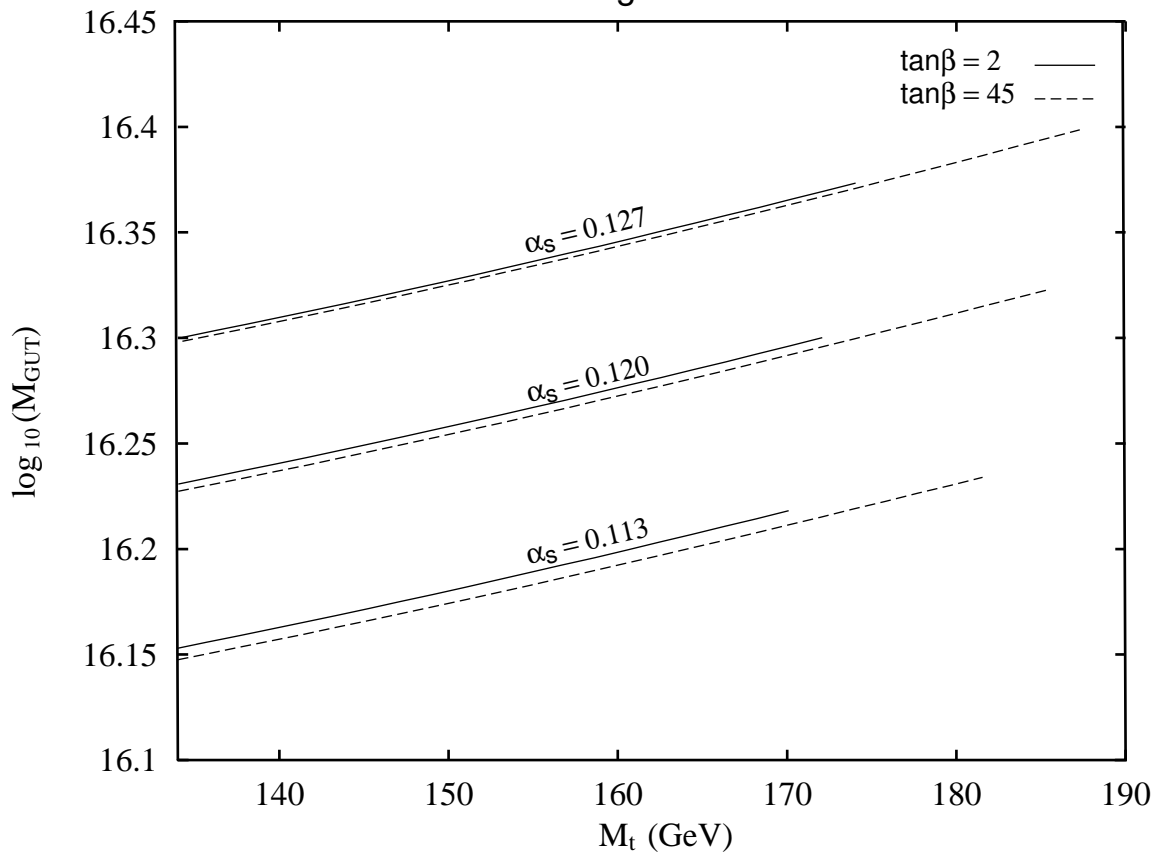




Figure 6

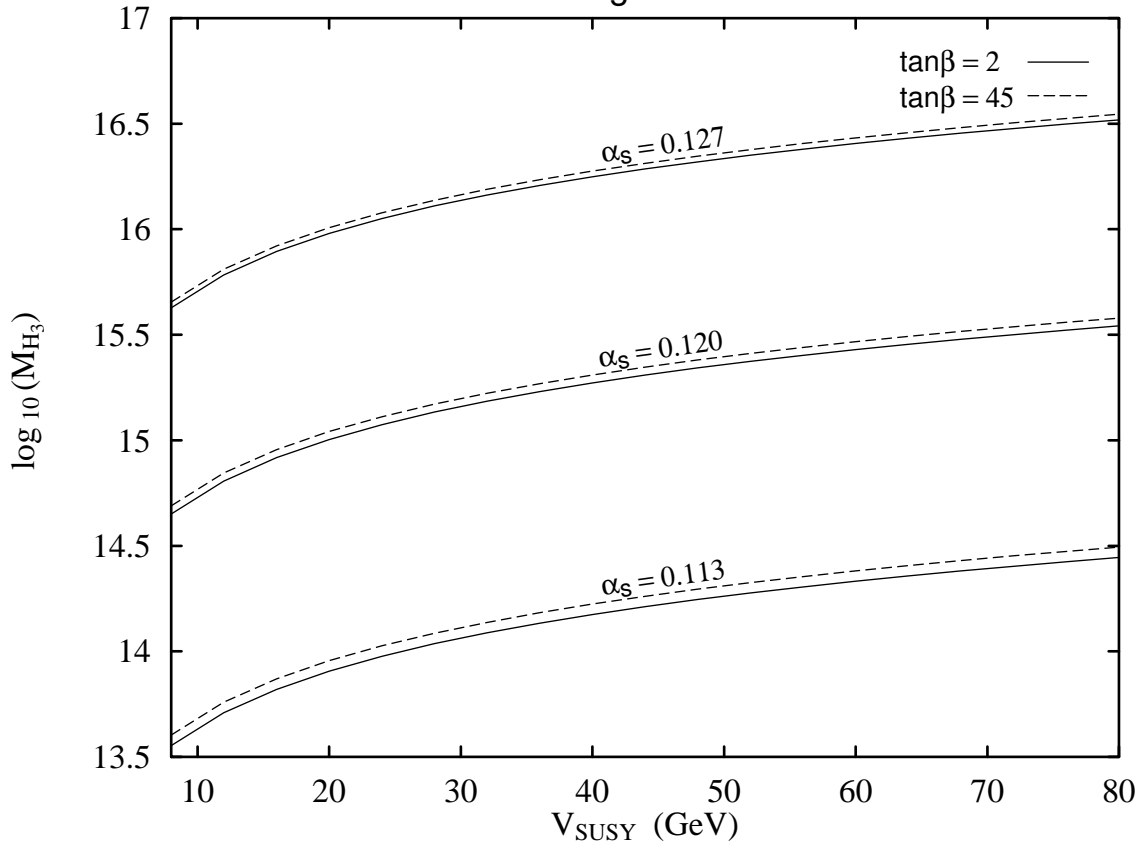


Figure 7

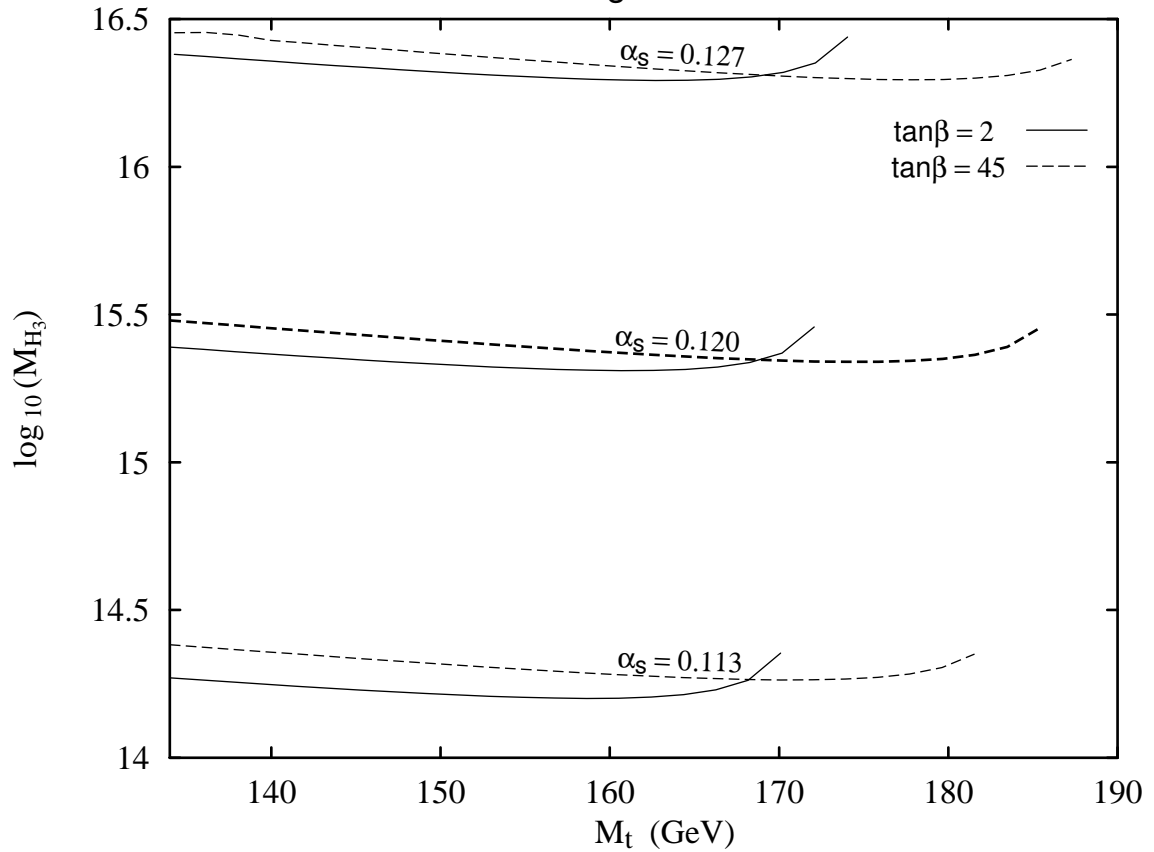




Figure 8

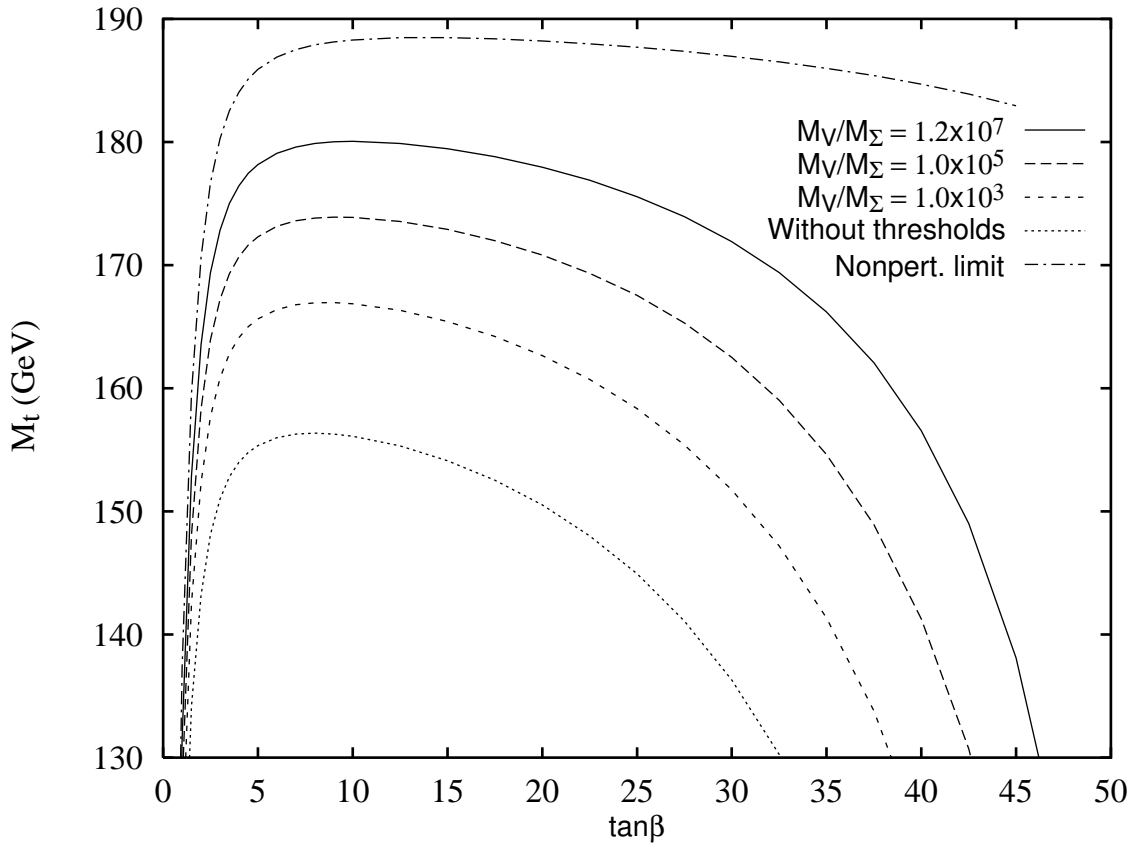


Figure 9

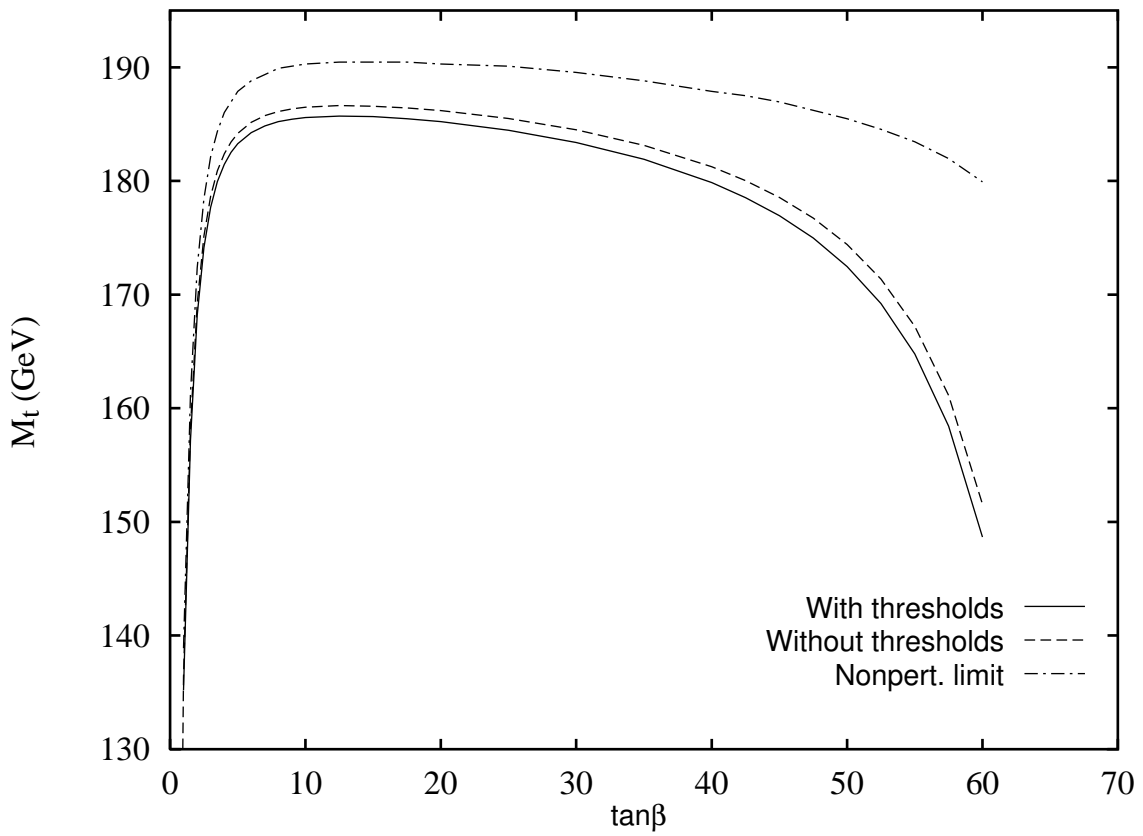




Figure 10

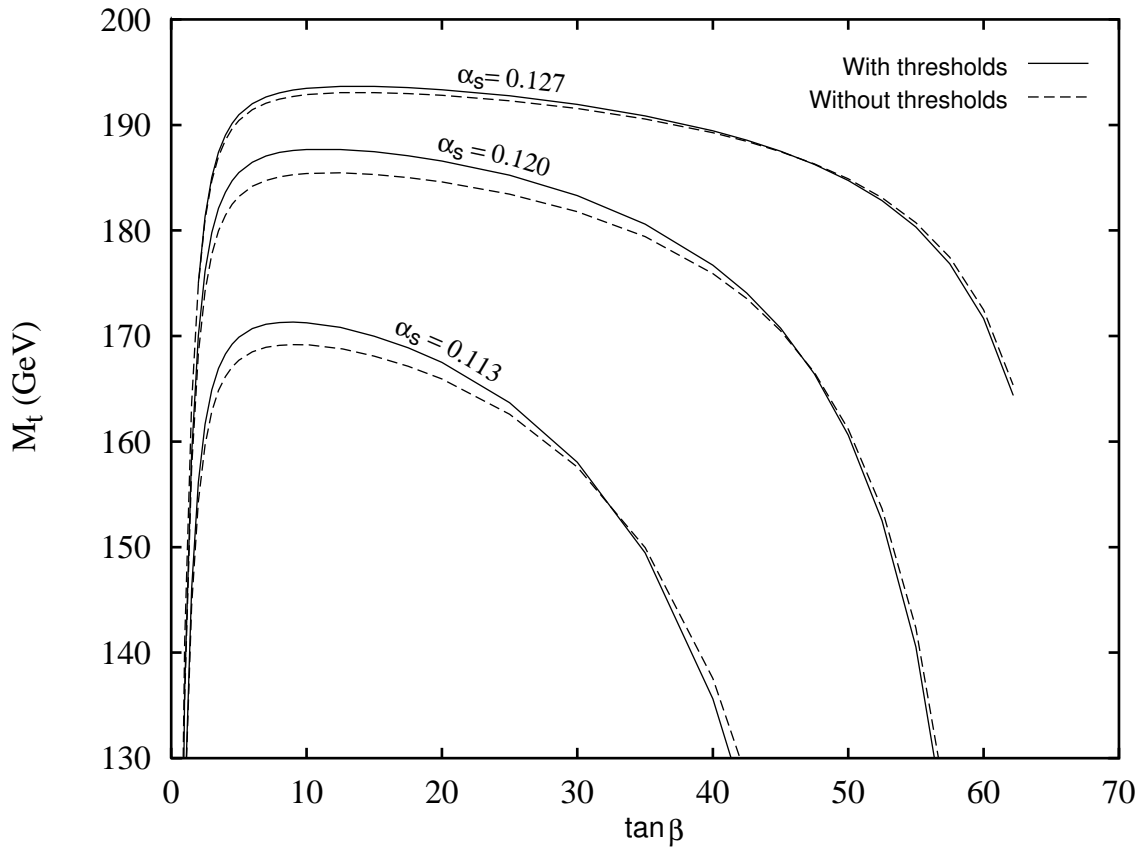


Figure 11

